Effects of Wrapping Chloride Contaminated Concrete with Fiber Reinforced Plastics

by

Emily Wason Berver, B.S.C.E.

Thesis

Presented to the Faculty of the Graduate School of

The University of Texas at Austin

in Partial Fulfillment

of the Requirements

for the Degree of

Master of Science in Engineering

The University of Texas at Austin

August 2001

Effects of Wrapping Chloride Contaminated Concrete with Fiber Reinforced Plastics

Approved by
Supervising Committee:

James O. Jirsa, Supervisor

David W. Fowler

Harovel G. Wheat

Dedication

To my husband,

Brendan Kelley Berver

Acknowledgements

I thank Dr. James O. Jirsa for his help and guidance throughout my research. His kindness, expertise, and advice are appreciated.

I thank Dr. David W. Fowler for his support that helped make this report possible. His enthusiasm contributed to a rewarding experience at The University of Texas at Austin.

I thank Dr. Harovel G. Wheat for her knowledge and her cheerful disposition to my inquiries.

I would like to express my appreciation to everyone at the Texas Department of Transportation. My thanks go to Jon Kilgore and Randy Cox for their support on this project. I would also like to thank the Lubbock District for their help in my research, especially Ron Baker, Jim Odem, and the maintenance crew.

I would also like to thank Paul Guggenheim of Delta Structural Technology, Inc. His generosity in the donation of time, labor, and materials has helped to make this project possible.

The staff and students at the Ferguson Structural Engineering Laboratory and the Construction Materials Research Group have been excellent. I greatly appreciate the atmosphere of cooperation and the willingness to offer a helping hand. I would especially like to thank Blake Stasney, Mike Bell, David Whitney, Mike Rung, Manuel Razo, and Brian Dahm for their involvement in this project.

Finally, I would like to give my love to my family. Their support and encouragement has been invaluable.

August 17, 2001

Abstract

Effects of Wrapping Chloride Contaminated Concrete with Fiber Reinforced Plastics

Emily Wason Berver, M.S.E.

The University of Texas at Austin, 2001

Supervisor: James O. Jirsa

Damage to concrete due to corrosion of steel reinforcement is a costly maintenance problem that affects infrastructure. Reinforced concrete structures located in an aggressive environment are susceptible. Fiber reinforced plastic composite wraps have recently been used to rehabilitate structures that have experienced damage due to corrosion. Little is known about the long-term performance of FRP composites in corrosion prevention. Corrosion monitoring of laboratory specimens and field research are discussed.

Table of Contents

List of Tables

List of Figures

Chapter 1

Introduction

1.1 INTRODUCTION TO CORROSION IN REINFORCED CONCRETE BRIDGES

In 1998, the Federal Highway Administration (FHWA) rated 29.6% of the nation's bridges as structurally deficient or functionally obsolete. While this number of problem structures is unacceptable, it has been declining over the last decade from a high of 34.6% in 1992. The FHWA strategic plan calls for less than 25% of the nation's bridges to be classified as deficient by 2008 (ASCE 2001).

With the increased demand on our nation's bridges and limited funding towards infrastructure, replacing deficient structures is not always a viable option. In the 21st century, engineers will increasingly need to design retrofits in order to preserve the infrastructure already in place.

The economic loss due to problems associated with corrosion of the steel reinforcing in reinforced concrete is estimated to be $50 billion per year in the United States. It is the single most expensive corrosion problem in the nation. It affects the integrity of thousands of bridges, roadbeds and overpasses (Jones 1996).

Concrete is typically a strong, durable, and long lasting building material. However, in an aggressive environment, a concrete structure may experience premature deterioration due to exposure to salts. While it may be expected that structures in a marine environment will be exposed to salts, structures located

above the freezing line are also exposed. This is due to the policy that started in the 1960s of applying deicing salts to roadways and bridge decks in order to keep them clear of ice. As a result, many bridges across the country have been experiencing problems associated with corrosion. The exposure to salt and water results in damage to the structure in the form of cracking, delamination, and spalling. This damage may cause structural problems and requires expensive rehabilitation. Overall, developing innovative ways to prevent corrosion from taking place and implementing long-term solutions to repair chloride contaminated concrete is a necessary endeavor.

A recent solution for repairing damage due to corrosion in reinforced concrete is to use fiber reinforced plastic (FRP) composite wrap. In addition to strengthening a concrete member, the FRP wrap is not subject to corrosion and may provide a barrier to protect the concrete from an aggressive environment. A potential concern is that by encapsulating concrete with FRP composite, moisture, chlorides, and oxygen may be trapped and cause the corrosion process to continue undetected. Figures 1.1 and 1.2 show a bridge bent before and after repair.

Figure 1.1 Corrosion damage to a bridge bent.

Figure 1.2 Bridge bent and column wrapped with FRP after repair of corrosion damage.

1.2 PREVIOUS RESEARCH

TxDOT Project 1774, "The Effect of Wrapping Chloride Contaminated Structural Concrete With Layers of Glass Fiber/Composites and Resin," was initiated in 1997 in order to address questions regarding the effectiveness of FRP composites for corrosion related repairs.

There are several ongoing field studies by other organizations that will also provide researchers information on the performance of FRP composite wrap in the repair and prevention of corrosion in reinforced concrete. There are not any significant findings to date from these field studies. Findings from previous laboratory studies will be discussed in Chapter 3. However, these studies rely on extreme exposures that are necessary for accelerated laboratory simulation of corrosion. While they may be used to predict behaviors that might happen in the field, they do not accurately reflect conditions that are found in the field.

In a study at the University of Sherbrooke, twelve circular columns were rehabilitated in 1996 after experiencing significant damage from corrosion. The columns were located on a bridge on Highway 10, near Sherbrooke, Quebec, Canada. Five of the columns were wrapped with glass FRP, four were wrapped with carbon FRP, and three were repaired with conventional repair materials. Existing chloride levels in the structures were not addressed other than to remove and repair the delaminated and spalled concrete prior to wrapping. Fiber optic sensors were installed to monitor axial deformations and circumferential expansion in each of the columns. Many of the sensors were damaged during the

wrapping process. Results from this study are still pending (Labossiere, Neale, and Martel 1997).

In a study at Purdue University, sponsored by the Indiana Department of Transportation, a field evaluation was performed in addition to a laboratory study on monitoring long-term performance of highway bridge columns retrofitted with advanced composite jackets. The concrete columns of a bridge at the junction of Interstate 69 and U.S. Highway 14 in Fort Wayne, Indiana were repaired with glass FRP in 1997 after experiencing deterioration due to corrosion and extreme temperatures. There was no mention in the report as to what other repairs were made to the columns, or if chloride contamination of the concrete was addressed. Thermocouples and strain gages were installed on three of the columns. Visual inspection was performed periodically over two years. Damage to the FRP wrap was observed due to auto collisions, and the damaged areas had increased during subsequent inspections. The increase in damage to the wrap was speculated to be caused by the glass fiber's sensitivity to moisture. No other findings from the field evaluation were reported (Teng, Sotelino, and Chen 2000).

1.3 PROJECT OBJECTIVES

The investigation for TxDOT Project 1774 consists of both a laboratory research program and a field research program. The objective is to determine the long-term effectiveness of repairs with FRP composite wrap. The laboratory study consists of reinforced concrete specimens that are subjected to an accelerated corrosive environment. Both chloride contaminated concrete and non-chloride

contaminated concrete are being evaluated. The field study consists of long-term monitoring of highway bridges that were wrapped with FRP. Corrosion rate probes were embedded into the structure prior to being wrapped.

This report will discuss the mechanisms of corrosion of steel embedded in concrete, the use of FRP composites, and corrosion monitoring techniques. The short-term findings from monitoring of both laboratory and field studies will be discussed and compared. Also, the initiation of an additional laboratory study on the use of corrosion inhibitors in conjunction with FRP composite wrap will be discussed.

Chapter 2

Corrosion of Steel in Concrete

2.1 MECHANISMS OF CORROSION

Corrosion is defined as the destructive result of chemical reactions between a metal or metal alloy and its environment. The process involves a transfer of an electronic charge in an aqueous solution (Jones 1996). In steel, corrosion results in the metallic iron being converted to the voluminous corrosion product ferric oxide (Mailvaganam 1992). Reinforcing steel is susceptible to uniform corrosion and pitting, that may be caused by several different mechanisms as will be discussed later.

New concrete typically has a pH of 12.5 or higher. The high alkalinity passivates the steel by forming a protective film of ferric oxides. This film prevents the reinforcing steel from corroding. However, certain factors can increase the likelihood of the passive film being broken down. These factors include development of the cracks in the concrete that extend to the steel, high permeability and/or high porosity of the concrete, inadequate concrete cover over the steel, or high levels of chlorides (Perkins 1997).

Once the passive film breaks down, an electrochemical reaction takes place. This reaction may be separated into two partial or half-cell electrochemical reactions. The first reaction is the oxidation reaction or anodic reaction [2.1]. The

second reaction is the reduction reaction or cathodic reaction [2.2]. The two half-cell reactions are expressed below:

$$\text{The anodic reaction: } Fe \rightarrow Fe^{2+} + 2e^{-} \qquad [2.1]$$

$$\text{The cathodic reaction: } 2e^{-} + H_2O + \tfrac{1}{2} O_2 \rightarrow 2OH^{-} \qquad [2.2]$$

This leads to the development of ferric oxide or “rust”. The formation of ferric oxide is expressed in the following equations (Broomfield 1997):

$$\text{Ferrous hydroxide: } Fe^{2+} + 2OH^{-} \rightarrow Fe(OH)_2 \qquad [2.3]$$

$$\text{Ferric hydroxide: } 4Fe(OH)_2 + O_2 + H_2O \rightarrow 4Fe(OH)_3 \qquad [2.4]$$

$$\text{Hydrated ferric oxide: } 2Fe(OH)_3 \rightarrow Fe_2O_3 \bullet H_2O \qquad [2.5]$$

The passivated area becomes the anode, and the remaining steel becomes the cathode. The moist concrete acts as an electrolyte, allowing the electrons to move from the anode to the cathode (Allen, Edwards, and Shaw 1993). The corrosion process is illustrated in Figure 2.1

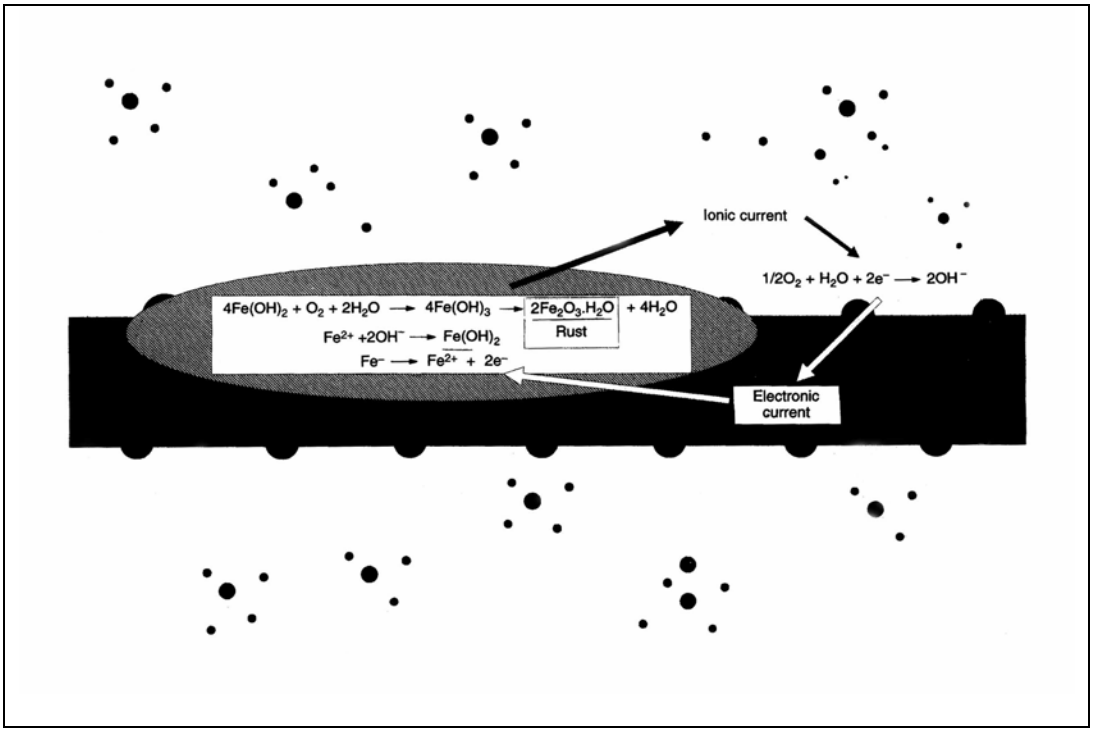

Figure 2.1 The corrosion process (Broomfield 1997).

When ferric oxide is formed it has a volume that is between two to ten times greater than the volume of the steel that it replaced. This volume increase places considerable tensile stresses on the concrete, which leads to cracking of the concrete (Broomfield 1997). After cracks have formed, the concrete may begin to separate at the level of the reinforcing along a plane parallel to the concrete surface. This separation is referred to as delamination. As the corrosion process continues, pieces of concrete may eventually break away or “spall” off. This process is illustrated in Figure 2.2: (a) is the exposure to corrosive environments,

(b) is the formation of cracks, and (c) is the formation of delamination and spalling (Scannell, Sohanghpurwala, and Islam).

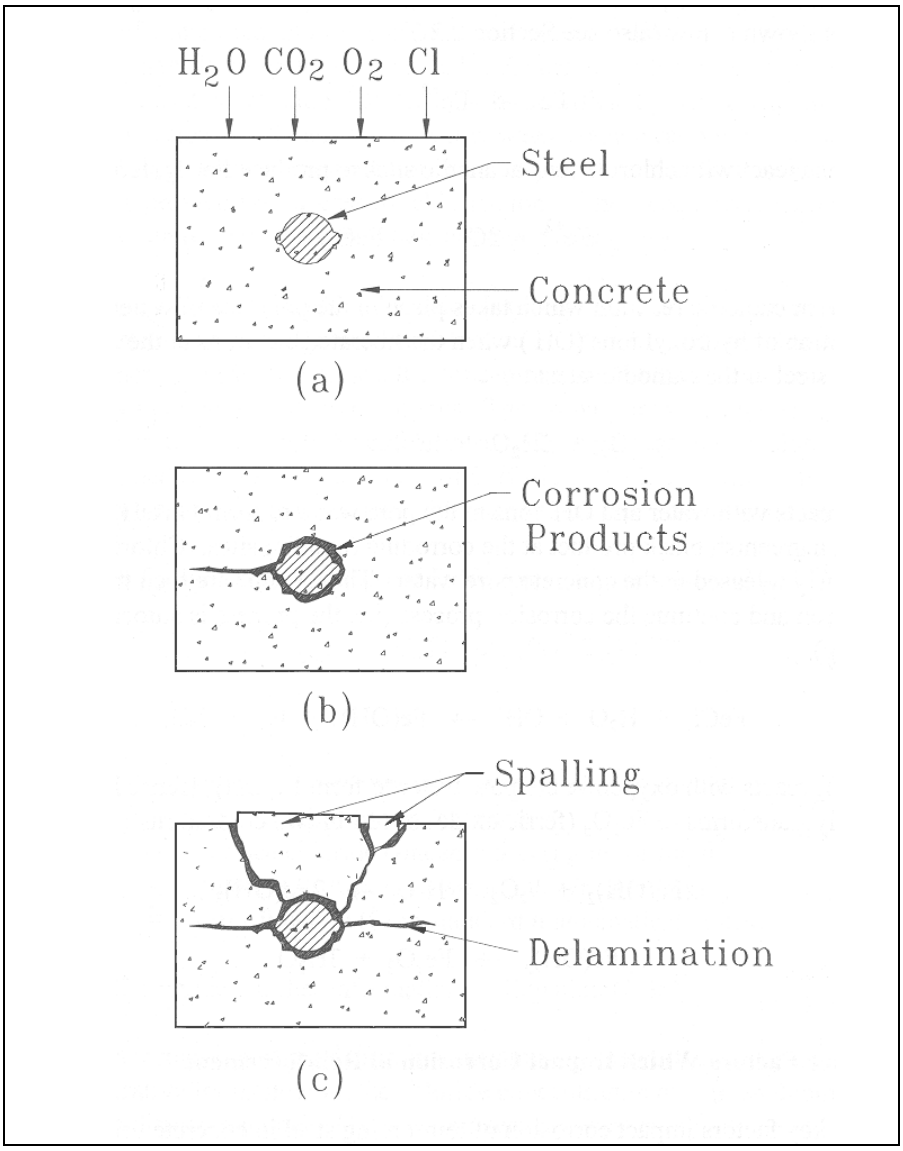

Figure 2.2 Consequences of corrosion of steel in concrete.

There are two main causes of corrosion of steel in reinforced concrete: carbonation of the concrete and chloride attack. Carbonation results when carbon dioxide in the air reacts with calcium hydroxide in the concrete, which causes a significant reduction of the pH. The carbon dioxide gas dissolves in the pore water to form an acid. The acid is then neutralized by the calcium hydroxide, which forms calcium carbonate. The pH level in the concrete drops as the calcium hydroxide reacts with the carbon dioxide (Kay 1992).

Carbonation is most common in concrete with a high water-cement ratio. It will most likely be found near the concrete surface and adjacent to cracks. The rate of penetration is proportional to the square root of time; therefore it slows down with increased depth (Allen, Edwards, and Shaw 1993). Carbonation does not significantly affect the strength of the concrete, but it will affect the steel if allowed to penetrate that far. The pH level of carbonated concrete may drop below 8; hence adjacent steel cannot maintain its passive film and will proceed to corrode (Broomfield 1997).

Chloride attack, which results in pitting, takes place when the concrete is exposed to high levels of chloride ions. Concrete may be exposed to chlorides through a number of different sources. The most common are exposure to deicing salts or seawater. Some other sources of chlorides include the use of chloride containing additives in the concrete mix or the use of chloride contaminated water or aggregates (Hansson and Sorensen 1990). The chloride ions cause very localized breakdowns in the passive film of the steel. Hence a small anode is formed and the rest of the passive film serves as the cathode. Due to the large

cathode-to-anode ratio, the rate of attack is accelerated and a pit is formed (Mailvaganam 1992).

Chloride thresholds are approximate due to variations in pH level of the concrete, amount of chlorides that are bound chemically or physically, and the amount of moisture found in the concrete. The most commonly quoted threshold is 1 lb of chloride per cubic yard of concrete, which is approximately 0.03% chlorides by weight of concrete and 0.22% chlorides by weight of cement, depending on the concrete mix. In laboratory tests (Broomfield 1997), the chloride threshold was found to be 0.4% chloride by weight of cement for cast-in-chlorides and 0.2% for diffused-in-chlorides. Table 2.1 lists the American Concrete Institute's recommended limits for chloride ion content in new structures (Gaynor 1987).

Table 2.1 Recommended limits for water-soluble chloride ion content in concrete, from ACI 201.2R-77

Category of concrete service	Maximum water-soluble chloride ion content, percent by weight of cement
Prestressed concrete	0.06
Conventionally reinforced concrete in a moist environment and exposed to chloride	0.10
Conventionally reinforced concrete in a moist environment but not exposed to chloride	0.15
Above ground construction where concrete will stay dry	No limit for corrosion

Cracking greatly increases the corrosion process. Carbonation is typically found along cracked surfaces, and penetrates into the concrete adjacent to the crack. Steel in carbonated concrete is more susceptible to chlorides since it is no longer passivated. Cracks that extend to the steel reinforcing provide a direct path for chlorides, moisture, and oxygen which creates an environment ideal for corrosion to take place (Mailvaganam 1992).

2.2 PREVENTION OF CORROSION

In order to prevent corrosion, care should be taken in the mixing and pouring of concrete. The concrete mix should have a low water-cement ratio to reduce permeability. The aggregate should be well graded in order to ensure a good adherence between the cement and aggregate. The concrete should be well consolidated when it is cast in order to prevent voids from forming. Care should also be taken to keep a minimum of 2 in. cover between the surface of the concrete and the reinforcing steel (Jones 1996).

In addition to quality workmanship, engineers have developed other solutions to reduce the possibility of corrosion. One solution is the use of corrosion inhibitors. Other solutions include modifying the reinforcing by using epoxy or zinc galvanized coatings. Another possibility is to use FRP bars instead of steel.

Corrosion inhibitors, such as calcium nitrite based additives, may be added to the concrete mix or applied to the concrete surface. They create a thin chemical layer at the steel surface, which inhibits corrosion. There is concern as to how

well corrosion inhibitors migrate to the steel when applied to the surface, and whether they are able to protect against localized pitting (Broomfield 1997). The use of corrosion inhibitors will be discussed in greater detail in Chapter 8.

Another method of preventing corrosion of the steel is to limit the ability of the reinforcement to corrode by using protective coatings or FRP instead of steel. Such reinforcement costs more than traditional black steel. The characteristics and behavior of such reinforcement continue to be investigated by researchers.

The use of fusion bonded epoxy coated reinforcing for corrosion protection has been around since the 1970s. It is the most popular of the corrosion protection strategies, and is used in forty-one states in the United States (Babaei and Hawkins 1991) Epoxy coating improves the performance of reinforcement in a corrosive environment provided that coating damage is minimized. Defects in the coating may result from improper fabrication or handling practices can cause a significant decrease in corrosion protection. Epoxy coated reinforcement has a lower ultimate bond strength than black steel that must be taken into account in the design.

Galvanized steel reinforcement has been in use since the 1930s. The zinc coating can remain passive in a lower pH level and can withstand higher chloride concentrations than black steel. Although the ultimate bond strength is often found to be nominally higher than black steel, the passivation of the zinc generates hydrogen, which may reduce the bond strength (Yeomans 1991). Galvanized steel reinforcement is not commonly used in the United States. The

Federal Highway Administration (FHWA) recommends that fusion bonded epoxy coated reinforcing be used instead of galvanized steel because galvanized steel is more susceptible to chloride attack. However, prevention of coating damage in galvanized steel is not as crucial due to the sacrificial nature of the zinc coating (Broomfield 1997).

FRP reinforcement has been in use since the 1980s. Over a dozen prestressed concrete pedestrian and roadway bridges have been built, primarily in Japan and Germany. These bridges use FRP cables instead of steel prestressing tendons. Unlike steel, FRP reinforcement does not corrode. Since it is a new material, the long-term strength, durability, and fatigue limits have not been resolved. Also, special attention must be paid to anchorage details, since FRP behaves differently than steel (Erki and Rizkalla 1993). The use of FRP reinforcing bars instead of steel reinforcing bars is an even newer development. The first roadway concrete bridge deck to have FRP reinforcing bars was built in West Virginia in 1996. FRP reinforcing bars have additional design issues because the physical properties of the reinforcement vary from manufacturer to manufacturer. Therefore design calculations must be made for the specific reinforcement used (Bassett 1998).

2.3 REPAIR METHODS

Common repair techniques for corrosion damage involve removing the cracked and spalled concrete over and around the reinforcing bars, cleaning or replacing badly corroded reinforcement, and replacing the concrete removed with

a patch. This method is tedious and often the repairs need to be made again in less than two years (Watson 2000).

When patching concrete, macrocell corrosion may form due to physical, chemical, and electrochemical dissimilarities between the existing concrete and the patch material. This is due to localized corrosion cells between the reinforcing in the existing chloride contaminated concrete and that in the new, patched area. The localized corrosion, referred to as a macrocell, accelerates the corrosion process in the repair area. This often leads to spalling of the patch (Whitmore, Abbott, and Velivasakis 1999).

To minimize the possibility of macrocell corrosion, it is necessary to remove all of the carbonated, chloride contaminated, and other unsound concrete. Then the steel reinforcing must be thoroughly cleaned or replaced to remove all corrosion products. Finally, the repair material should be similar to the existing sound concrete, to reduce electrochemical differences due to different oxygen permeabilities of the two materials (Gu, et al. 1997).

Other techniques used for repair and prevention of corrosion involve use of latex modified mortars in repair patches, injection of cracks with polymer resins, cathodic protection of reinforcement, chloride extraction, and more recently the use of fiber reinforced plastics (Perkins 1997).

Polymers have been used in cementitious mortars since the 1950s. Admixtures containing latex polymers may replace a portion of the mixing water in the repair mortar. It functions as a water reducing plasticizer, which lowers the water-cement ratio and reduces the permeability of the mortar. It also improves

the bond between the patch material and the existing concrete (Allen, Edwards, and Shaw 1993).

Crack injection is primarily used to repair deep cracks and to improve the structural strength of a concrete member that is compromised due to a crack. In crack injection, epoxy, polyurethane, or polyester resin is injected into a crack after any corrosion product, dirt, and/or grit is removed. The polymer resin bonds the concrete across the crack and seals the crack against the ingress of water and reduces the ingress of carbon dioxide (Perkins 1997).

Cathodic protection reduces the corrosion of a metal exposed to an aqueous electrolyte. An anode, either impressed current or sacrificial, is connected electrically to the steel reinforcing. This causes a cathodic polarization of the steel reinforcing, which may reduce or prevent corrosion (Jones 1996).

Chloride extraction is an electrochemical process to move chloride ions away from the steel reinforcement in chloride contaminated concrete. A voltage is applied to an external mesh that is installed on the surface of the concrete. The mesh becomes a positively charged anode and attracts the negatively charged chloride ions. Hydroxyl ions are produced at the negatively charged steel reinforcement, which causes the pH to increase and the concrete to become more alkaline (Kay 1992).

The use of fiber reinforced plastics for repair of concrete and prevention of corrosion will be discussed in the following chapters.

Chapter 3

Fiber Reinforced Plastic Composites

3.1 INTRODUCTION TO FRP COMPOSITES

Fiber reinforced plastic (FRP) composites consist of fiber reinforcement that is suspended in a polymer resin matrix. The fibers provide increased stiffness and tensile capacity, and the resin offers high compressive strength along with binding the fibers together. Three different types of fibers: glass, carbon, and aramid may be used depending on application and budget. Glass is the least expensive of the fibers. Carbon is considerably more expensive, and aramid is the most expensive. Glass, carbon, and aramid FRP composites are abbreviated GFRP, CFRP, and AFRP respectively. Table 3.1 includes properties of the different types of FRP as well as steel.

Table 3.1 Basic Properties of Glass, Carbon, and Aramid FRP Compared to Steel (Bassett 1998)

Property	Glass FRP	Carbon FRP	Aramid FRP	Steel
Tensile strength (ksi)	200-250	240-350	170-300	200-270
Modulus of elasticity (Gsi)	7-9	22-24	7-11	27-29
Elongation	0.03-0.45	0.01-0.015	0.02-0.26	0.04
Coefficient of thermal expansion (10^{-6}/°F)	5.5	0.0	-0.5	6.5
Specific gravity	2.4	1.6	1.25	7.9

Glass fibers are divided into three classes: electrical, structural, and corrosion resistance. Electrical, E-glass, is the most commonly used for civil engineering applications. It is the most economical, and also is an excellent electrical insulator. Structural, S-glass, has a higher strength and corrosion resistance than E-glass. Corrosion resistant glass, C-glass, has better resistance to acids and bases than S-glass, but is not commonly used in civil engineering. Glass fibers creep under sustained loads, and degrade under increased temperature. These factors have to be taken into consideration in the design (Tang 1997).

Carbon fibers are made from polyacrylonitrile (PAN), pitch, or rayon polymer precursors. They are available in bundles of untwisted carbon filaments, referred to as "tow". They are available in several different modulus categories ranging from standard (33 – 35 Msi) to ultrahigh (50 – 70 Msi). Carbon fibers have a very high fatigue and creep resistance and are more brittle than glass or aramid fibers. Carbon fibers are also susceptible to galvanic corrosion when placed next to a metal (Bassett 1998).

Aramid fibers are synthetic organic fibers consisting of aromatic polyamides. The commercial grade of aramid fibers is known as Kevlar®. They have excellent fatigue and creep resistance. When used in a composite, the fibers can have difficulty achieving a chemical or mechanical bond with the resin. Aramid fibers also have a low compressive strength, so they are not well suited for applications involving high compressive loads (Mallick 1997).

Structural applications of composites generally use long, continuous fibers, as opposed to short, discontinuous fibers that are for applications such as automobile bodies. The most common forms of fibers are rovings, tows, and fabrics. Rovings are similar to tows, except they are bundles of glass or aramid fibers, rather than carbon fibers. Fabrics consist of small bundles of fibers that are woven together to provide strength in both the 0° (warp) direction and the 90° (weft) direction (Bassett 1998).

There are three different methods for manufacturing commercial composite products: pultrusion, filament winding, and hand layup. Pultrusion is the process of pulling fibers through a resin bath and then through a heated die to produce a structural shape with a constant cross section. Pultrusion is used to manufacture rods, beams, and channels. Filament winding is the automated process of winding resin saturated fibers around a mandrel to produce a circular shape. This method is primarily used to manufacture tanks, pipes, and poles, but has also been used as an automated method to encapsulate bridge columns. Hand layup involves saturating sheets of fabric with resin by hand or machine, and then applying it by hand to an existing structure (Ballinger 1991). This method is primarily used to produce laminates and wraps that are used in retrofits. Figure 3.1 is an example of the hand layup method being used in the field.

Figure 3.1 FRP composite wrap being applied to the bent of a bridge.

Fibers typically occupy 30 to 70% of the matrix volume in a composite. The rest is occupied by the resin system. Resin systems consist of two classes, thermoplastics and thermosets. Thermoplastics are not used in structural applications because they do not cure permanently. The polymers in a thermoset resin irreversibly cross link, which causes the resin to remain solid at elevated temperatures after it has cured. The most common resin systems used are unsaturated polyesters, epoxies, and vinyl esters (Tang 1997).

Unsaturated polyesters account for the majority of the resins used. Their quick curing rate and affordable cost makes them ideal for pultrusion. Epoxies are typically the most expensive resins. They are generally used for applications that require high performance. The high viscosity of epoxy resins limits their use to

filament winding and hand layup manufacturing. Vinyl esters have the workability of epoxies and the fast curing rates of polyesters. They have higher physical properties than polyesters, and cost less than epoxies (Mallick 1997).

The research study discussed herein involves fiber composite wraps. There are many advantages of using FRP composites over steel. The strength-to-mass density ratio is 10 to 15 times higher than steel. Overall, FRP materials have very high strength-to-weight and stiffness-to-weight ratios. These properties allow FRP composites to be used to strengthen a structure without adding any significant additional weight to the structure. They are also corrosion resistant and have a low axial coefficient of thermal expansion. These characteristics offer advantages over steel in extreme environments (Erki and Rizkalla1993).

Prior to the development of externally applied FRPs, steel jackets were often used. Steel jackets increase the stiffness, strength, and energy absorption of the concrete, along with enhancing ductility and providing additional shear strength. (Mirmiran and Shahawy 1997). A major drawback of steel jackets is the installation. It is very difficult to fit steel jackets and requires the use of heavy clamping tools and welding, resulting in high installation costs. Also steel jackets are not practical in an aggressive environment due to their susceptibility to corrosion.

Unlike steel jackets, FRP materials are easy to handle, can conform to the shape of existing elements, and can be applied quickly. In the case of retrofitting, this means that the repair time will be shorter than other methods of repair. Shorter repair times result in savings in labor and construction related costs and

benefits the public by reducing the time a structure must be closed. When calculating the overall cost effectiveness and lifetime expectancy for the repair, the advantages of FRP composites may offset the high initial cost (Bassett 1998).

There are several disadvantages which have limited the use of FRP composites in the field of civil engineering. From the point of view of material properties, high cost, low modulus of elasticity, low failure strain, and little information about long-term durability are prime disadvantages. Another disadvantage is that FRP composites are new materials, and engineers are unfamiliar with their properties or applications. For implementation in infrastructure applications, a drawback is the lack of predictive models and design guidelines (Karbhari, Seible, and Hegemier 1996).

In a study performed by the University of Central Florida, the behavior of FRP encapsulated columns was compared to different confinement models. The results were that the use of FRP significantly increased the strength and ductility of the concrete. The researchers also found that the characteristics of confinement using FRP are different than the characteristics of confinement using steel. Steel is an elastoplastic material and FRP materials are linearly elastic, but most models for confinement do not account for this. The study showed that many confinement models overestimated the strength of FRP encapsulated concrete. Until models based on FRP are developed, the factor of safety for design of confinement in FRP encapsulated concrete should be increased. A higher factor of safety will decrease the cost effectiveness of FRP materials (Mirmiran and Shahawy1997).

3.2 SEISMIC APPLICATIONS

FRP materials have already been established as a method for strengthening concrete and preventing seismic damage. Studies in the last decade have shown that wrapping FRP fabric around the perimeter of concrete columns improves ductility, strength, and confinement of the column (Toutanji and Balaguru1998).

Concrete structures built prior to the 1970s are expected to have the worst response in the event of an earthquake. This is due to the poor detailing resulting in a lack of ductility in reinforced concrete members. Concrete with poorly detailed reinforcement has little capacity to absorb the energy imposed on the structure during seismic loading. Changes to the 1976 Uniform Building Code increased the ductility requirements and structures designed using recent codes have performed much better in recent earthquakes (Feld and Carper 1997). Figure 3.2 is an example of a nonductile failure.

Figure 3.2 Highway bridge column after the 1994 Northridge earthquake (Courtesy of EERC, University of California, Berkeley).

By wrapping columns with FRP, the high tensile strength of the composite increases the confinement of concrete in the column. The confinement provided by the FRP composite causes the concrete to fail at a larger strain thereby increasing the ductility of the column. The lateral restraint provided by the FRP increases the compressive strength of the concrete confined within the wrapping and results in higher load-carrying capacity of the column. The lateral confinement also provides additional restraint for buckling of the longitudinal reinforcing. FRP composites have the flexibility to be wrapped around either circular or rectangular columns, although sharp corners must be avoided. The low weight and negligible increase in stiffness of FRP composites offers advantages over steel jacketing of columns (Saadatmanesh, Ehsani, and Li 1994).

Wrapping technology received considerable attention in Japan. Columns were strengthened by externally bonding sheets of carbon fibers to enhance resistance to seismic loadings. After the superior performance of carbon FRP encapsulated columns in the 1995 Kobe earthquake in Japan, use of the technology increased further. As of 1996, over 1000 column strengthening projects in Japan have used FRP composite wrap (Thomas, et al 1996).

In the United States, 15 columns on the bridge ramps of Interstate 5 and Highway 2 in Los Angeles, California were wrapped with glass FRP composites in 1991 as part of a seismic retrofit program initiated by the California Department of Transportation. The columns were 6 feet in diameter and ranged from 18 to 55 feet in height. They were located 15 miles southwest of Northridge. The columns showed no damage following the 1994 Northridge earthquake. After the Northridge earthquake, the use of FRP composite wrap has steadily increased in California (Fyfe 1995).

3.3 APPLICATIONS IN CORROSION REPAIR AND PREVENTION

Since FRP composite materials are not susceptible to corrosion, engineers have been exploring the possibilities of encapsulating concrete with FRP instead of steel jackets. Currently FRP composite wraps are being investigated for strengthening of bridges that are deteriorating due to corrosion and also to prevent future corrosion activity.

Watson recommends the use of FRP composite wrap for non-seismic repairs and upgrades of highway bridges. One of the advantages he cites in using

FRP composite wrap is that it “Protects the concrete with an impervious barrier that will prevent de-icing chlorides from attacking the steel rebar,” (Watson 2000). In the second edition of *Construction Failures*, the authors Feld and Carper state that “applying an impervious coating over contaminated concrete is not a valid solution” to repairing corrosion damage due to chlorides (Feld and Carper 1997). Leeming and Peshkam, in their analysis of the advantages of FRP plates, state that one of the advantages of FRP composites over steel plates is that it is not necessary to remove all chloride contaminated concrete because the composite material would stifle any further corrosion (Leeming and Peshkam 1995). In another analysis of the advantages of FRP over steel plates by Emmons, Vaysburd, and Thomas, the authors disagree with Leeming’s and Peshkam’s conclusion that FRP encapsulation will stop the corrosion process. They state that unless the corrosion problem has been properly determined and addressed, encapsulation “will most likely accelerate the corrosion process in the existing structure,” (Emmons, Vaysburd, and Thomas 1998).

Overall, there has been very little research in the long-term effect of FRP composite wrap on the prevention of corrosion of steel reinforcing in concrete. In an investigation by Ohta, et al., they evaluated the rehabilitation of deteriorated prestressed concrete beams. The bridge was a three-span post-tensioned prestressed concrete bridge with simple tee-beams, built in 1957, and located near the Sea of Japan. In 1977, the bridge was rehabilitated after showing signs of severe cracking. The cracks were injected with an epoxy grout. The beams experiencing cracks were strengthened with a 4.5-mm steel plate bonded to the

lower flange and two layers of GFRP composite wrap were applied to the web. The rest of the beams had one layer of GFRP applied to the entire surface. The rehabilitation was evaluated in 1990 when the bridge was scheduled to be demolished. The researchers found that the FRP prevented further chlorides from penetrating the concrete. They also found that the deterioration of the bridge due to corrosion of the steel reinforcing bars and sheaths had continued due to insufficient measures that were taken to address the chloride contamination of the concrete at the time of rehabilitation (Ohta, et al. 1992).

On the Bryant Patton Bridges in Florida, it was found that fiberglass jackets applied to bridge piles in a marine environment had accelerated the corrosion process. Capillary action allowed moisture to rise from the submerged portion of the pile, but the fiberglass jacket prevented the concrete from drying out. The combination of moisture and the high levels of chlorides in the unrepaired portions of the pile resulted in severe damage due to corrosion, as seen in Figure 3.3 (Sohanghpurwala and Scannell 1994).

Figure 3.3 Concrete pile that had previously been repaired with a fiberglass jacket.

In a laboratory study at Purdue University previously mentioned in Chapter 1, researchers concluded that FRP composite materials provide excellent protection against aggressive environmental conditions. In the study, five 20 in. x 10 in. reinforced concrete beams were exposed to 56 weeks of wet/dry cycles of 5% saline water. The specimens consisted of new concrete; there was no attempt to replicate conditions that might be found in damaged concrete. One beam was unwrapped, one beam was coated with epoxy, one was wrapped with one layer of

GFRP, and two beams were wrapped with two layers of GFRP. At the end of the study, the unwrapped specimen was the only one that showed signs of corrosion activity (Teng, Sotelino, and Chen 2000).

3.4 LONG-TERM BEHAVIOR

The long-term behavior of FRP composite materials used in infrastructure is not fully understood. One concern is whether the long-term durability of the material will remain the same, or if the effects of moisture, freezing environment, and/or ultraviolet light will cause the material to degrade and compromise the expected performance of the material. Most composite materials have not been in service long enough to accurately evaluate their durability.

Brandt Goldsworthy reports that composites will have a service life considerably longer than traditional materials. He cites that the strength of composite materials used in submarines and electric utility poles was 5 to 7% higher after 30 years of service. The increase in strength is due to the continuous curing of the resin systems. Goldsworthy also states that the UV degradation of composites is self-limiting. After the surface oxidizes, it protects the rest of the material from further degradation (Bassett 1998).

In the aforementioned investigation by Ohta, et al., they found the tensile strength of the FRP was reduced by 60% after 13 years of exposure. In the load tests on the beams, the overall contribution of the rehabilitation to the load carrying capacity was significantly smaller than the degree expected.

A study performed jointly by the University of Alabama and Rutgers University, Toutanji and Balaguru, examined the durability of carbon and glass FRP materials externally applied to concrete and subjected to different environments. The environments used in the study were room temperature, wet/dry cycles using salt water, and freeze/thaw cycles.

Twenty-four concrete cylinders that were 305 mm long and 76 mm in diameter were wrapped with two layers of FRP material. The different parameters were unwrapped cylinders, cylinders wrapped with carbon FRP (CFRP), and cylinders wrapped with glass FRP (GFRP). Each parameter was subjected to different environments. One set was kept at room temperature for 75 days. Another set was exposed to 3000 wet/dry cycles using 3.5% sodium chloride solution. The cycle consisted of 4 hours wet followed by 2 hours dry. The last set was exposed to 300 freeze/thaw cycles. The cycles ranged in temperature from 4.4°C to –17.8°C within 4 hours. After the exposure cycles were completed, the specimens were loaded axially until failure.

The results indicated that for the CFRP wrapped cylinders in a room temperature environment, the compressive strength increased by 200%. GFRP wrapped cylinders in this same environment showed a 100% increase in compressive strength compared to the unwrapped specimens. In the wet/dry environment, the wrapped cylinders experienced less than 10% reduction in strength. In the freeze/thaw environment, the wrapped specimens experienced a 20 to 28% reduction in strength while the unwrapped specimen disintegrated.

Overall, the FRP encapsulated concrete showed an increase in strength over the unwrapped concrete. The ductility for the GFRP cylinders decreased considerably after exposure to harsh environments. The wrapped cylinders exhibited more catastrophic failures after exposure to the freeze/thaw cycles than the other environments (Toutanji and Balaguru 1998).

In a similar study by Soudki and Green, the behavior of columns wrapped with CFRP was investigated. The column specimens were 150 mm by 300 mm cylinders, half of which were reinforced with steel, and the other half plain concrete. The parameters were unwrapped, or wrapped with one or two layers of CFRP. The cylinders were exposed to 200 freeze/thaw cycles, and then subjected to axial compression tests. The cycles ranged from 18°C to –18°C within 24 hours. They found that one layer of CFRP increased the strength up to 57%, compared to unwrapped specimens exposed to the same environment. The second layer of CFRP increased the strength by an additional 30%. They also found that the specimens exposed to freeze/thaw cycles failed in a more catastrophic manner than the specimens that were not exposed (Soudki and Green 1997).

The Ministry of Transportation in Ontario is currently sponsoring an ongoing research project by The University of Toronto on using FRP materials to repair damaged chloride contaminated concrete columns. The purpose of the study is to test the effectiveness of repairing damaged concrete with different types of grout and then wrapping with GFRP composites (Sheikh, et al. 1999).

The study involved subjecting reinforced concrete columns, 1524 mm long and 406 mm in diameter, to accelerated corrosion. A steel tank was installed

around each column and then filled with a 2% sodium chloride solution. The steel reinforcing was connected to a voltage source in order to form a corrosion cell. The columns were subjected to accelerated corrosion for seven months, resulting in light to moderate corrosion of the longitudinal reinforcement and more severe corrosion of the spiral reinforcement. The damaged concrete was removed and then the columns were repaired using different mortars and polymer coatings. After the repairs were made, the columns were wrapped with two layers of GFRP. The repaired columns, along with an undamaged column and an unrepaired column, were each subjected to an axial load until failure. The results of the tests found that the maximum load carried by the columns repaired with FRP composite was similar in value to the maximum load carried by the column that had not experienced damage due to corrosion. The FRP encapsulated columns were more ductile than the undamaged column. The unrepaired column failed in an explosive manner rather than a ductile failure (Sheikh, et al. 1999). In this study, the FRP encapsulation compensated for the loss of steel resulting from corrosion.

Chapter 4

Corrosion Monitoring Methods

4.1 INTRODUCTION TO CORROSION MONITORING

Monitoring of corrosion activity is essential for establishing preventive maintenance and repair procedures. Monitoring may range from visual observation to taking measurements to assess presence or rate of corrosion. Visual observation is often used to assess whether corrosion is the cause of damage. More sophisticated methods may be used to determine whether corrosion is taking place before the concrete becomes damaged, and to assess the corrosion rate.

4.2 VISUAL INSPECTION

Visual inspection is used to determine the condition of a concrete structure. An inspector can assess to what extent a structure is damaged, and the cause of the damage. It is the simplest method to determine if concrete damage is the result of corrosion. A visual inspection is conducted by examining crack patterns, looking for rust stains and spalling, and checking for delamination of the concrete cover (Scannell, Sohanghpurwala, and Islam 1996).

Mapping crack patterns and determining crack size is one of the first steps in a visual inspection. Cracks resulting from the formation of rust are generally parallel to the length of the reinforcing and are a good indication that corrosion activity is present. Although any rust stains should be noted, they are not as

reliable as an indication of corrosion. Rust stain may be caused by contamination of the aggregates with iron pyrites (Allen, Edwards, and Shaw 1993). The size and location of concrete spalls should be noted, since they reflect serious distress.

A hammer survey is the most cost effective method to determine the extent of delamination. It is quicker and less expensive than methods involving radar, ultrasonic, or infrared thermography, and often more accurate (Broomfield 1997). However, new, less expensive, more mobile instruments are likely to be available in the future. A hammer survey is conducted by tapping concrete with a medium weight hammer and listening for a hollow sound. The hollow sounding areas are then marked as areas of delamination.

The presence of carbonation or chlorides can be determined by simple field tests. Carbonation is identified by spraying freshly exposed concrete with a solution of phenolphthalein in diluted ethyl alcohol. The solution changes from colorless to purple-pink as the pH rises above 10. Carbonated concrete will remain colorless and uncarbonated concrete will become stained. There are several chemical tests that can be performed on site to detect chlorides. A sample of powdered concrete is collected and dissolved in a chemical agent. Special indicator paper is then dipped into the solution to determine the percentage of chlorides by mass of concrete (Allen, Edwards, and Shaw 1993).

While visual inspection is useful to assess the overall structure, it is difficult to determine the onset of corrosion activity.

4.3 HALF-CELL POTENTIAL

The use of half–cell potential measurements for corrosion testing was developed in the 1960s and is covered by ASTM Specification C876. Although it does not determine the rate of corrosion, it does estimate the likelihood of corrosion taking place. Since the corrosion process causes an electrical potential to be generated, the half-cell provides a reference against which the corrosion potential can be measured. The corrosion potential, also known as E_{corr}, can be compared to criteria established through laboratory testing.

The half-cell consists of a reference electrode of a metal contained in an electrolyte solution saturated with one of its own salts. The reference electrode is in a rigid plastic or glass tube with a porous plug. The most commonly used reference electrodes are copper/copper sulfate ($Cu/CuSO_4$) and saturated calomel (SCE) (CRC 1991). Since the ASTM Specification C876 is for a $Cu/CuSO_4$ reference electrode, if a SCE reference electrode is used instead, the potentials should be converted to $Cu/CuSO_4$ equivalent potentials (ASTM 1989).

The test is conducted by connecting the reference electrode to the negative terminal of a high impedance voltmeter. A direct electrical connection is made from the steel reinforcing to the positive terminal of the voltmeter. Reinforcement is usually electrically continuous in a structure so that only one electrical connection is needed. A wetted sponge at the end of the reference electrode forms a liquid bridge between the cell and the concrete. A schematic for the half-cell potential test is shown in Figure 4.1.

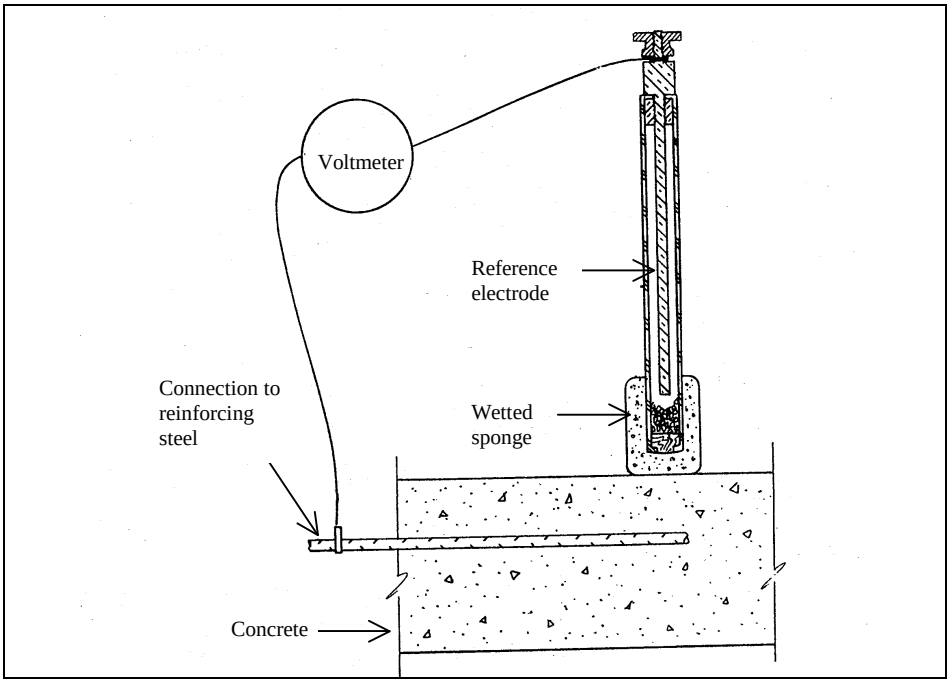

Figure 4.1 Copper-Copper Sulfate Half-cell Circuitry (ASTM 1989).

Half-cell potential readings are typically taken in a grid pattern, generally at 4 ft. spacing on a bridge deck. The reference electrode is placed against the concrete until the reading on the voltmeter stabilizes. The results then can be plotted in an equipotential contour diagram, similar to the example in Figure 4.2.

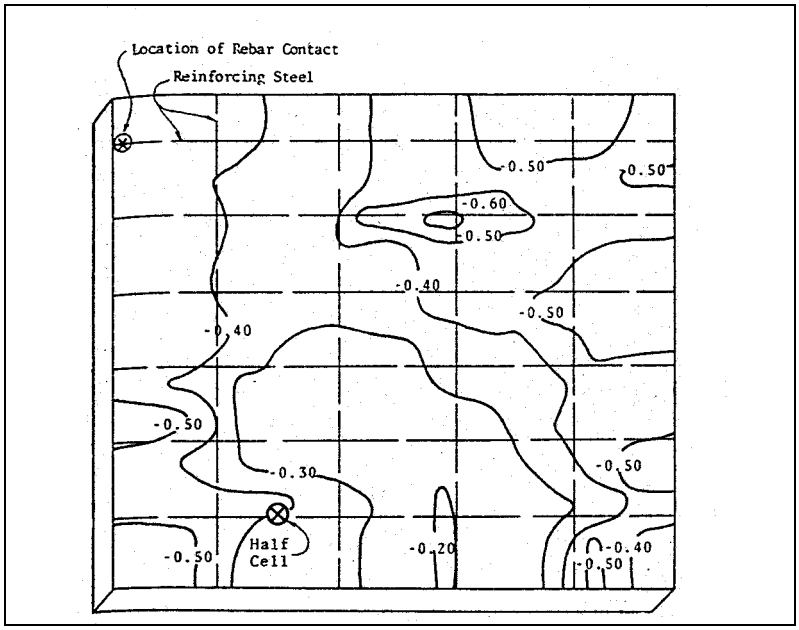

Figure 4.2 Equipotential contour diagram (ASTM 1989).

The diagram illustrates areas that have a high probability for corrosion to be occurring, and areas that are likely to be passive. Interpretation of E_{corr} readings with respect to a copper/copper sulfate reference electrode is summarized in Table 4.1.

Table 4.1 ASTM interpretation of half-cell readings

E_{corr} (mV)	Corrosion Probability	Corrosion Risk
>0	N/A	Invalid data
0 to -200	10% probability of corrosion	Low risk
-200 to -350	Activity is uncertain	Intermediate risk
< -350	90% probability of corrosion	High risk
< -500	> 90% probability of corrosion	Severe corrosion

There are limitations to the effectiveness of half-cell potential. The method may not be used on coated reinforcing or concrete with coated surfaces. Another drawback is that the potentials are measured at the concrete surface and not at the reinforcing. Because of this, the potential measurements are very sensitive to moisture content, thickness of the concrete cover, resistivity of the concrete, carbonation, and chloride ingress (Ohtsu, Yamamoto, and Matsuyama 1997).

4.4 LINEAR POLARIZATION

Linear polarization, also known as polarization resistance, is a method well suited for measuring the corrosion rate of metals embedded in concrete. There are several portable corrosion rate measurement devices available for nondestructive testing of concrete structures. Four of these devices that operate on linear polarization techniques: the PR-Monitor, the 3LP Device, the Gecor

Device, and the NSC Device, were evaluated by the FHWA's Strategic Highway Research Program.

Linear polarization was derived from experimental data that showed that the slope of the linear curve of applied cathodic and anodic current vs. potential is inversely proportional to the corrosion rate. Figure 4.3 illustrates how linear polarization is derived graphically (Jones 1996).

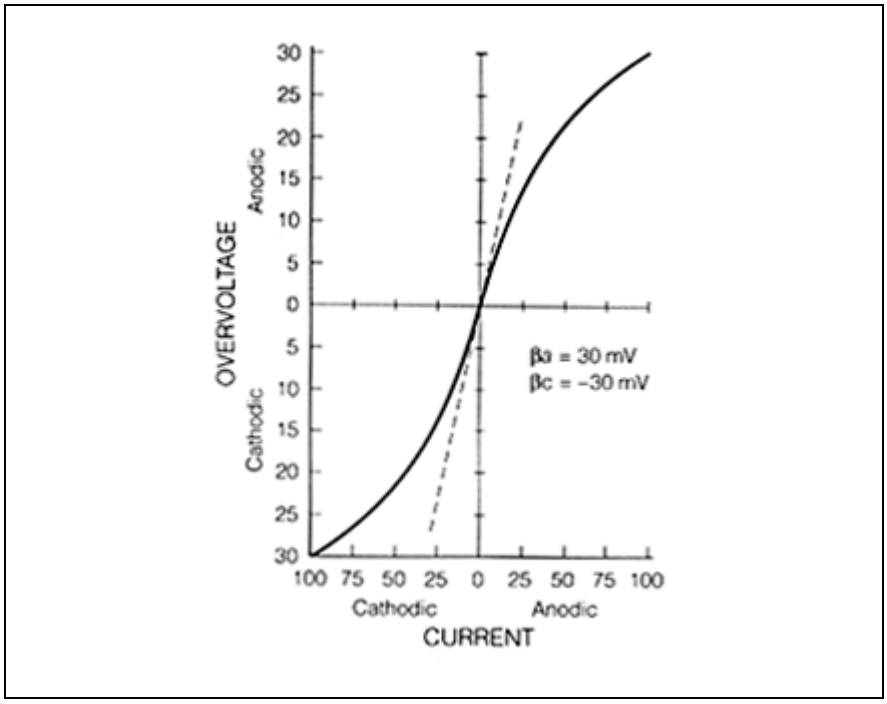

Figure 4.3 Hypothetical anodic and cathodic polarization curve.

This method was developed as a nondestructive method for corrosion monitoring. Before linear polarization, most corrosion rate data were collected by measuring the weight loss of metal coupons exposed to an aggressive

environment. Not only is linear polarization considerably faster, it is better suited for corrosion rate testing outside of the laboratory (Jones 1996).

In concrete, linear polarization is performed by polarizing the reinforcing steel with an electric current, and then measuring its effect on the half-cell potential. A reference electrode is incorporated with a variable low voltage DC power supply. The system is connected to a microprocessor that runs the calculations and stores the data (Broomfield 1997).

Overvoltages, ε_c for the cathodic region and ε_a for the anodic region, are related to the corrosion potential by equation [4.1]. The extent of the linearity depends on the cathodic, β_c, and anodic, βa, Tafel constants selected. The relationship of the corrosion rate, i_{corr}, in terms of current density to the cathodic and anodic applied current densities, i_c and i_a, the Tafel constants, and the overvoltages is expressed in equation [4.2] (Jones 1996).

$$\varepsilon_{c/a} = E_{c/a} - E_{corr} \qquad [4.1]$$

$$\varepsilon_{c/a} = \beta_{c/a} \log i_{c/a}/i_{corr} \qquad [4.2]$$

The polarization resistance, R_p, is equal to the ratio of the change in potential over the applied current. The corrosion rate is equal to the proportionality constant *B* divided by the polarization resistance [4.3] (Jones 1996). The proportionality constant *B* is a function of the Tafel constants [4.4], and for concrete is typically from 26 to 52 mV depending on the passive or active condition of the steel. A corrosion rate in μm/yr is calculated from the

polarization resistance in equation [4.5], where *A* is the surface area of the steel measured. In many other fields, the electrical resistance of the medium that the metal is in can be neglected when calculating the polarization resistance. The electrical resistance of concrete is significant enough that measured R_p will be higher than the actual $R_{p.}$ Therefore, the solution resistance of the concrete needs to be taken into consideration when calculating R_p (Broomfield 1997).

$$i_{corr} = B / R_P \qquad [4.3]$$

$$B = \beta_a\beta_c / [2.3 (\beta_a + \beta_c)] \qquad [4.4]$$

$$X = (11 \times 10^6 B) / (R_p A) \qquad [4.5]$$

The major advantage of linear polarization is that it is the only method that determines a corrosion rate. A corrosion rate gives the engineer an indication of the extent of corrosion taking place. One disadvantage of linear polarization is that the rate is an instantaneous rate, which reflects the conditions at the time the test was run. Another disadvantage is that the test is sensitive to factors such as humidity and temperature. Corrosion rate measurements will increase in warm conditions. Since the resistivity of concrete decreases when the concrete is wet, corrosion rate measurements increase in wet conditions (Scannell, Sohanghpurwala, and Islam 1996).

Another disadvantage is that assumptions may have to be made about the area of steel being measured. It is difficult to calculate the exact area being polarized since the impressed current “fans out” from the electrode. A guard ring

system confines the area of the impressed current, allowing for a more accurate estimation of the area of steel being measured. Figures 4.4 and 4.5 show schematics of linear polarization devices (Broomfield 1997).

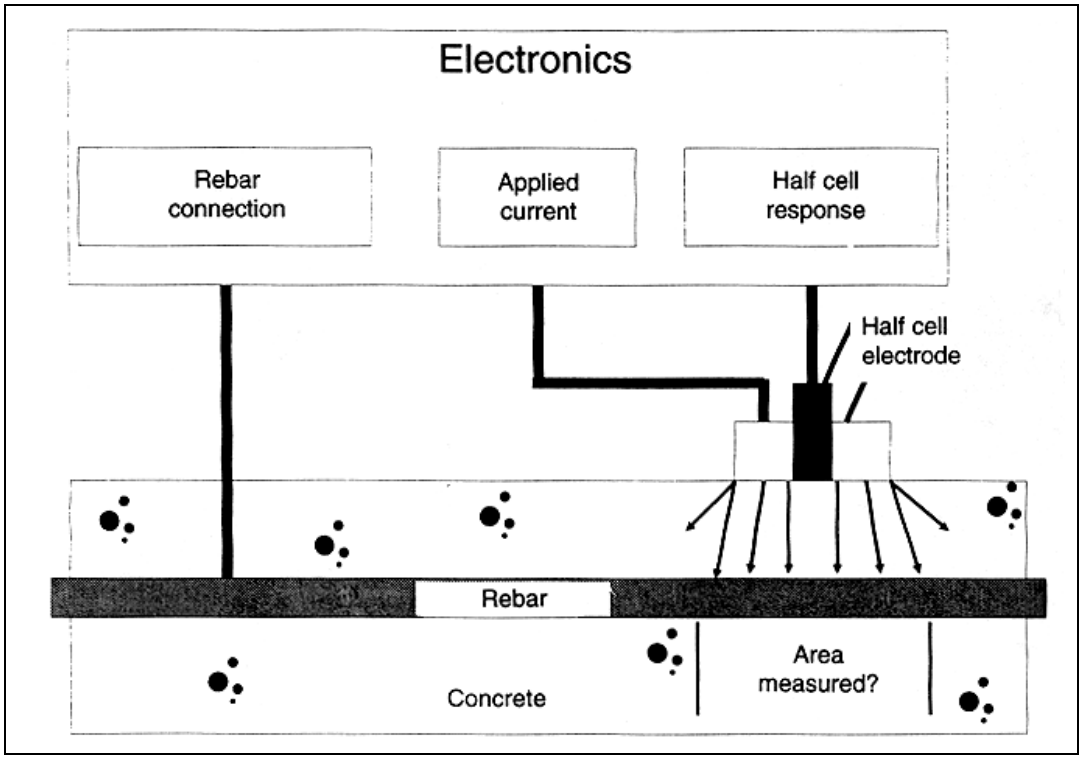

Figure 4.4 Schematic of linear polarization device (Broomfield 1997).

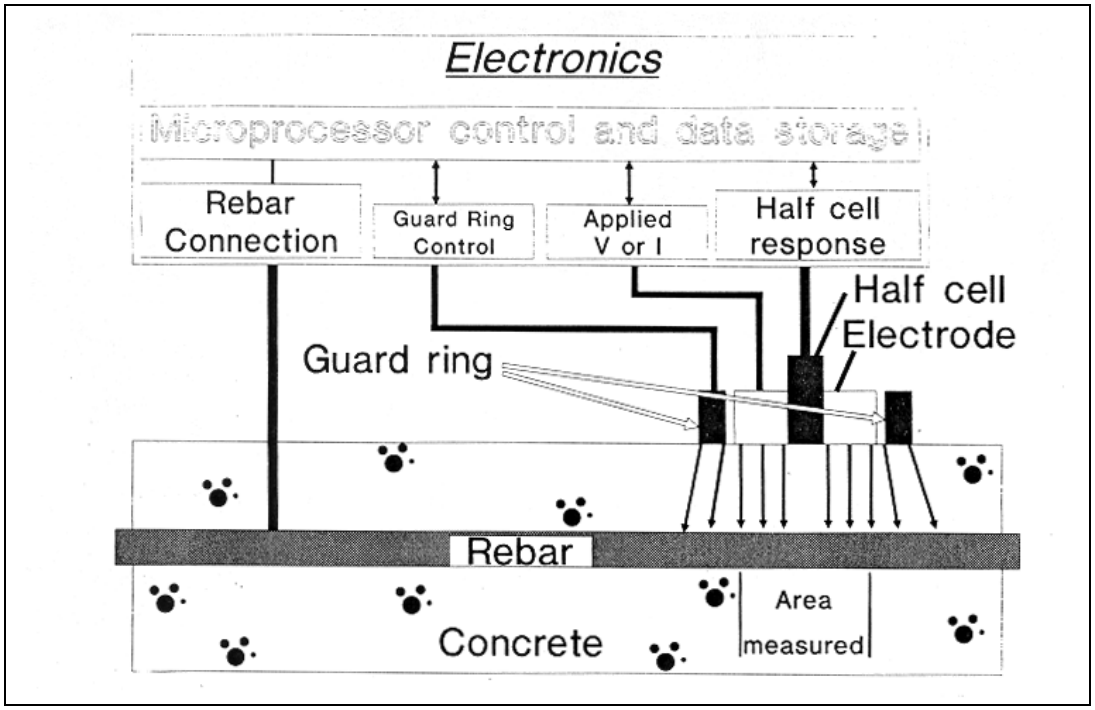

Figure 4.5 Schematic of linear polarization device with a senor controlled guard ring (Broomfield 1997).

The set up for linear polarization is similar to that of half-cell potential in that a connection to the reinforcing must be made. The reference electrode is placed over a portion of concrete where the size of reinforcing is known. Corrosion rate measurements generally take longer to run than half-cell potential measurements. Interpretations of values for i_{corr} are summarized in Tables 4.2 and 4.3 (Broomfield 1997).

Table 4.2 Interpretation of Linear Polarization Results

i_{corr} ($\mu A/cm^2$)	Corrosion Level
< 0.1	Passive condition
0.1 to 0.5	Low to moderate corrosion
0.5 to 1.0	Moderate to high corrosion
> 1.0	High corrosion

Table 4.3 Correlation of corrosion rates to rust growth and section loss

i_{corr} ($\mu A/cm^2$)	Rust growth ($\mu m/yr$)	Section loss ($\mu m/yr$)
0.1	3	1.1
0.5	17.3	5.7
1.0	34	11.5
10	345	115

4.5 LONG-TERM MONITORING

For long-term corrosion monitoring, embedded monitoring probes may be desired. Typically they are used in cathodic protection monitoring systems, but they are ideal for any system where the concrete or reinforcing is not readily accessible, or a large number of readings are needed over a period of time.

One method of embedded probes is to embed a half-cell reference electrode as close to the reinforcing as possible. Half-cell potential measurements are then taken from lead wires that extend out of the concrete. An electrical connection to the steel still needs to be made in order to complete the half-cell circuit. By embedding the reference electrode, the potential measurements are more accurate since they are taken at the steel rather than at the concrete surface (Ohtsu, Yamamoto, and Matsuyama 1997).

Another type of monitoring probe allows for linear polarization measurements to be made, so the corrosion rate can be determined. This type of probe consists of a stainless steel auxiliary electrode, a reference electrode, and a short length of reinforcement steel. This probe is usually encased in a concrete prism. An electrical connection is made from the probe to the steel reinforcing in the vicinity of the probe. By using a probe, it eliminates any assumptions about the area of steel being measured since the length of reinforcing is already known (John, et al. 1995). These probes are usually not affected by temperature change, but moisture content and changes in chloride levels in the concrete will affect the corrosion rate measurements (Perkins 1997).

Chapter 5

Project Organization

5.1 TXDOT PROJECT 1774

Project 1774 is a long-term monitoring project to evaluate the effectiveness of FRP composite wrap for the prevention of corrosion in chloride contaminated concrete. The objective is to compare the findings from laboratory tests to findings from field installations.

5.2 LABORATORY PHASE

The laboratory phase was designed to replicate different parameters that represent worst-case scenarios found in the field, and to observe their effect on corrosion. The specimens are exposed to an accelerated corrosion environment, consisting of alternating wet and dry cycles of 3.5% saline water. The following parameters were chosen:

- Specimen geometry
- Chloride content in the concrete mix
- Cracking condition
- Type of repair material
- Application of a corrosion inhibitor
- Type of wrapping system

- Length of wrapped surface
- Condition of the surface (wet or dry) when the wrap was applied

5.2.1 SPECIMEN GEOMETRY

The specimens consisted of two shapes, cylinders and rectangular blocks. The cylinders were modeled to represent bridge columns, and the rectangular blocks were modeled to represent portions of bridge bents located at points where bridge deck runoff exposes the bent to water containing deicing salts. The cylinders were 36 in. long and 10 in. in diameter. The rectangular blocks were 36 in. long with a 10 in. by 10 in. cross section. The reinforcement consisted of four #6 grade 60 bars. The transverse reinforcing for the cylinders consisted of nine ¼-in. plain steel wire circular hoops spaced at 4 in. The rectangular blocks have ¼-in. plain steel wire that form three U-shaped stirrups spaced at 10 in. The steel cage was tied together with metal ties in order to assure electrical continuity. The reinforcement extended 3 in. past the concrete to allow easy access for making electrical connections to the steel. The specimens had 1 in. of concrete cover that was maintained by using plastic chairs. Figures 5.1 to 5.4 illustrate the specimen geometry.

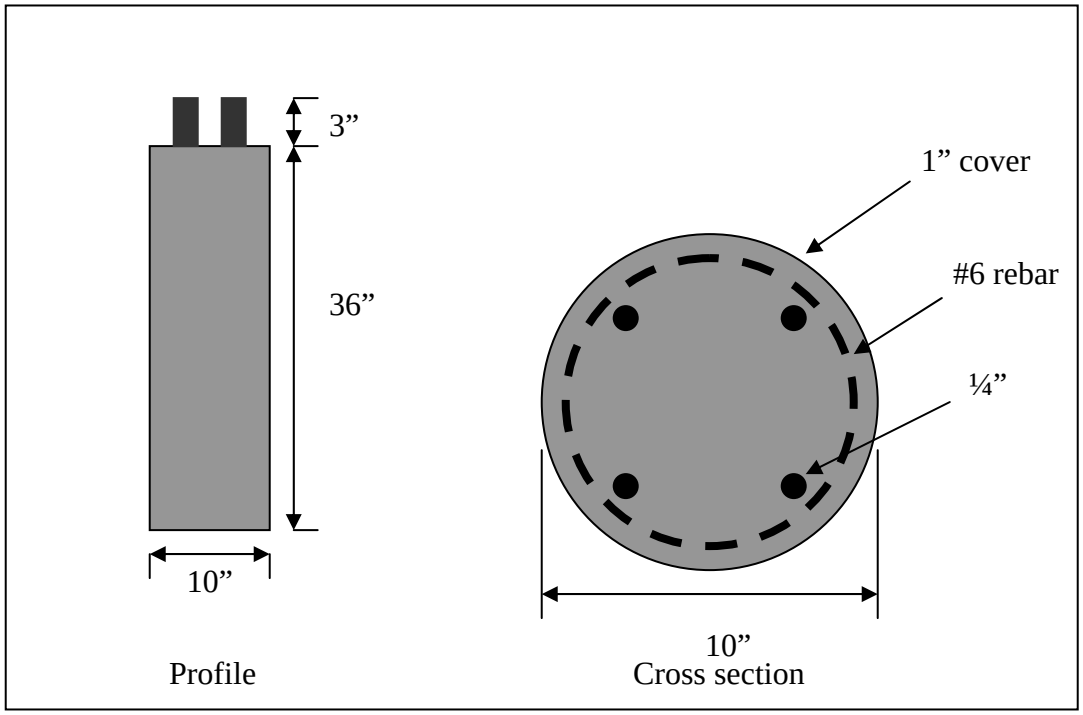

Figure 5.1 Geometry of cylinder specimens.

Figure 5.2 Typical cylinder specimen.

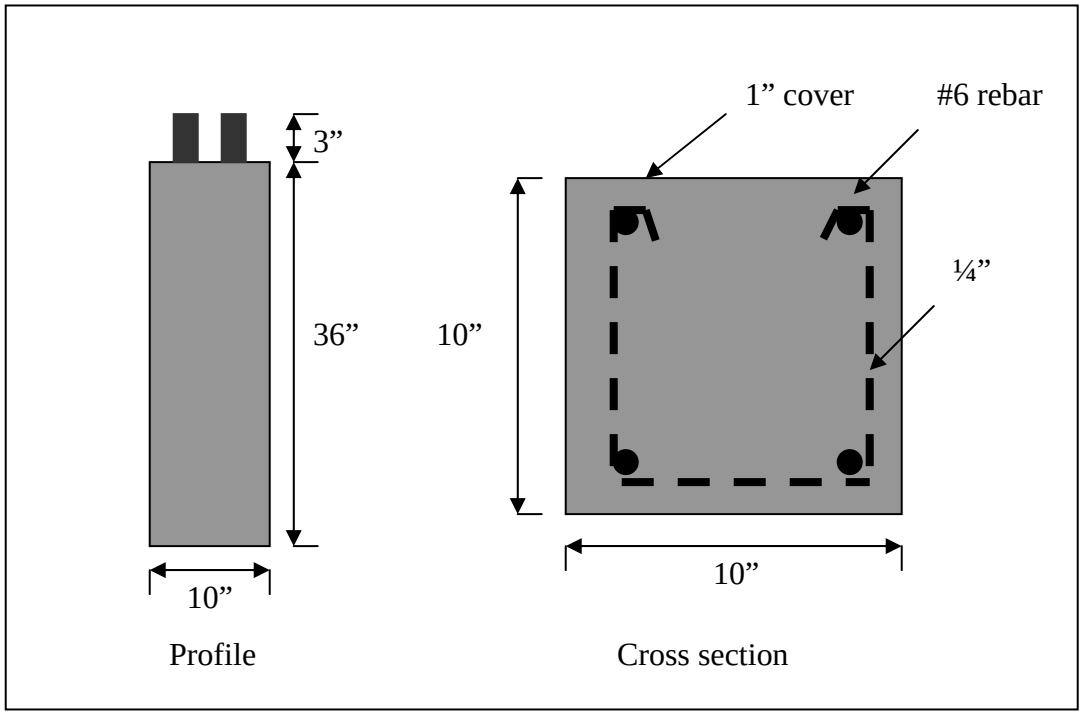

Figure 5.3 Geometry of rectangular block specimens.

Figure 5.4 Typical rectangular block specimen.

5.2.2 CONCRETE

A low quality, highly permeable mix was used for the specimens. In order to insure permeability, the selected water-cement ratio was 0.7. An air entrainment additive was also added to the mix. In order to simulate chloride contaminated concrete, half of the specimens had cast-in-chlorides added to the mix. Food grade salt was added to produce a 3.5% saline solution. The concrete mix mixture properties are shown in Table 5.1.

Table 5.1 Concrete mix design

Item	Amount (lbs./yd^3)
Cement	393
Coarse Ag. (3/4-in. crushed limestone)	1970
Fine Ag. (Colorado River sand)	1620
Water	275
Total	4258

The percentage of chlorides found in sodium chloride, NaCl, is calculated in the following equations. (Gaynor 1987).

Molecular weight: $NaCl = 23 + 35.5 = 58.5$ [5.1]

Cl^- as a percentage of molecular weight: $35.5/58.5 = 60.7\%$ [5.2]

For this mix design, approximately 9.6 lbs. of salt per cubic yd. of concrete were added to make the chloride contaminated concrete mix (FSEL

1999). Equations 5.3 and 5.4 calculate the percentage of chlorides per weight of concrete, and percentage of chlorides per weight of cement respectively.

$$[(9.6 lb/yd^3)(0.607) / (4258 lb/yd^3 + 9.6 lb/yd^3)] \times 100\% = 0.137\% \quad [5.3]$$

$$[(9.6 lb/yd^3)(0.607) / 393 lb/yd^3] \times 100\% = 1.48\% \quad [5.4]$$

The percentage of chlorides in the chloride contaminated mix well exceeds the threshold of 0.4% chlorides by weight of cement for cast-in-chlorides. A survey by the Building Research Establishment has found that the possibility of corrosion is highly probable if the percentage of chlorides by weight of cement exceeds 1% (Allen, et al. 1993).

5.2.3 SIMULATION OF EXISTING FIELD CONDITIONS

In order to simulate existing cracks within a structure, some of the specimens were subjected to flexural cracking prior to being wrapped. The cracks were created by applying a point load in the center of the specimen using a Universal Testing Machine. The specimens were loaded until crack widths of 0.01 to 0.013 in. were observed, which is the maximum crack width allowed for exterior exposure by ACI 10.6.4 (ACI 1995). The cylinders were loaded on two sides; the rectangular blocks were only loaded on the topside. Figure 5.5 shows a typical cracked specimen.

Figure 5.5 Cracked cylinder specimen.

Two types of repair material, an epoxy grout and a latex-modified concrete, were chosen. Both repair materials are approved for use on TxDOT projects. The materials were manufactured by Sika™ Corporation. The epoxy grout used was Sikadur 42, Grout Pak, and the latex-modified concrete was SikaTop 122 Plus.

Portions of concrete on the specimens were removed to the level of the reinforcing with a chipping hammer. All loose dust was removed with a pressure air hose, and the reinforcing was scrubbed with a wire brush to remove any dirt and/or corrosion product. The repair material was applied according to the manufacturer's specifications. Formwork was used for large patches. Small repair areas were dry packed (Fuentes 1999).

A surface applied corrosion inhibitor was applied to some of the specimens prior to the application of the wrap. Sika™ Ferrogard 903, manufactured by Sika™ Corporation was applied according to the manufacturer's specification. It was applied with paint rollers to the concrete surface after it was cleaned with a pressure air hose (Fuentes 1999). Ferrogard 903 is a modified amino alcohol inhibitor that migrates to the steel reinforcing in order to form a protective coating on the steel surface (Sika 1996).

5.2.4 WRAPPING MATERIALS AND PROCEDURES

The specimens were either wrapped with Fibrwrap®, or a similar generic brand, or were not wrapped. The wrap was applied according to the manufacturer's instructions.

The fabric was saturated with resin by paint rollers. Three layers of FRP wrap were applied by the hand layup method with a 6 in. overlap. After each layer was applied, air bubbles were pushed out by hand before the next layer was applied. After the composite had achieved a tacky feel to the surface, the specimens were examined for any voids. A thickened epoxy mix was injected into the voids. The composite was painted with Sherwin Williams® Hi Bald Aliphatic Polyurethane within 72 hours of application in order to provide UV protection (Fuentes 1999).

Fibrwrap refers to the TYFO S Fibrwrap®system manufactured by Hexcel Fyfe Co. This system consists of TYFO™ SEH 51 saturated with TYFO™ S epoxy matrix. The TYFO S Fibrwrap® System is the most common GFRP

composite wrapping system used in civil infrastructure. This system was used in the studies in Canada, California, and Indiana that were discussed in Chapters 1 and 3.

TYFO S Fibrwrap® System has been tested extensively to demonstrate its ability to increase strength and ductility of concrete without increasing the stiffness. The system is also designed to expand when corrosion causes expansion of concrete. The system has undergone 1000 hour testing for ozone, 140°F temperatures, -40°F temperatures, water, salt water, alkaline soil, and ultraviolet light. The testing showed no significant loss in strength and no failure modes due to environmental effects (Fyfe 1995).

TYFO™ SEH 51 is a woven fabric of E-glass rovings, with a weight of 27.2 oz/yd^2. In the 90°, or weft, direction of the fabric, Kevlar® fibers are woven in with the glass fibers to increase strength in the vertical direction. TYFO™ S epoxy system is a two-part ambient temperature epoxy resin matrix. (Delta 2000).

The generic system was developed by the IMPACT Laboratory of the Texas Materials Institute. The generic system consisted of Knytex Reinforcement Fabric A 260-50 by Owens Corning, which is a unidirectional, woven E-glass fabric. It has a weight of 25.7 oz/yd. Two resin systems were used. One was an epoxy system similar to the Fibrwrap system, and the other was a vinyl ester resin. The epoxy system was manufactured by Shell Chemical Company and consisted of EPON™ Resin 862 with a polyamine curing agent, EPI-CURE™ 3234. The vinyl ester system was DERAKANE™ 411-C50 manufactured by the

Dow Chemical Company (Fuentes 1999). The generic system's ability to withstand environmental effects is currently being tested.

Some specimens were not wrapped in order to serve as controls. This was to allow for evaluation of single parameters, and to compare the overall performance of the composite material to specimens that were not repaired with the FRP wrap.

Since the length of the wrap may vary on bridge columns, two different lengths of FRP wrap were used on the cylinder specimens. The first length was 24 in., which simulated wrapping to the waterline. The wrap was placed on the upper two feet of the specimens, leaving the bottom one foot of the specimen unwrapped. Therefore the portion of the column that would be subjected the most to the wet/dry cycles was not wrapped. The second length was 36 in., which simulated wrapping the entire length of the column. In this case, a larger portion of the composite would be subjected to the wet/dry cycles. The bottoms of the cylinder specimens were not wrapped since it is not feasible to wrap the bottom of a column.

For the rectangular blocks, the downstream end was wrapped along with all four sides of the block. The upstream end, which has the reinforcing extending out, was not wrapped. The wrap length for the rectangular blocks varies from 24 to 36 in.

The last parameter was the surface condition at the time of the application of the wrap. Since columns in a marine environment may require wrapping below the waterline, the composite material has to adhere to the wet surface. Four

cylinder specimens were placed in buckets containing 3.5% saline water for 24 hours prior to encapsulation. The remaining twenty-five specimens had air-dried surfaces at the time of encapsulation (Fuentes 1999).

Access holes, 1 ¼-in. in diameter, were cored into the FRP composite in order to provide access to the concrete surface for the reference electrode. The holes are located at a distance of 16 in. from the bottom of the cylinder specimens, which is 4 in. above the waterline. On the rectangular blocks, the access hole is located on the lower left corner of the downstream end. The access holes are sealed during exposure in order to prevent moisture from infiltrating. Grease was applied to the exposed steel reinforcing in order to protect it from corrosion. Figures 5.6 and 5.7 are typical wrapped specimens. Each specimen is described in detail in Appendix A.

Figure 5.6 Wrapped cylinder specimen.

Figure 5.7 Wrapped rectangular block specimen.

5.3 FIELD PHASE

Field monitoring was conducted on the substructures of highway overpass bridges in Lubbock and Slayton, TX. Table 5.2 lists the location of the structures in the study. The structures were evaluated before and after they were repaired and wrapped with FRP composites. The system used was TYFO S Fibrwrap®, which is the same system that is being evaluated in the laboratory phase. The FRP composite wrap was applied by Delta Structural Technology, Inc. The work was completed in fall 1999.

Table 5.2 Location of structures repaired with FRP composite

Structure #	City	Interchange
#1 - #2	Lubbock	State Loop 289 over Municipal Drive
#3 - #8	Lubbock	US 62/82 & State Loop 289
#9 - #10	Slaton	US 84 over FM 41
#11 - #12	Slaton	US 84 over FM 400

The bridges were experiencing severe damage due to corrosion. The damage consisted of cracking, spalling, and delamination of the concrete cover on the downstream portions of the bents, and also on some of the columns. Figures 5.8 to 5.10 show typical corrosion damage found on the substructure. The damage correlated with the drainage paths for water on the bridge deck. The bents had a slight slope so that water ran to the lower end as shown in Figs. 5.8 and 5.9.

Figure 5.8 Damage to an endcap of Structure #5.

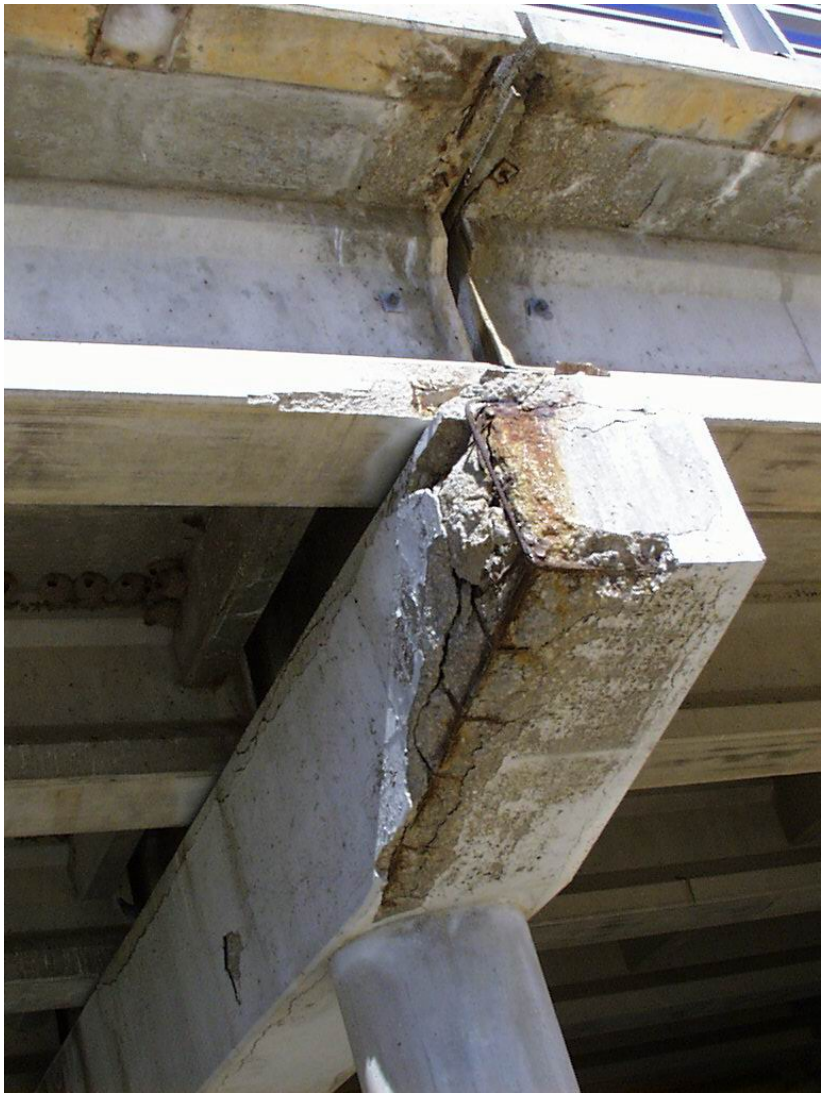

Figure 5.9 Delamination on an endcap of Structure #8.

Figure 5.10 Cracking on column of Structure #12.

The project specified the removal of all unsound concrete, and cleaning and/or replacement of reinforcement in order to remove all of the corrosion products. The concrete was then patched with Shotpatch® 21F by Master Builders Technologies®, Inc.

After the damaged areas were repaired, the concrete was sprayed with Sherwin Williams® Macropoxy 920 Pre-Prime (Verhulst 1999). Macropoxy 920 Pre-Prime is a rust penetrating epoxy pre-primer designed for use over marginally prepared surfaces. It may be used as a high performance primer/sealer (Sherwin Williams 2001).

After the primer was applied, the concrete surface was ground to provide a smooth finish. Then it was coated with a layer of epoxy thickened with Cab-O-Sil TS 720 manufactured by Cabot Corporation.

The glass fabric was saturated with resin by a saturation machine and then applied to the substructure by the hand layup method. Three layers of FRP wrap were applied in a manner similar to that described in the laboratory phase. Figure 5.11 shows Structure #1 after repairs have been made, and before the FRP composite has been installed. Figure 5.12 shows the parallel structure, Structure #2 after encapsulation.

Figure 5.11 Structure #1 prepared for encapsulation.

Figure 5.12 Structure #2 encapsulated with FRP wrap.

In order to monitor the performance of the FRP composite in a corrosive environment, a non-destructive method was required. Embedded probes were installed for long-term monitoring, and because the concrete surface and steel reinforcing were not readily accessible after the structure was wrapped. The probes that were used were manufactured by Concorr, Inc. The probe consists of a reference electrode, and a counter electrode encased in a mortar block. The overall dimensions are 2 3/8-in. x 2 3/8-in. x 5 in. Figure 5.13 and 5.14 are a schematic and cross section of the probe respectively.

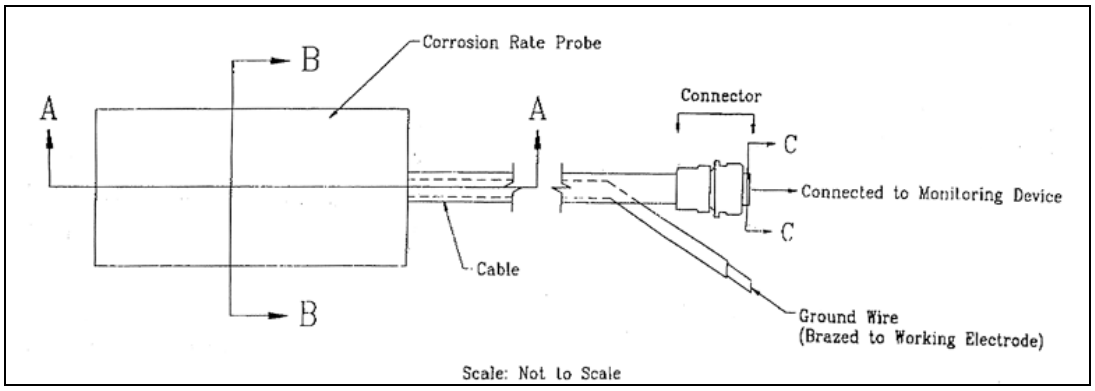

Figure 5.13 Concorr corrosion rate probe and connection cable (Concorr 1998).

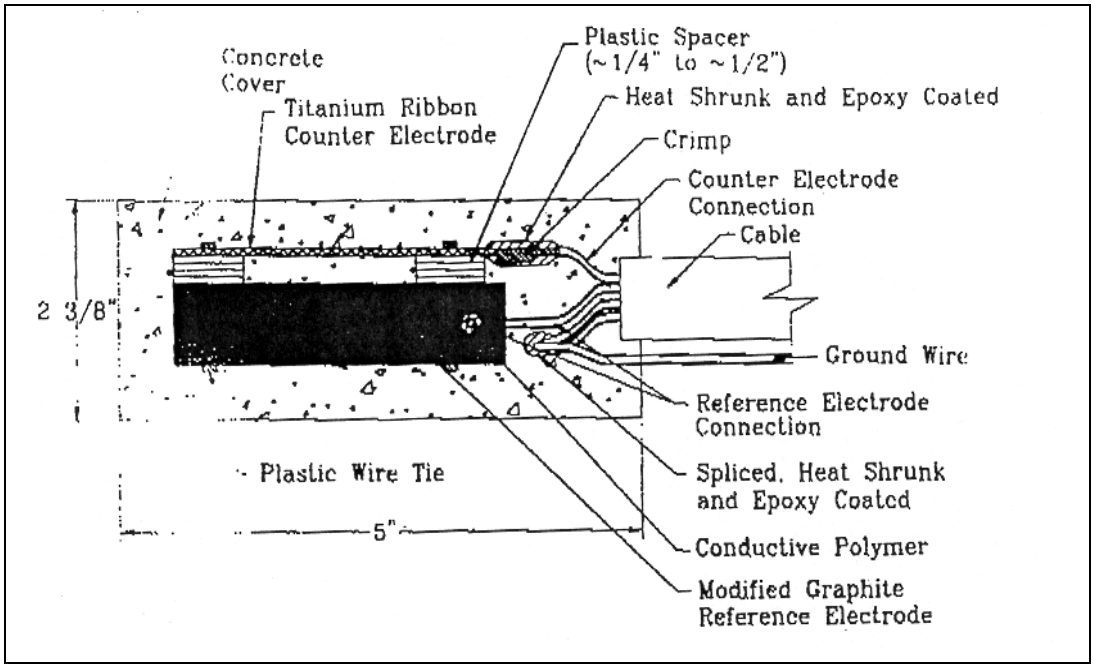

Figure 5.14 Lengthwise section of the corrosion rate probe (Concorr 1998).

The reference electrode is modified graphite, and the counter electrode is a titanium ribbon that is mounted on the reference electrode. The electrodes are connected to a cable that leads out of the probe. At the end of the cable is a six-pin connector that connects to the PR-Monitor. The PR-Monitor, manufactured by Cortest Instrument Systems, Inc., is a corrosion rate measurement device designed for testing of reinforced concrete. It uses the polarization resistance technique to directly determine the corrosion rate of the steel reinforcing.

The embedded probes were installed after the damaged concrete was removed and before the repair material was placed. The probes were placed next to the longitudinal reinforcing. An electrical connection was made from the probe

to the reinforcing. Nine probes were embedded in three separate structures. The probes were installed near the downstream endcaps of the bent. Figure 5.15 shows a probe after it has been installed.

Figure 5.15 Installed probe on Structure #7.

The area of steel being polarized is the surface area of the reinforcing in the direct vicinity of the probe. In this case, it is the circumference of each reinforcing bar multiplied by the length of the probe. Table 5.3 indicates locations of each embedded probe. The designation “left” or “right” is from the perspective of looking at the structure from the downstream end of the bent.

Table 5.3 Probe installation locations

ID#	Structure	Bent	Beam Face	Distance from End (ft.)	Steel Area (in^2)
7.1	#7	7	Left	7.5	44.30
7.2	#7	7	Right	4	44.30
8.1	#8	4	Left	4	44.30
8.2	#8	4	Right	4	44.30
8.3	#8	5	Left	4	44.30
8.4	#8	5	Right	4	22.15
12.1	#12	1	Left	4	44.30
12.2	#12	1	Right	4	44.30
12.3	#12	3	Left	4	44.30

Chapter 6

Laboratory Data

6.1 SCOPE OF PROJECT

The laboratory specimens described in Chapter 5 were monitored from spring 1999 to spring 2001. During that time, the specimens were exposed to wet/dry cycles, in order to accelerate the corrosion process. The wet/dry cycle consisted of a soaking (wet) period of one week in a 3.5% saline solution followed by a two-week drying period. During the wet period, the lower one foot of the cylinders (columns) was immersed in salt water. During the drying cycle, the water was removed to a level below the bottom of the cylinder specimens. This was to create a splash zone effect for the cylinder specimens. The rectangular block specimens (bents) had saline water irrigated over the top surface. Mats were placed over the tops to provide even distribution of the water. The blocks were placed at a slight incline, allowing for the water runoff to flow towards the downstream end. Figure 6.1 is a photograph of the cylinder specimens in the exposure tank.

Figure 6.1 Cylinder specimens in the exposure tank.

Due to the planned long-term exposure studies, this report will concentrate on fourteen specimens that were monitored, removed from exposure testing, and evaluated. In May 2000, eight specimens, which will be referred to as Group A, were removed after being exposed to fifteen cycles. In February 2001, six more specimens, which will be referred to as Group B, were removed after being exposed to twenty-six cycles. The properties of the specimens are listed in Table 6.1.

Table 6.1 Specimen Parameters

Specimen*	Cast-in-chlorides	FRP Wrap		Resin system	Initial concrete condition	Concrete repair material+	Corrosion Inhibitor
		Fabric type	Length, in				
Group A							
CC7	Chlorides	Fibrwrap	24	TYFO S	Cracked		
CC18	Chlorides	None			Cracked		
CNC8		None			Cracked		Ferrogard
CNC13		Generic	24	Epoxy	Cracked		Ferrogard
CNC14		Generic	36	Epoxy	Cracked		Ferrogard
CNC19		Generic	24	Epoxy	Uncracked		
RC4	Chlorides	None			Cracked		
RC7	Chlorides	Generic	30	Epoxy	Cracked		
Group B							
CC3	Chlorides	Fibrwrap	24	TYFO S	Uncracked	EG	
CC5	Chlorides	Generic	36	Epoxy	Cracked	EG	
CC6	Chlorides	Generic	36	Vinyl Ester	Cracked	EG	Ferrogard
CNC10		Fibrwrap	24	TYFO S	Cracked		
RNC6		Fibrwrap	30	Epoxy	Cracked	LMC	
RNC7		None			Cracked		

* The first letter represents the specimen geometry (C for cylinder, R for rectangular block). The following letters denote which concrete mix was used (C for cast-in-chlorides, NC for no chlorides).

+ The notation EG is for the epoxy grout, and the notation LMC is for the latex-modified concrete.

6.2 CORROSION MONITORING

Corrosion monitoring is necessary in order to provide some insight into the likelihood of corrosion activity taking place. This is especially crucial in structures wrapped with FRP composites, since the wrap prevents visual inspection for signs of corrosion activity, e.g. cracking and staining.

The laboratory specimens were monitored by half-cell potential using a saturated calomel reference electrode. The procedure followed ASTM Standard C 876, which is described in Chapter 4. The readings were then converted to equivalent copper/copper sulfate results. The half-cell readings are listed in Appendix B.

Readings were taken after every four wet/dry cycles for the wrapped specimens during the exposure period. Readings were taken after every cycle for the unwrapped specimens for the first year and a half of monitoring. After eighteen months of exposure, it was well established that corrosion was taking place in the unwrapped specimens. The readings indicated a high probability that corrosion was taking place. In addition, cracks were forming parallel to the reinforcing in specimens that were not cracked prior to exposure, as illustrated in Figure 6.2. After eighteen months of exposure, readings were taken after every four cycles on all of the specimens. Linear polarization testing was performed on the cylinders in Group B in order to compare results with the amount of corrosion activity found in the specimen after it was opened.

Figure 6.2 Longitudinal cracks forming on an uncracked specimen.

6.2.1 HALF-CELL POTENTIAL RESULTS

The changes in half-cell potential readings over time are illustrated for each group in the following graphs.

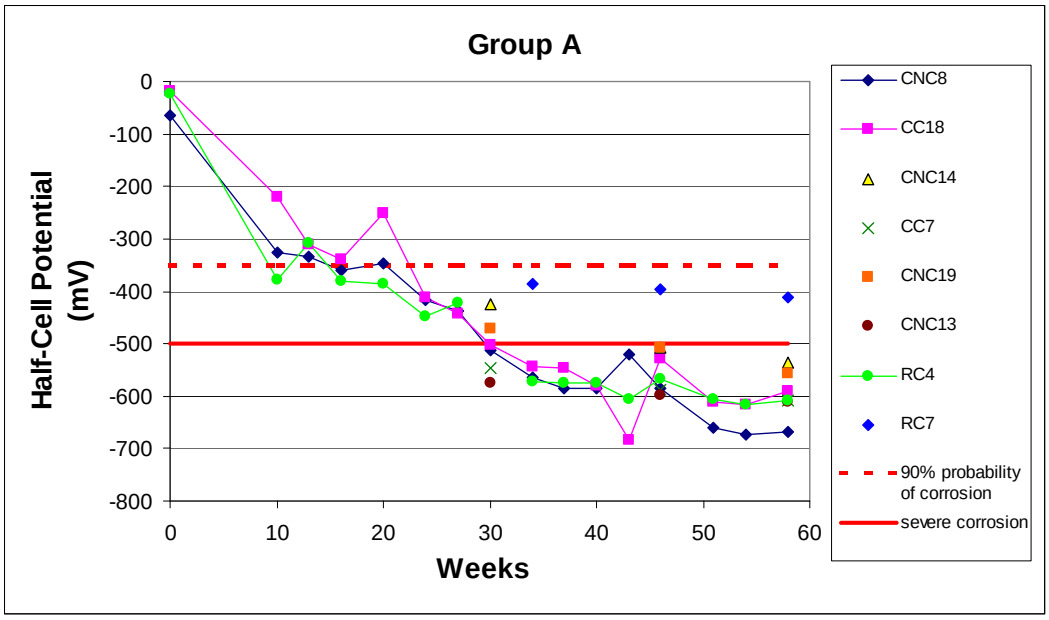

Figure 6.3 Half-cell potential vs. time for Group A.

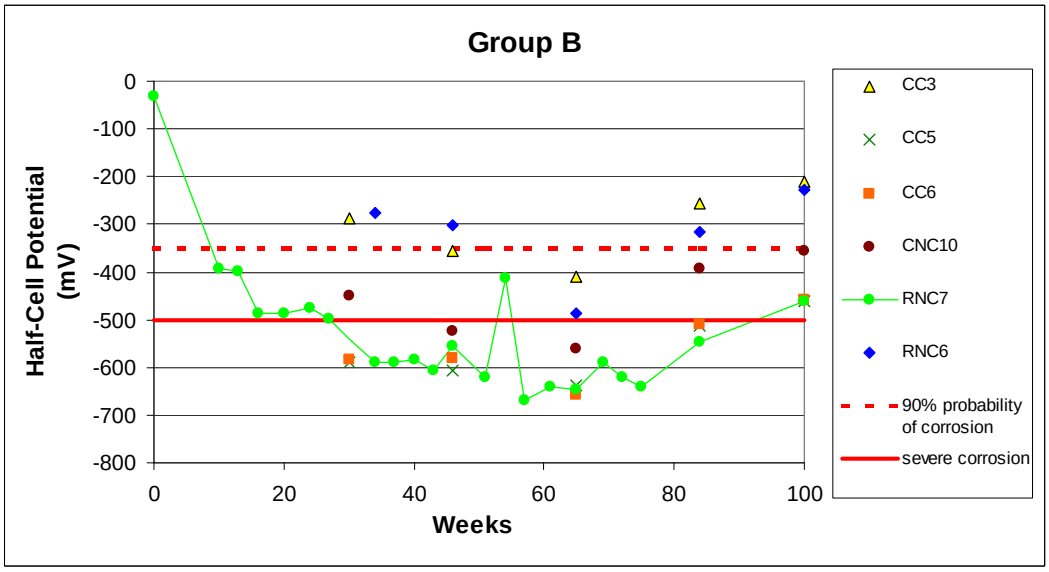

Figure 6.4 Half-cell potential vs. time for Group B.

The half-cell potential readings were generally below –500 mV for the unwrapped specimens, which indicates a strong likelihood of cracks forming in the concrete due to the formation of corrosion products. Both cracks and rust stains were observed on the unwrapped specimens. The readings for the wrapped specimens were typically less negative than the unwrapped specimens. Shortly after the exposure started, the readings indicate that all of the specimens crossed out of the range of 90% probability of the steel being passive. The readings fluctuate over time, which is probably due to changes in moisture levels in the concrete.

The next set of graphs show the readings over time for selected parameters. In Figure 6.5, half-cell potential for cylinders that were cast with the chloride free mix and have different wrap lengths and cracking conditions are plotted. Figure 6.6 shows the same parameters for cylinders that had the cast-in-chlorides. In Figure 6.7, values for wrapped and unwrapped rectangular blocks for both concrete mixes are compared.

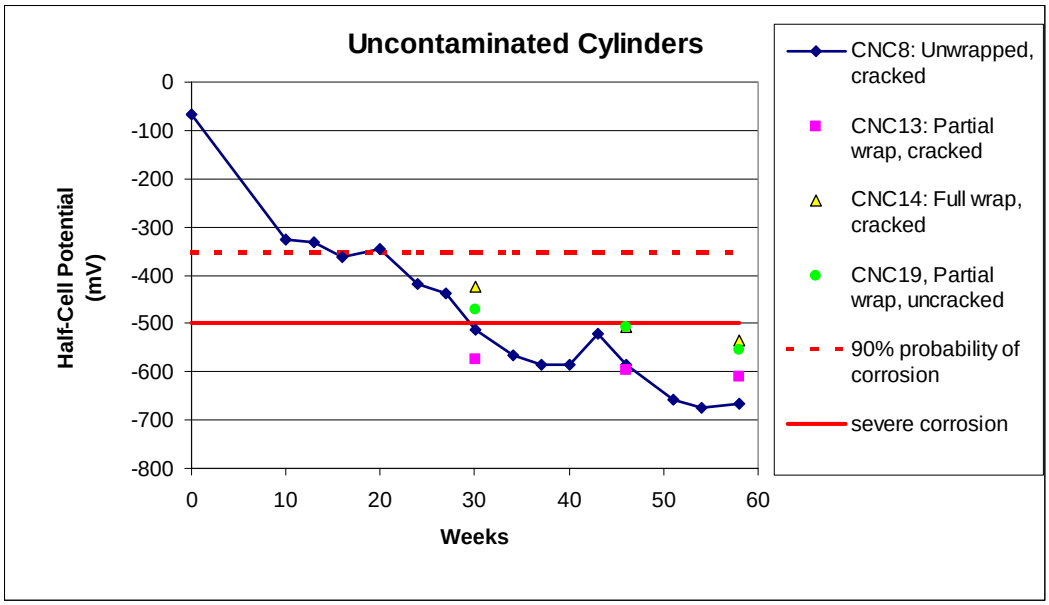

Figure 6.5 Uncontaminated concrete cylinders with different parameters.

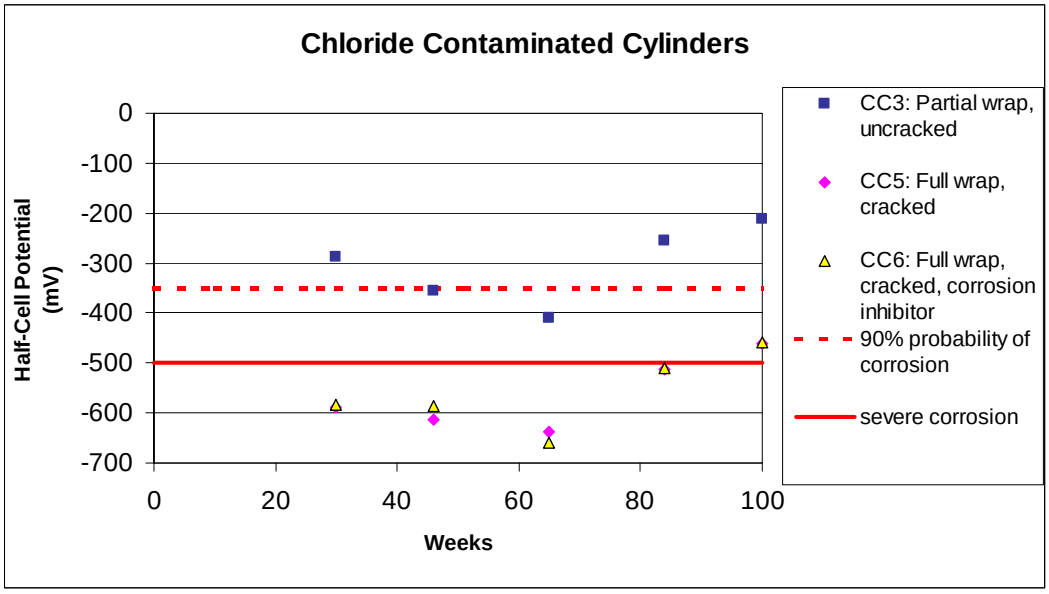

Figure 6.6 Chloride contaminated concrete cylinders with different parameters.

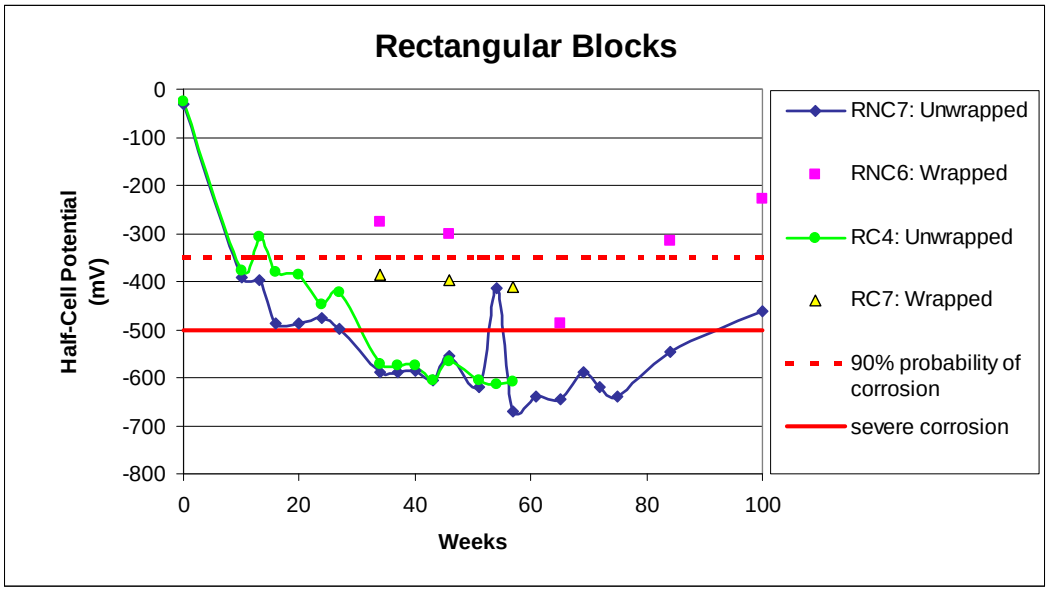

Figure 6.7 Half-cell potential vs. time for rectangular blocks.

For the cylinders without the cast-in-chlorides, there was not a noticeable difference in the half-cell potential values for the different parameters. The values suggested that corrosion activity was most likely taking place in all of the specimens. For the cylinders with the cast-in-chlorides, there was a noticeable difference between the values for the uncracked specimen compared to the values for the cracked specimens. For the rectangular blocks, the wrapped specimens had less negative values than the unwrapped specimens. The readings from the unwrapped specimens were very close in value. For the wrapped specimens, the specimen with the cast-in-chlorides was more negative than the non-chloride specimen.

The variation in readings for the different parameters is likely to be partially due to the location where the readings were taken. For the rectangular

blocks, the readings were taken at the downstream end. The downstream end for the unwrapped specimens was subjected to the saline water runoff, whereas the concrete at the downstream end for the wrapped specimens was much more likely to stay dry because it was covered with the wrap.

Due to the nature of the wrapping process, the partially wrapped cylinder specimens had the same amount of unwrapped concrete in the water as the unwrapped specimens. Since the half-cell potential measurements for the cylinders was taken 4 in. above the waterline, it is likely that the measurements for the partially wrapped specimens were affected by corrosion activity that might be taking place in the unwrapped portion below. Also, unlike the rectangular block, moisture could infiltrate the concrete above the splash zone by capillary action. Therefore the section of the wrapped cylinder specimens that were being monitored were not as likely to remain as dry as the downstream ends of the rectangular blocks.

6.2.2 LINEAR POLARIZATION RESULTS

Linear polarization was used on the cylinder specimens in Group B in order to determine the corrosion rate of the steel reinforcing. The test was performed at two locations on each specimen. The first location was at 4 in. above the waterline, which allowed for comparison with the half-cell potential readings, see Table 6.2. The second location was in the middle of the splash zone, 6 in. above the bottom of the specimen, which is where the most corrosion activity was expected to occur.

The PR-Monitor uses a copper/copper sulfate reference electrode with a sensor controlled guard ring. The circuit is completed with a large clamp that is used to make an electrical connection to the reinforcing steel. There is a five-pin connector that connects the half-cell and the sensor controlled guard ring to the instrument. Prior to running the test, the instrument monitors the free corrosion potential for a period of at least two minutes to confirm that there is no potential drift present that might affect the accuracy of the measurements. After the drift is within acceptable limits, less than 2 mV/min, the instrument starts measuring the overvoltages. At the end of the polarization cycle, an AC signal is applied from a high frequency generator in order to measure the solution resistance of the concrete. The computer then calculates the polarization resistance and the corrosion rate. Figure 6.8 shows the PR-Monitor in place for the linear polarization testing of the cylinder specimens.

Figure 6.8 PR-Monitor test setup on specimen CC5.

The testing was performed after the FRP composite wrap had been removed from the specimens. The clamp was connected to the reinforcing bar that was being polarized. The test could not be performed on the lower portion of specimen CC3 because the epoxy resin from the composite had encased the entire portion of concrete below the wrap. The corrosion rate data sheets for the tests may be found in Appendix C. The results from the tests are shown in Table 6.3 and Figure 6.9.

Table 6.2 Comparison of Half-Cell Potential and PR-Monitor

Specimen	E_{corr} Half-Cell Potential (mV)	E_{corr} PR-Monitor (mV)
CC3	-212	-275
CC5	-460	-411
CC6	-459	-458
CNC10	-356	-275

The values for E_{corr} from the half-cell potential testing and the linear polarization testing agree well. The first set of values was taken when the specimens were removed from the exposure tank. They were taken with the saturated calomel reference electrode and then converted to the equivalent copper/copper sulfate reading. The second set of values was obtained from the linear polarization testing, which was six weeks later. They were taken with a copper/copper sulfate reference electrode. The E_{corr} measurements were consistently higher in the splash zone compared to those above the splash zone, as noted in Table 6.3.

Table 6.3 Linear Polarization Data from Group B

Specimen	Location	
	Splash zone	4 in. above the waterline
CC3		
E_{corr} (mV)	N/A	-248
I_{corr} ($\mu A/cm^2$)	N/A	0.74
Rate (mpy)	N/A	0.34
CC5		
E_{corr} (mV)	-475	-411
I_{corr} ($\mu A/cm^2$)	4.88	4.27
Rate (mpy)	2.23	1.95
CC6		
E_{corr} (mV)	-504	-458
I_{corr} ($\mu A/cm^2$)	3.09	5.23
Rate (mpy)	1.41	2.39
CNC10		
E_{corr} (mV)	-549	-275
I_{corr} ($\mu A/cm^2$)	8.45	1.27
Rate (mpy)	3.86	0.58

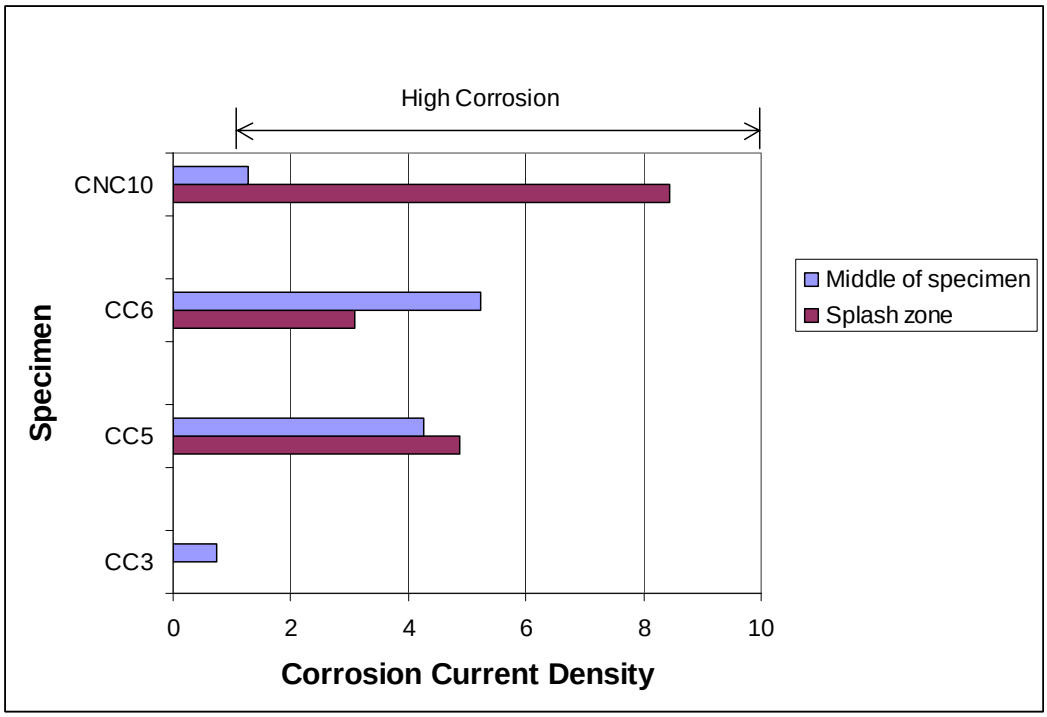

Figure 6.9 Corrosion current density ($\mu A/cm^2$) values for Group B.

The results from the linear polarization tests indicate that severe corrosion is taking place in most of the specimens. Specimen CC3 was the only specimen to fall into the moderate corrosion rate level. From visual observations of the specimens, there were no outward signs of corrosion activity on the middle portions of CC3 and CNC10. There was minimum cracking on CC3, and CNC10 did not have the cast-in-chlorides. The lower portion of CNC10 showed signs of corrosion activity as seen in Figure 6.10. Rust stains were visible at both locations on specimen CC6, and in the splash zone of CC5.

Figure 6.10 Evidence of corrosion activity in the splash zone of specimen CNC10.

6.3 TESTING OF SPECIMENS

Before opening the specimens, they were allowed to dry in order to remove any moisture remaining in the concrete. After Group A was removed from the exposure tank; it was left to air dry for six weeks prior to being evaluated. Group B was left to air dry for eight weeks prior to being evaluated. The cracks on the specimens were mapped and measured to determine the largest crack size observable. Chloride content determination tests were run on all of the specimens. Pull-off bond tests were run on the wrapped rectangular block in Group B.

6.3.1 CRACK MAPPING

Since cracks provide direct access for oxygen, moisture, and salts to enter the concrete, it is important to note their size and location. ACI recommends that cracks should be smaller than 0.004 in. in order to be watertight (ACI 1992). Group A was mapped prior to the wrap being removed. Group B was mapped after the wrap was removed. The crack locations were marked on the concrete. Then the crack size was measured with a crack comparator. Table 6.4 lists the maximum crack sizes observed.

Table 6.4 Crack Size Data

Specimen	Maximum Crack Size (in)
CC7	0.01
CC18	0.02
CNC8	0.007
CNC13	0.016
CNC14	N/A: Fully wrapped
CNC19	0.002
RC7	N/A: Fully wrapped
RC4	0.025
CC3	0.002
CC5	0.016
CC6	0.009
CNC10	0.005
RNC6	0.013
RNC7	0.025

It is likely that there were larger cracks on most of the wrapped specimens in Group A that were not observed due to being covered by the FRP wrap. The two uncracked specimens, CNC19 and CC3, both had hairline cracks that formed during the exposure period. The rest of the specimens had cracks larger than the recommended 0.004 in.

6.3.2 CHLORIDE DETERMINATION

In addition to crack size, it is important to determine the chloride content of the concrete. The chloride content indicates whether the chloride threshold has been reached, and whether the FRP composite wrap prevents the ingress of chlorides. The chloride threshold is approximately 0.03% chloride by weight of concrete. The chloride content calculated for the cast-in-chlorides mix was 0.137% chloride by weight of concrete.

Chloride content tests were run on the specimens to determine the chloride content in the concrete after exposure. A James Instruments CL-500 test was used. Samples were taken using a hammer drill with a ½-in. bit. For Group A, the first ½-in. of concrete was removed and discarded, and then samples were taken to the depth of 1 ¼-in. For the cylinders, the sample locations were 6 in. from the top, and 6 in. from the bottom. For the rectangular blocks, the sample locations were the center of the top face of the block, and the center of the side face of the block. For Group B, the chloride content tests were used to determine if the chloride levels changed at different depths of the cover. The first ¼-in. was discarded, and then samples were taken at depths of ½-in. and 1 in. The concrete

cover over the reinforcing steel was located at the depth of 1 in. The samples were taken at the same level that the half-cell potential measurements were taken. This was at 4 in. above the water line for the cylinders, and at the lower left corner of the downstream end for the rectangular blocks. The results from the chloride content tests are listed in Tables 6.5 and 6.6.

Table 6.5 Results from chloride tests for Group A at 1 ¼-in. depth

Specimen	Chloride Content by Weight of Concrete			
Cylinders	6 in. from top		6 in. from bottom	
	% Cl^-	Surface	% Cl^-	Surface
CC7	.14	FRP	.30	Bare
CC18	.62	Bare	.26	Bare
CNC8	.001	Bare	.33	Bare
CNC13	.002	FRP	.24	Bare
CNC14	.002	FRP	.04	FRP
CNC19	.002	FRP	.26	Bare
Rectangular Blocks	Top		Vertical	
	% Cl^-	Surface	% Cl^-	Surface
RC4	.33	Bare	.36	Bare
RC7	.12	FRP	.12	FRP

Table 6.6 Results from chloride tests for Group B

Specimen	Chloride Content by Weight of Concrete			
Cylinders	Depth of ½-in.		Depth of 1 in.	
	% Cl^-	Surface	% Cl^-	Surface
CC3	.09	FRP	.08	FRP
CC5	.16	FRP	.08	FRP
CC6	.16	FRP	.13	FRP
CNC10	.003	FRP	.003	FRP
Rectangular Blocks	Depth of ½ in.		Depth of 1in.	
	% Cl^-	Surface	% Cl^-	Surface
RNC6	.002	FRP	.002	FRP
RNC7	.21	Bare	.21	Bare

The difference in levels of chlorides found in the rectangular block specimens indicates that the FRP wrap provides a barrier for chlorides. This is evident by the very low levels of chlorides found in RNC6 as compared to RNC7. Both specimens were cast with the chloride-free mix and exposed in the same way. The percentages of chlorides in the unwrapped specimen were two orders of magnitude larger than the wrapped specimen. In specimens RC4 and RC7, the chloride levels in the wrapped specimen were slightly lower than the predicted chloride levels for the chloride contaminated specimens. The chloride levels in the unwrapped specimen were considerably higher.

The samples from the lower portion of the cylinders, which was located in the splash zone, had a chloride content of 0.24 to 0.33% for all exposed concrete. Specimen CNC14, which was a chloride free specimen, was the only cylinder that was wrapped the full length. It had the lowest chloride content in the splash zone for the cylinders. The chloride content in the splash zone of CNC14 was still above the threshold of 0.03%. This indicates that the chlorides permeated through the bottom of the column in order to contaminate the concrete.

The specimens in Group B had very little difference in chloride levels with respect to depth of the concrete cover. The variance in chloride levels from 0.08 to 0.16% for the wrapped chloride contaminated specimens was most likely due to some unevenness in the distribution of the chlorides in the mix and that some of the powder samples may have contained portions of the larger aggregates, which would not contain chlorides.

6.3.3 BOND TEST

The strengthening benefits of FRP composite wrapping systems are dependant on a strong adhesion between the wrap and the concrete surface. Without sufficient bond, the external strengthening benefits of the wrap are lost. When FRP composite wrap is applied by the hand layup method, the resin also serves as the system adhesive. If this adhesive layer deteriorates due to environmental effects, the bond between the concrete surface and the FRP composite deteriorates.

The bond of the FRP composite wrap was tested on specimen RNC6. The rectangular block specimen was chosen because the geometry was not as conducive to applying the wrap as the cylinders. It was difficult to maintain the tension required to apply the wrap (Fuentes 1999). Also a flat surface was required in order to perform the pull-off test.

The test was performed with a DYNA Z16 Pull-off Tester manufactured by Proceq. The pull-off tester measures the load required to cause a tensile failure in the concrete. From it, the compressive strength of the concrete can be estimated. The bond between the concrete and repair material can be evaluated by the location of the failure (Long and Murray 1995).

To carry out the test, two 2 in. diameter cores were partially cored into the center of the top face and the side face of the specimen to a depth of ½-in. One was near the upstream end and one was near the downstream end. A 50 mm. steel disk was then epoxied onto the FRP composite wrap at the end of the core. The disk was then fastened into the DYNA Z16 Pull-off tester, and slowly pulled until failure occurred. The device measured the force at failure. Figure 6.11 shows the test setup and Table 6.7 lists the results from the pull-off tests.

Figure 6.11 Test setup for DYNA Z16 Pull-Off Tester.

Table 6.7 Results from pull-off test for RNC6

Test #	Location	Depth of Failure (in)	Failure Strength (N/mm^2)	Failure Strength (psi)
1	Top, downstream end	¼	0.7	101.5
2	Top, upstream end	0	1.22	176.9
3	Side, downstream end	1/8	1.3	188.5
4	Side, upstream end	1/8	1.63	236.4

All of the tests failed in the substrate except for test #2, which failed at the bond between the wrap and the concrete surface, as shown in Figure 6.12. This indicates that the bond strength was stronger than the concrete tensile strength for

most of the specimen. The top face had the most severe exposure, so it is reasonable that the tensile strength was lower. The upstream end was most likely to have moisture seep under the wrap, which may have resulted in the failure at the epoxy bond in that location. The differences in failure strength are also possibility due to the fact that concrete is not an isotropic material. In addition, the low failure strength in the substrate during test #1 may have also been caused by cracks in the specimens. The difference in values of failure stress does indicate that there is some variation in the adhesion of the FRP wrap to the concrete surface.

Figure 6.12 Failure at the epoxy/concrete interface on Test #2.

The pull-off strengths agreed well with the study by Abu-Tair, Burley, and Rigden of bond strength of repair materials subjected to different loading and exposure conditions. In their pull-off tests, the average failure stress for concrete repaired with an epoxy mortar, a polymer modified cementitious mortar, and a portland cement concrete repair material was 1.63 N/mm^2, 1.39 N/mm^2, and 1.06 N/mm^2 respectively (Abu-Tair, Burley, and Rigden 1995).

6.4 OPENING OF SPECIMENS, GROUP A

The unwrapped specimens were opened by first removing the outer 1 in. of concrete cover with a chipping hammer. The concrete core was then examined for corrosion products. Then the concrete core was broken into small pieces with the chipping hammer. The concrete pieces were removed, and the remaining steel reinforcing cage was then examined for signs of corrosion activity.

The FRP composite wrap prevented easy removal of the concrete cover. The specimens were scored four times lengthwise with a concrete saw in order to provide access to the concrete surface. The concrete cover along the score was loosened with the chipping hammer. The wrap generally pulled away from the concrete along the score. This allowed for the wrap to be removed. Although the concrete along the scores was damaged due to the chipping hammer, there was very little damage to the rest of the concrete surface after the wrap was removed. Once the FRP composite wrap was removed, the specimens were opened and examined the same way as the unwrapped specimens. Table 6.8 summarizes the observations noted for Group A.

Table 6.8 Observations from opening of Group A

Specimen	Corrosion activity
CC7	The top 2’ were wrapped. Epoxy that had dripped down from the wrap covered half of the exposed surface on the bottom 1’. Heavy corrosion was found on bars and stirrups near cracks. Minor corrosion was found throughout the upper 2’.
CC18	The entire surface was exposed. A small honeycombed area was located at the bottom of the specimen. Areas of heavy corrosion were found throughout on the bars and stirrups near cracks and also near the honeycombed area. A small amount of section loss was found at the lower ends of two bars near the honeycombing.
CNC8	The entire surface was exposed. A honeycombed area was at the bottom of the specimen. Heavy corrosion with substantial section loss was found on the bottom stirrup near the honeycombing. Moderate corrosion was found on the lower half of the bar by the honeycombing and on the lower 5 stirrups.
CNC13	The top 2’ were wrapped. A corrosion inhibitor was applied. Light to moderate corrosion was found on the lower 6” of the bars and on the bottom 2 stirrups. Corrosion activity corresponded with crack locations.
CNC14	The entire surface was wrapped. A corrosion inhibitor was applied. Moisture was found trapped beneath the wrap in the splash zone. Minor to moderate corrosion was found on the lower 6” of 1 bar and on the bottom 2 stirrups near where the moisture was found.
CNC19	The top 2’ were wrapped. The specimen was not cracked prior to exposure. Moderate corrosion was found near crack locations on the lower 1’ of 2 bars. Minor corrosion was found on the lower 3 stirrups.
RC4	The entire surface was exposed. Moderate corrosion was found throughout the bottom 2 bars and on all 3 stirrups.
RC7	The entire surface was wrapped. Moisture was found trapped underneath the wrap on the bottom face at the upstream end. Moderate corrosion was found on the upper stirrup near where the moisture was found. Minor corrosion was found throughout the bottom 2 bars.

Corrosion activity generally corresponded with cracks and honeycombing found within the concrete. Specimens with cast-in-chlorides had corrosion activity throughout the specimen whereas the specimens without cast-in-chlorides had corrosion only in the splash zone and a few inches above the splash zone.

The wrapped specimens had less corrosion activity than the unwrapped specimens. Moisture was found trapped between the FRP composite wrap and the concrete surface in specimens CNC14 and RC7, both of which were fully

wrapped. Figure 6.13 shows moisture that was found at the interface of the wrap and the concrete surface on specimen CNC14.

Corrosion activity appeared less severe on the specimens that were treated with the Sika™ Ferrogard 903. Corrosion activity in specimen CNC19, which was not treated with the corrosion inhibitor, was found on the stirrups throughout the splash zone even though the specimen was not cracked prior to exposure. Corrosion activity in specimens CNC13 and CNC14, which were treated with the corrosion inhibitor, was near the crack locations. Very little corrosion activity was found in the uncracked portions of CNC13.

Figure 6.13 Moisture trapped beneath the surface in the splash zone of specimen CNC14.

6.5 OPENING OF SPECIMENS, GROUP B

In order to perform the linear polarization testing, the FRP composite wrap had to be removed with minimal damage to the concrete surface. It was noticed in Group A that the wrap could be pried away from the concrete along the scores. Therefore the specimens were scored twice lengthwise with a concrete saw. The wrap was then pried off with a crowbar. The epoxy resin that had dripped down from the composite and encased the bottom portion of CC3 could not be removed. The generic system with the vinyl ester was the easiest to remove. The Fibrwrap® system was the most difficult to remove. This method resulted in very little damage to the concrete surface. As a result, the entire surface of the wrapped specimens could be examined for cracks, and the linear polarization testing could be performed. After the wrap was removed, the specimen were opened the same way as Group A. Table 6.9 summarizes the observations noted for each specimen for Group B.

Table 6.9 Observations from opening of Group B

Specimen	Corrosion activity
CC3	The top 2' were wrapped. The bottom 1' was covered with epoxy resin that had dripped down from the wrap. The specimen was not cracked prior to exposure. An epoxy grout patch covered the bottom 1' of the specimen. Corrosion activity was found mainly in the splash zone, which was also where the patch was located. A small amount of moderate corrosion was found at the lower ends of the bars. Half of the surface area of the bottom 4 stirrups was covered with minor to moderate corrosion.
CC5	The entire surface was wrapped. An epoxy grout patch covered the top 6" of the specimen. A small honeycombed area was located at the bottom of the specimen. Small areas of moderate corrosion were found on the bars near cracks throughout. Minor corrosion was found on the lower 6 stirrups, with moderate corrosion on the bottom stirrup at the honeycombing. Heavy corrosion with minor section loss was found on the top stirrup at the patch.
CC6	The entire surface was wrapped. Moisture was trapped beneath the wrap in the splash zone. An epoxy grout patch covered the top 1' of the specimen. A corrosion inhibitor was applied. Moderate corrosion was found on bars at crack locations and near where the moisture was found. Minor corrosion was found on the lower 5 stirrups. Heavy corrosion was found on the upper 4 stirrups at the patch.
CNC10	The top 2' were wrapped. Corrosion activity corresponded with crack locations. Heavy corrosion was found on the lower 6" of bars and on lower 2 stirrups. One bar had an area of moderate corrosion just above the splash zone. No corrosion activity was found on the upper 18" of the specimen.
RNC6	The entire surface was wrapped. A small amount of moisture was trapped at the upstream end of the top face of the specimen. A latex-modified concrete patch covered the downstream end of one of the side faces. Isolated minor corrosion was found along the bars and stirrups near the patch. Heavy rust was found on all of the bars near the end of the wrap. Heavy rust with substantial section loss was found on the top stirrup.
RNC7	The entire surface was exposed. A longitudinal crack had formed at the location of the bottom bars. Heavy corrosion was found throughout the bars, with moderate to heavy corrosion found on stirrups near crack locations.

Due to the longer exposure time, the corrosion activity was more severe in Group B than Group A. Corrosion activity also corresponded with the crack locations, although more corrosion was found away from cracks. This is mainly due to the fact that most of the specimens had cast-in-chlorides.

Moisture was found trapped beneath the wrap for two of the fully wrapped specimens, CC6 and RNC6. No moisture was found in specimen CC5, even though it was fully wrapped. Corrosion activity near the location of trapped moisture was greater than in other areas of the specimen. Specimen RNC6 experienced section loss in the stirrup due to the trapped moisture as shown in Figure 6.14.

Figure 6.14 Section loss on the upstream stirrup of specimen RNC6.

Unlike Group A, corrosion activity was also found in the upper half of the cylinder specimens. Heavy corrosion was found at the patches in the chloride contaminated concrete indicating that macrocells had formed between the concrete and the uncontaminated repair material for the cylinder specimens. The macrocells were found both in the splash zone and several feet above the splash

zone in encapsulated concrete. Figure 6.15 shows the corrosion activity found in the top portion of specimen CC5. A macrocell also formed between the uncontaminated concrete and the repair material in RNC6, but the corrosion activity was not as extensive. This was most likely due to fact that the existing concrete did not contain chlorides.

Figure 6.15 Macrocell formation in the top portion of specimen CC5.

There was no sign of decreased corrosion due to the use of the corrosion inhibitor in Group B. Corrosion activity was more extensive throughout specimen CC6, which was treated with Sika™ Ferrogard 903, compared to CC5 which was not treated.

6.6 DISCUSSION OF RESULTS

Both the half-cell potential readings over time and the linear polarization indicate the likelihood of corrosion activity taking place. Opening of the specimens found corrosion activity to varying degrees was taking place in each specimen.

The chloride tests confirmed that the FRP composite wrap prevents chlorides from permeating the concrete. As a result, very little corrosion activity was found in portions of uncontaminated concrete that was free of cracks and repair material. However, corrosion activity was present throughout the wrapped portions of the chloride contaminated specimens. This indicates that although the FRP composite wrap provides a barrier to chlorides and moisture, corrosion activity may continue in the cracked chloride contaminated concrete. Corrosion activity was also accelerated by the formation of macrocells between the existing concrete and repair material.

Corrosion activity was found in the splash zones of all of the cylinder specimens. Chlorides were found in the lower portions of all of the cylinder specimens including the fully wrapped cylinder without the cast-in-chlorides. The FRP composite wrap did not prevent chloride ingress in and just above the splash zone.

Lastly, in four out of five of the fully wrapped specimens, moisture was found trapped beneath the wrap resulting in accelerated corrosion activity in that area. For the cylinder specimens, it resulted in corrosion activity taking place in the splash zone. For the rectangular blocks, the area of corrosion activity due to

trapped moisture was found at the upstream end rather than the downstream end. As a result, the activity did not register on the half-cell potential monitoring since the downstream end was the area being monitored. The results from the linear polarization showed that the half-cell potentials varied depending on the location where they were taken. The ASTM standard suggests an interval of 4 ft. for a bridge deck. In the case of the laboratory specimens, the half-cell potential could vary substantially in an interval of 10 in.

The following figures help to quantify the corrosion rate measurements taken from the linear polarization testing. Figure 6.16 shows the steel reinforcing that was polarized in the splash zone of CNC10. It had the highest corrosion rate measurement, 3.86 mpy. The concrete was not wrapped with FRP composite in that area. Figure 6.17 shows the steel reinforcing that was polarized in the splash zone of CC6. The concrete was wrapped with FRP composite in that area. The corrosion rate was 1.41 mpy. Figure 6.18 shows the steel reinforcing that was polarized in the middle portion of CC3. It had the lowest corrosion rate measurement, 0.34 mpy, and the only measurement that was in the moderate corrosion rate level. The concrete was wrapped with FRP composite in that area. As shown in the following figures, the corrosion rate was consistent with the extent of corrosion activity. Photographs of the steel reinforcing cage for each specimen in both groups may be found in Appendix D.

Figure 6.16 Steel reinforcing of CNC10 with a corrosion rate of 3.86 mpy.

Figure 6.17 Steel reinforcing of CC6 with a corrosion rate of 1.41 mpy.

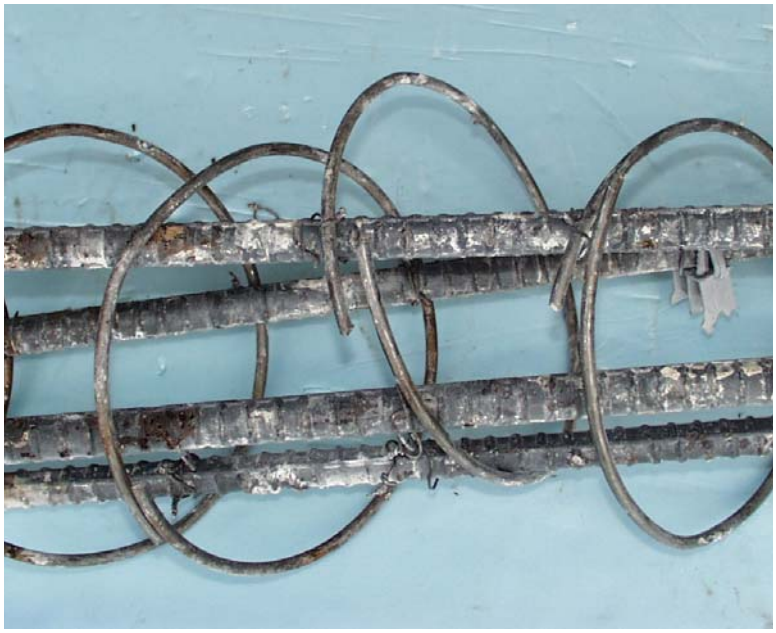

Figure 6.18 Steel reinforcing of CC3 with a corrosion rate of 0.34 mpy.

Chapter 7

Field Data

7.1 SCOPE OF PROJECT

The field installation described in Chapter 5 has been monitored for twelve months during 2000 to 2001, visually and using embedded probes. The condition of the structures was evaluated prior to repair and encapsulation with FRP composite wrap. Readings from the embedded probes have been monitored approximately every six months. The objective is to determine the likelihood of corrosion activity continuing after the FRP composite was installed.

7.2 FIELD RESULTS PRIOR TO REPAIRS

In the summer of 1998, the structures were evaluated to determine the extent of the corrosion activity. The testing was performed prior to repairs. Three different linear polarization devices were used: the 3LP device, the PR-Monitor, and the Gecor device. This was done to determine how well each device operated in the field. The E_{corr} values for the PR-Monitor and the Gecor device were more consistent than the 3LP device. The corrosion current density was higher on the PR-Monitor than the Gecor device. The 3LP device produced inconsistent results, which may have been due to technical difficulties with the reference electrode. The linear polarization was performed 10 to 20 feet from the downstream end of the bent in order to be able to connect to the steel and to avoid the delaminated

areas. The results indicated that the steel was mostly passive. This is reasonable since the measurements were taken at places that showed little to no damage (Verhulst 1999). The results are summarized in Table 7.1 and Figure 7.1.

Table 7.1 Corrosion Rate Measurement Data (July 1998)

Device	Location (Structure #)					
	#8	#7	#1	#5	#10	#11
3LP						
E_{corr} (mV)	-40	N/A	-100	-270	N/A	-157
I_{corr} ($\mu A/cm^2$)	0.1347	N/A	0.0431	0.063	N/A	0.6207
PR-Monitor						
E_{corr} (mV)	-108	-79.2	-102.7	-74.9	-66.8	-144.5
I_{corr} ($\mu A/cm^2$)	0.0219	0.46	0.0044	0.018	0.15	0.302
Rate (mpy)	0.01	0.21	0.002	0.008	0.069	0.138
Gecor						
E_{corr} (mV)	-83.8	-78.3	-116.4	-41.4	-49.8	-113
I_{corr} ($\mu A/cm^2$)	0.01	0.001	0.009	0.003	0.008	0.022
Interpretation	Passive	Passive	Passive	Passive	Passive	Passive

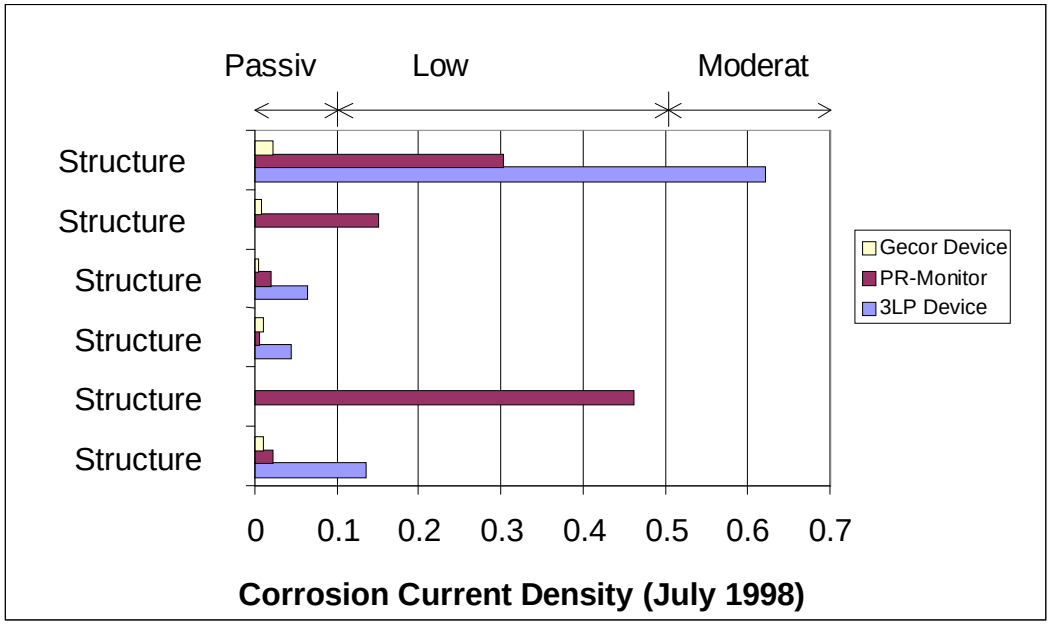

Figure 7.1 Corrosion current density ($\mu A/cm^2$) values from different equipment.

The chloride content with respect to depth was determined at different locations. This was done to classify the possibility of corrosion conditions for the structures. The samples were taken using a hammer drill with a ¾-in. bit. The first ½-in. was discarded to eliminate surface imperfections or inconsistencies. Samples were taken at the depth of 1 in., 1.5 in., and 2 in. The results are listed in Table 7.2.

Table 7.2 Chloride percentages by weight of concrete (FSEL 1999)

Location	Depth (in.)		
	0.5 – 1.0	1.0 – 1.5	1.5 – 2.0
Structure #8 – 10 ft. from the downstream end.	0.12	0.034	0.038
Structure #8 – 2.5 ft. from the downstream end.	0.17	0.21	0.20
Structure #7 – 20 ft. from the downstream end.	0.19	0.18	0.15
Structure #7 – 12 ft. from the downstream end.	0.21	0.28	0.16
Structure #3 – 22 ft. above the ground on the west face of the column.	0.26	0.29	0.19
Structure #2 – 17 ft. from the downstream end.	0.31	0.22	0.16
Structure #2 – 25 ft. from the downstream end (left of the center column).	0.056	0.08	0.042
Structure #1 – Directly on the downstream endcap.	0.01	0.0056	0.0035
Structure #5 – Directly on the spalled downstream endcap.	0.45	0.38	0.21
Structure #5 – 10 ft. from the downstream end (some spalling present).	0.082	0.043	0.0035
Structure #10 – Between columns away from the downstream end.	0.003	0.003	0.003
Structure #11 – On the top of the bent.	0.018	0.02	0.018

The shaded boxes indicate the three locations where the chloride threshold had not been reached. The chloride levels in most of the locations were higher than the threshold of 0.03% chloride by weight of concrete. This means that many of the locations tested have a sufficient level of chlorides to allow for the onset of

corrosion. The highest levels of chlorides were found in areas that were already damaged. However, high levels of chlorides were found in Structure #7 and #2 in locations that were 10 to 25 feet away from the downstream end.

A pachometer was used to determine the depth to the steel reinforcing. The depth of cover was found to be 2.5 in. Given that eight of the twelve locations were above the threshold of 0.03% at a depth of 2 in., it is likely that chloride contamination is occurring at the depth of the reinforcing steel (Verhulst 1999).

7.3 MONITORING RESULTS

Three trips were made to Lubbock, TX in order to collect data from the field installations. Readings were taken with the PR-Monitor. The tops of the bridge bents were accessed using a lift truck provided by TxDOT. The lead cables from the embedded probes protruded out from the FRP wrap on the top of the bents. The six-pinned connector at the end of the cable was plugged into a connecting cable from the PR-Monitor. The linear polarization test was run by using a program on the laptop console on the PR-Monitor. The PR-Monitor operates in the same manner as described in Chapter 6, except that the embedded probe replaces the half-cell and sensor controlled guard ring assembly. Figure 7.2 shows the PR-Monitor being used in the field.

Figure 7.2 PR-Monitor test setup for Structure #12.

The embedded probes were installed in three bridges: Structure #7, Structure #8, and Structure #12. Corrosion rate measurements for probe 12.3 could not be taken due to invalid data. Possible damage to the probe or the connection to the steel may have been the cause of the problem. The linear polarization tests were performed in May 2000, October 2000, and May 2001. The corrosion rate data sheets for the tests may be found in Appendix E. The results are summarized in Table 7.3 and Figure 7.3.

Table 7.3 Linear Polarization Data

Probe ID #	Date	E_{corr} (mV)	I_{corr} (mV)	Rate (mpy)
7.1	May 2000	-244	0.57	0.26
	October 2000	-251	0.37	0.17
	May 2001	-253	0.37	0.17
7.2	May 2000	-477	1.60	0.73
	October 2000	-426	1.09	0.50
	May 2001	-528	1.82	0.83
8.1	May 2000	-329	0.44	0.20
	October 2000	-306	0.24	0.11
	May 2001	-344	0.44	0.20
8.2	May 2000	-362	1.36	0.62
	October 2000	-352	0.94	0.43
	May 2001	-384	1.42	0.65
8.3	May 2000	-377	0.57	0.26
	October 2000	-392	0.33	0.15
	May 2001	-395	1.23	0.56
8.4	May 2000	-351	0.99	0.45
	October 2000	-461	0.79	0.36
	May 2001	-359	1.31	0.60
12.1	May 2000	-305	3.37	1.54
	October 2000	-316	0.59	0.27
	May 2001	-392	2.19	1.00
12.2	May 2000	-384	2.69	1.23
	October 2000	-303	2.08	0.95
	May 2001	-436	2.45	1.12
12.3	May 2000	N/A	N/A	N/A
	October 2000	N/A	N/A	N/A
	May 2001	N/A	N/A	N/A

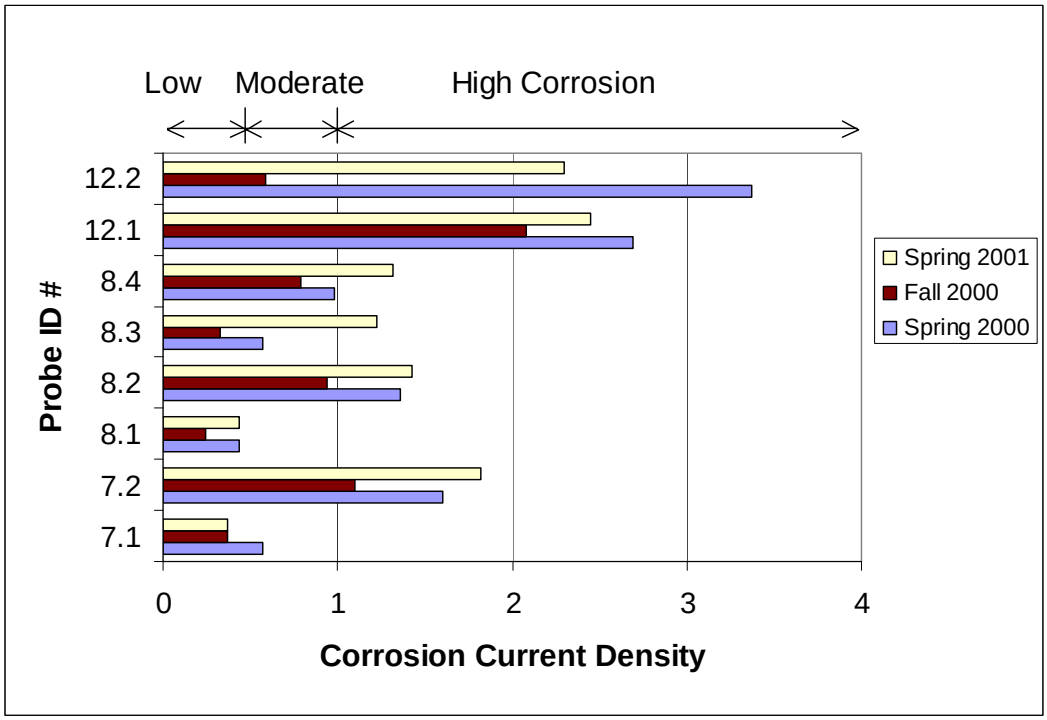

Figure 7.3 Corrosion current density ($\mu A/cm^2$) for corrosion monitoring.

Many of the half-cell potential values are more negative than –350 mV, indicating that corrosion is likely to be taking place. Many of the corrosion rate readings indicate that moderate to heavy corrosion activity is taking place. The readings were higher in the spring than in the fall. This is probably due to higher temperatures and moisture levels in the spring. The corrosion rate measurements for Structure #12 were noticeably higher than the other structures.

The corrosion rates from the linear polarization testing were substantially higher than the corrosion rates from linear polarization testing performed before the repairs were made. The difference is most likely due to the fact that the embedded probes are located 4 to 7 feet from the downstream end in areas where corrosion activity was noted before the repairs were made, while the pre-repair linear polarization testing was performed 10 to 20 feet from the downstream end in areas that did not show signs of corrosion activity.

7.4 OBSERVATION OF FIELD INSTALLATION

The bents that had the embedded probes were examined each time the linear polarization testing was performed. Moderate debris accumulation was found on top of all of the bents. The FRP composite on the bridge bents had been cut around the bearing pads. In some places, the wrap was finished with epoxy to seal it around the bearing pad; in other places it was not. The finishes around the bearing pads near probes 7.1, 8.3, and 8.4 seemed to have the best seals. There was a 1 in. gap between the wrap and the bearing pad near the location of probes 12.1 and 12.2. This allowed for exposed concrete on the top of the bent as shown in Figure 7.4. Figure 7.5 shows the finish around the bearing pad near probe 7.2. Figure 7.6 shows the finish around the bearing pad near probe 8.3, and is an example of how the wrap around the bearing pad may be sealed off. However, little is known about the viability of the seal if there are movements of the girder and bearing pad.

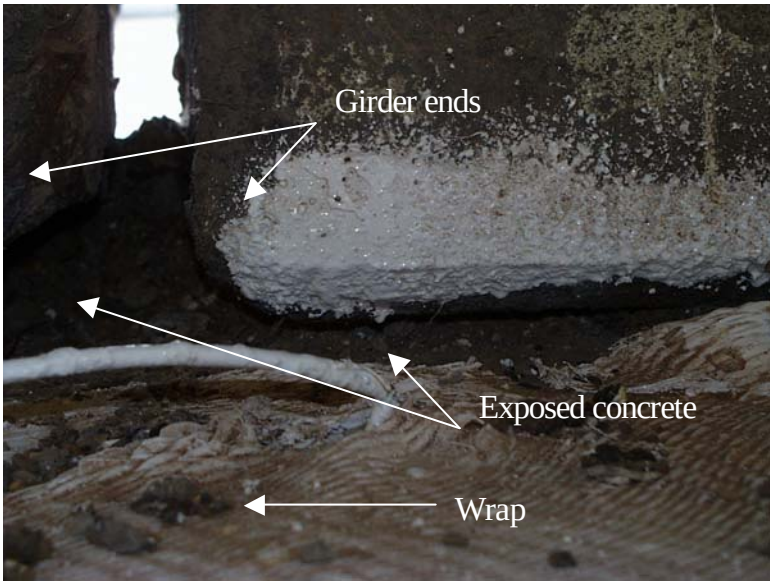

Figure 7.4 Finish of FRP wrap around girders of Structure #12.

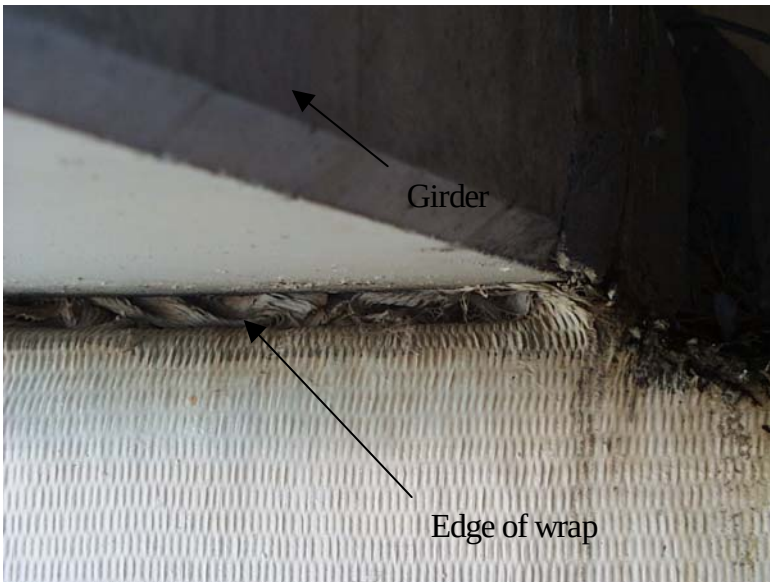

Figure 7.5 Finish of FRP wrap around girders of Structure #7.

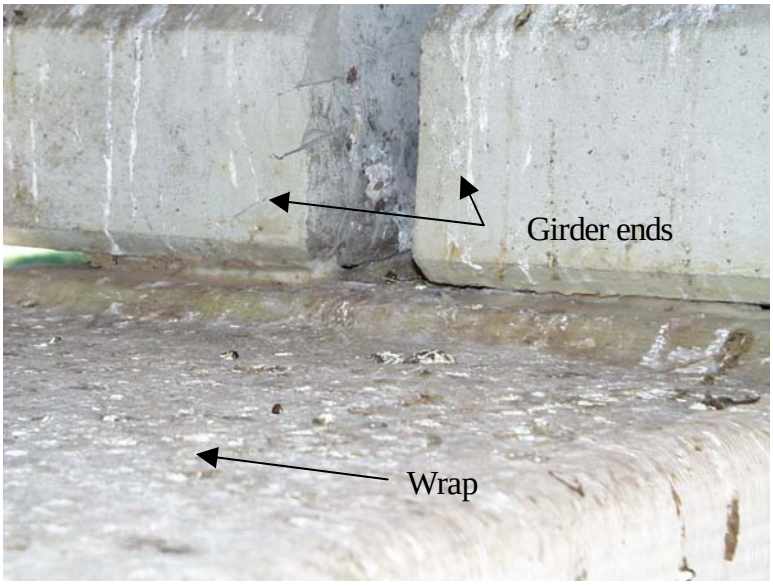

Figure 7.6 Finish of FRP wrap around girders of Structure #8.

There is some correlation between the finish of the wrap and the corrosion rate measurements. The readings from probe 7.1, and the readings from Structure #8, were generally lower than the readings from probes 7.2, 12.1, and 12.2. Cracks were found on the ends of the girders near probes 8.3 and 8.4. Cracks with rust stains were found on the ends of the girders near probes 7.2, 12.1, and 12.2. The cracks may be an indication of exposure to runoff containing deicing salts.

In May 2001, all of the structures were visually inspected. On several of the columns, the FRP composite wrap was damaged as a result of vehicle impact. This damage will undoubtedly influence the performance of the FRP composite. In the field study in Indiana, researchers noticed that collision damage to the FRP wrap worsened over time because the damaged areas were more sensitive to the

effects of a harsh environment. Figure 7.7 shows the worst damage noticed on the structures at the Lubbock site.

Figure 7.7 Vehicular collision damage on column of Structure #2.

At the time of the visual inspection, the bridge decks were being replaced on Structures #1 to #8 because of corrosion damage. On many of the bridges substructures there were rust stains that had resulted from corrosion activity that was taking place in the superstructure above. However, on Structure #1, there were signs of corrosion activity taking place in one of the bents. Rust stains were found at the seam of the FRP wrap on the bottom of the fourth bent on both sides of the north column. There were no indications that the stains had resulted from corrosion activity in superstructure. Figure 7.8 is a photograph of the rust stains.

Figure 5.8 Rust stains on bent of Structure #1.

7.5 COMPARISON OF RESULTS FROM THE LABORATORY AND THE FIELD

The linear polarization and half-cell potentials both indicate a strong probability that corrosion activity is taking place near the probe locations. The staining found on one of the bents indicates that there may also be corrosion activity in other locations that are not being monitored.

The chloride measurements indicate high levels of chloride in many locations in the structures. These locations include areas that were then repaired and areas that were most likely not repaired. The specifications for the repairs

called for the removal of all unsound concrete. The chloride content determination indicates that the structures are likely to contain sound but chloride contaminated concrete. This means that there may be macrocells forming between the repair material and the existing concrete similar to that found in the laboratory specimens. It is also likely that chloride contaminated concrete was encapsulated with FRP composite wrap.

Moisture may be able to enter into the concrete through the exposed concrete surface around the bearing pads on the bents where the FRP wrap was not sealed. The laboratory specimens showed that moisture that seeped into the concrete near the edge of the FRP wrap could become trapped, resulting in accelerated corrosion in that area. It is possible that moisture is being trapped in the bents near the bearing pads. This could be causing accelerated corrosion, which would explain the higher corrosion rate measurements found in Structure #12.

It should be noted that the embedded probes were originally planned to be installed closer to the endcaps. This was because the downstream endcaps showed the most damage in the field before repairs were made. It was expected that the endcaps would be the most susceptible place for any corrosion that might take place after encapsulation. Due to the construction timing, the embedded probes were installed 4 to 7 feet away from the downstream end of the bent because the endcaps had already been repaired. In most cases, the embedded probes were installed near the bearing pads.

It is quite possible that the corrosion activity that is taking place near the bearing pads is more severe than corrosion activity in the endcaps. When the laboratory study was initiated, it was expected that the downstream ends of the rectangular blocks would be the area that was most likely to experience corrosion activity. Instead, the most severe corrosion activity was found at the upstream ends of the rectangular blocks where the moisture had become trapped underneath the wrap.

Chapter 8

Corrosion Inhibitors

8.1 INTRODUCTION TO CORROSION INHIBITORS

In order to further study the issue of corrosion prevention in FRP encapsulated chloride contaminated concrete, an additional laboratory study was developed to investigate the effectiveness of surface applied corrosion inhibitors. Three different commercially available corrosion inhibitors were selected to be studied.

The objective of this additional study is to find out whether the use of a surface applied corrosion inhibitor will prevent corrosion activity chloride contaminated concrete in members where FRP composite wraps serve as a barrier for moisture and further chloride ingress.

8.2 TYPES OF CORROSION INHIBITORS

Corrosion inhibitors are found in two forms, admixtures and liquid coatings that are applied to the surface. The first chemicals tested as corrosion inhibitors were additives containing sodium nitrite, potassium chromate, sodium benzoate, stannous chloride, and calcium nitrite. Calcium nitrite was the only product that became commercially available because it was found to improve the properties of hardened concrete. Inhibitors with sodium or potassium bases were found to be detrimental to concrete strength and to cause alkali-aggregate

reaction. In 1983, the Federal Highway Administration concluded that using calcium nitrate as an admixture could provide more than an order of magnitude reduction in the corrosion rate. More recent tests have found that the use of calcium nitrite as an admixture will provide corrosion protection for diffused chlorides up to a level of 16 lb/yd^3 (Berke 1991). This is substantially higher than the chloride threshold of 1 lb/yd^3.

The calcium nitrite delays the onset of corrosion initiation and controls the rate of corrosion by stabilizing the passivating layer of iron-oxide film. It chemically reacts with the passivating layer of the embedded steel so that it remains intact when it comes into contact with chlorides (Perkins 1997). Calcium nitrite is an anodic inhibitor. It prevents corrosion activity by suppressing the anodic reaction.

The use of a calcium nitrite admixture is limited to new construction. For rehabilitation, corrosion inhibitors are available in the form of a surface applied liquid. These products migrate through the concrete surface in order to provide a protective film on the reinforcing steel. Some surface applied corrosion inhibitors are calcium nitrite based. Since nitrites pose an environmental threat, many of the newer surface applied corrosion inhibitors use organic and inorganic materials instead. Most are based on amine salts. Some are water based and some are alcohol based. Noncalcium nitrite based inhibitors are usually mixed inhibitors in that they act as both anodic and cathodic inhibitors. In addition to providing a protective film on the anode, they suppress the cathodic reaction by forming a

barrier at the cathodic site that prevents oxygen from reaching the steel (Shaw 1997).

Laboratory testing of surface applied corrosion inhibitors have concluded that they can reduce corrosion. However, most of these tests have been sponsored by the product manufacturers and have also been performed on new concrete. Very little is known about the performance of corrosion inhibitors for repaired construction. The effect the corrosion inhibitor has on the reinforcing outside of the repair area is unknown. In addition, little is known about how well it protects steel that is actively corroding, or under conditions that cause macrocells to form (Krauss, Gu, and Vaysburd 1999). Since surface applied corrosion inhibitors have only been available since the 1990s, results from laboratory and field testing are limited. There have been no systematic studies reported on the effectiveness of surface applied corrosion inhibitors on existing structures or chloride contaminated concrete.

8.3 DESCRIPTION OF TEST SPECIMENS WITH CORROSION INHIBITORS

In TxDOT Project 1774, an additional laboratory study was designed to investigate the effectiveness of three commercially available surface applied corrosion inhibitors. The preliminary findings from the laboratory study discussed in Chapter 6 indicated that the use of FRP composite wrap alone on chloride contaminated concrete did not prevent corrosion activity. The objective of the additional test program is to evaluate the effectiveness of FRP composite wrap in prevention of corrosion activity when used in conjunction with a surface applied

corrosion inhibitor. For consistency with the initial study, similar specimens were fabricated. The properties for each specimen are listed in Table 8.1.

Table 8.1 Specimen Parameters for Corrosion Inhibitor Study

Specimen #	Concrete Condition	Corrosion Inhibitor	Wrap Length (in)	Probe Installation
1	Cracked	Surtreat	24	
2	Cracked	Surtreat	36	VETEK
3	Uncracked	Surtreat	24	
4	Uncracked	Surtreat	36	
5	Cracked	Cortec	24	
6	Cracked	Cortec	36	VETEK
7	Uncracked	Cortec	24	
8	Uncracked	Cortec	36	
9	Cracked	Sika	24	
10	Cracked	Sika	36	VETEK
11	Uncracked	Sika	24	
12	Uncracked	Sika	36	
13	Cracked	None	24	
14	Cracked	None	36	VETEK
15	Uncracked	None	24	
16	Uncracked	None	36	
17	Cracked	None	None	VETEK

The specimen geometry, cast-in-chloride concrete mix, and cracking conditions for the specimens in this study are the same as the ones described in Chapter 5. Only cylinder (column) specimens were used.

One FRP composite system TYFO S Fibrwrap® was used because it is commercially available and is being used on TxDOT projects. The specimens were wrapped either to the waterline with a 24 in. partial wrap, or a 36 in. full length wrap.

Three commercially available surface applied corrosion inhibitors were selected. The manufacturer's data sheet for each product may be found in Appendix F. The products used are described below:

- Total Performance System (TPS), manufactured by Surtreat® International. TPS uses a water soluble chemical formulation that controls the pH level in concrete and ties up chlorides and drives salts to the surface of the concrete.
- MCI 2020, manufactured by Cortec® Corp. MCI 2020 is a water-based blend of surfactants and amine salts that migrates to the steel reinforcing. It forms a monomolecular protective layer on the reinforcing steel.
- FerroGard-903, manufactured by Sika™ Corp. Ferrogard 903 is a modified amino alcohol inhibitor that migrates to the steel reinforcing in order to form a thin protective coating on the steel surface. The film inhibits corrosion and displaces chlorides.

In constructing the previous cylinder specimens, poor consolidation at the time of casting resulted in severe honeycombing. For the new specimens, procedures were changed to improve consolidation. The formwork consisted of

36 in. high cardboard sonoforms that were firmly anchored to prevent them from floating up when the concrete was cast. Twenty-six specimens were cast. The temperature was 65°F during the time of placement. The concrete slump was 6 ½-in. The concrete was placed into the form from an overhead chute in one lift. An immersion-type vibrator was placed in the form prior to the concrete placement and slowly pulled out as the concrete was added in order to assure good consolidation throughout the specimen. After the concrete was placed, the top surface was struck off and troweled. The specimens were covered with heavy damp clothes and a plastic sheet to cure for 28 days. All but one of the specimens were well consolidated and had smooth finishes. The average 28 day concrete cylinder strength was 3520 psi.

Half of the specimens were cracked as desrcibed in Chapter 5. The specimens with the most uniform cracking patterns were selected for the experiement.

The application of the corrosion inhibitors and the FRP wrap was done by Delta Structural Technology, Inc. The surface of the specimens was cleaned off with an air hose prior to application of the surface applied corrosion inhibitors. The inhibitors were then applied with a low pressure sprayer according to the manufacturer's instructions. A separate sprayer was used for each type od inhibitor. All of the corrosion inhibitors were applied at a rate of 100 ft^2/gal. The Surtreat TPS was applied using three coats. The specimens were subjected to a light rinse after the second and third application. The Cortec MCI 2020 was applied using two coats and rinsed after each coat. The Sika Ferrogard 903 was

applied using three coats and rinsed after each coat. The specimens that were not being treated with covered with a plastic drop cloth to prevent contamination. Figure 8.1 shows the application of the corrosion inhibitor.

Figure 8.1 Application of a surface applied corrosion inhibitor to the specimens.

Before the wrap was applied, the surface of the specimens were prepared by applying an epoxy filler thickened with Cab-O-Sil®, to create a smooth even surface. The glass fabric was saturated with the epoxy resin using a paint roller. The wrap was then applied to the specimens using the hand layup method. Three layers were applied with a 6 in. overlap. After each layer was applied, the surface was smoothed out by hand in order to remove air pockets. The specimens were cured for 24 hours and then inspected for voids under the wrap. Any voids

detected were injected with epoxy. The specimens were painted with Sherwin Williams® Hi Bald Aliphatic Polyurethane paint. Afterwards, they were left to cure an additional six days, bringing the total curing time to seven days. Figures 8.2 through 8.4 show the application of the FRP composite wrap.

Figure 8.2 Filling voids with a thickened epoxy filler.

Figure 8.3 Saturating glass fabric with epoxy resin.

Figure 8.4 Applying FRP wrap to the concrete specimen.

8.4 MONITORING AND EXPOSURE

The specimens will be monitored using half-cell potential. The specimens were prepared for taking readings in the wrapped sections in the same manner as described in Chapter 5. In addition to taking half-cell potential measurements at the concrete surface, embedded half-cell probes were installed in five of the specimens. By embedding the half-cell reference electrode, the potential measurements are taken at the steel rather than at the concrete surface. This reduces error related to properties of the concrete such as moisture content, thickness of the concrete cover, and resistivity of the concrete. It also offers the added benefit that measurements may be taken at any time without having to unseal a portion of the FRP composite.

The VETEK System manufactured by Corrosion Monitoring Systems was chosen for the embedded half-cell probes. The system consists of two separate reference electrodes. Both electrodes are wrapped in a permeable, nonconducting PVC covering. The probes monitor the steel for a distance of approximately 10 cm from the probe location. A separate connection to the steel must be made for each reinforcing bar being monitored. The V2000 Monitoring Electrode consists of a solid silver/silver chloride wire electrode. The V1500 Monitoring Electrode is a pure gold wire electrode. Both electrodes monitor corrosion activity, and when used together they provide information on the chloride concentration in the concrete. The chloride concentration is found by taking the difference in potential readings between the gold reference electrode and the silver reference electrode

and plotting it on the graph in Figure 8.5. The manufacturer's guide for interpreting the results for each probe is summarized in Tables 8.2 (CMS 2000).

Table 8.2 Interpretation of Readings for the VETEK System

V2000 (silver) E_{corr} (mV)	V1500 (gold) E_{corr} (mV)	Corrosion Risk
0 to 300	100 to -150	No active corrosion in the vicinity of the probe
300 to 400	-150 to –200	Damage of the passive layer has begun
> 400	< -200	Active corrosion is taking place

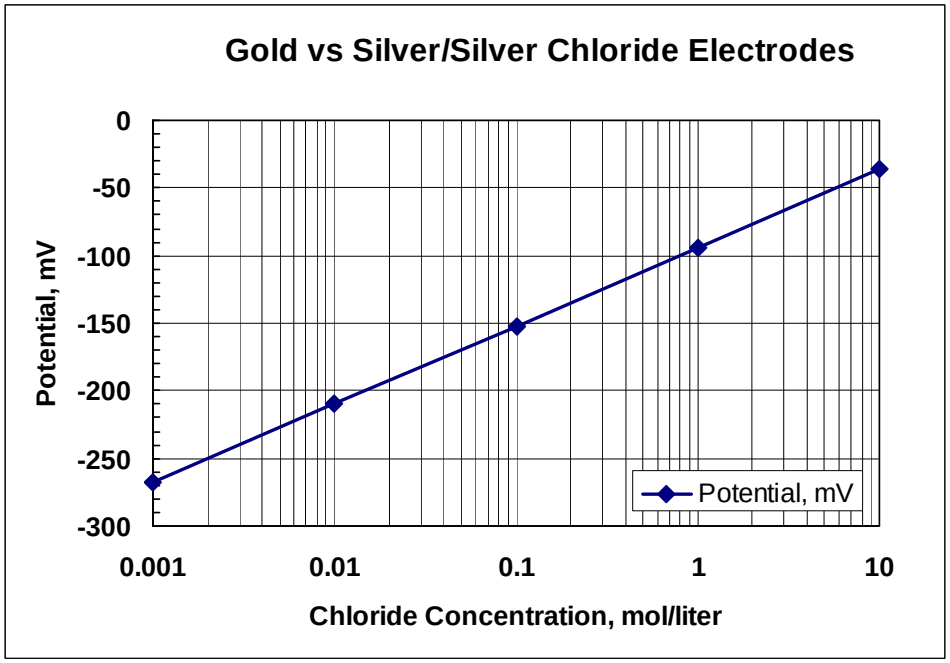

Figure 8.5 Chloride determination of VETEK System.

The silver/silver chloride probe may be converted to an equivalent copper/copper sulfate value by subtracting the reading from –94 mV (Broomfield 1997).

The probes were installed by drilling a 1 in. hole into the concrete up to the steel reinforcing. The probes were then bent into a circle and placed in the hole. Care was taken to prevent the wires in the two reference electrodes from coming into direct contact, which could result in an electrical short. After the probes were placed, the hole was then filled with a sand/cement concrete mix as specified by the manufacturer. The location of the installation was 4 in. above the waterline. A connection was made to the steel reinforcing bar being monitored by using the steel connector that was included with the system. The installation of the VETEK system is shown in Figures 8.6 and 8.7.

Figure 8.6 Installation of the embedded reference electrodes.

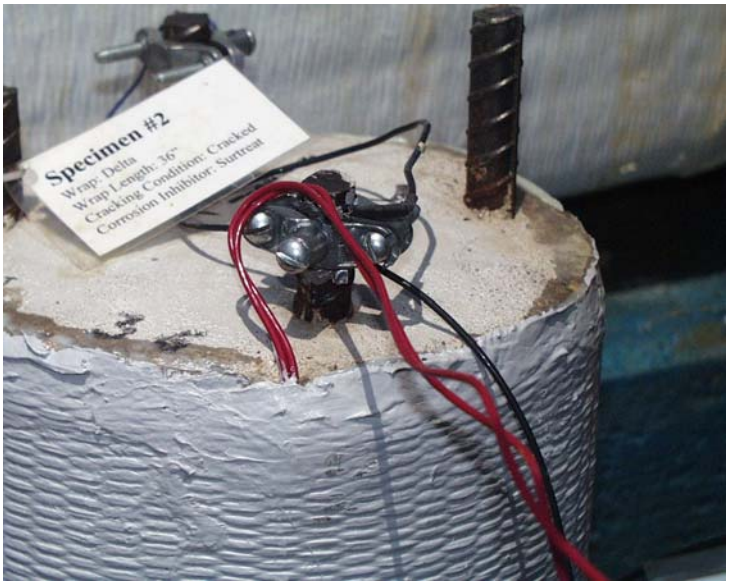

Figure 8.7 Wires from the embedded probes and the connection to the steel.

Unlike traditional half-cell measurements, the electrical connection to the steel reinforcing is made to the negative terminal of the voltmeter. The reference electrode is connected to the positive terminal of the voltmeter. This results in readings that are positive rather than negative.

Before the specimens were placed in the exposure tank, half-cell potential measurements were taken for each specimen. The results are listed in Tables 8.3 through 8.5.

Table 8.3 Half-cell Potential Readings

Specimen	E_{corr} (mV)	Interpretation
1	-212	Intermediate Risk
2	-225	Intermediate Risk
3	-211	Intermediate Risk
4	-295	Intermediate Risk
5	-298	Intermediate Risk
6	-243	Intermediate Risk
7	-186	Low Risk
8	-306	Intermediate Risk
9	-238	Intermediate Risk
10	-200	Low Risk
11	-229	Intermediate Risk
12	-279	Intermediate Risk
13	-179	Low Risk
14	-244	Intermediate Risk
15	-184	Low Risk
16	-262	Intermediate Risk
17	-100	Low Risk

Table 8.4 Embedded Probe Readings

Specimen	Gold probe (mV)	Silver probe (mV)	VETEK interpretation of Corrosion Activity	$Cu/CuSO_4$ Equivalent (mV)	ASTM Interpretation of Corrosion Activity
2	183	190	No corrosion	-284	Uncertain
6	8	435	Corrosion	-529	Corrosion
10	-6	186	No corrosion	-280	Uncertain
14	9	3	No corrosion	-97	Low probability
17	0	0	No corrosion	-94	Low probability

Table 8.5 Chloride Measurements from Embedded Probes

Specimen	Difference between probe reading	Chloride Level (mols/L)	Interpretation
2	-7	32	High levels
6	-427	0	Low levels
10	-192	0.02	Low levels
14	6	53	High levels
17	0	42	High levels

There is some general agreement between the half-cell potential readings taken at the concrete surface and the half-cell potential readings taken from the embedded probe. The E_{corr} values for the embedded probe readings are typically more negative than E_{corr} for the standard half-cell potential when both values were converted to the copper/copper sulfate equivalents. There is a distinct possibility

that a macrocell may have formed at the location of the embedded probe due to the difference in chlorides between the concrete and the concrete grout that was used to fill in the hole after the probes were placed. Also the half-cell measurements that are taken at the concrete surface are taken on a different reinforcing bar than the one that is being monitored with the embedded probes. Therefore different levels of corrosion activity may be taking place on each bar at the location of 4 in. above the waterline.

The specimens treated with the corrosion inhibitors appear to have lower chloride levels than the untreated specimens. The measurements indicated that the specimens treated with the Cortec and Sika corrosion inhibitors had substantially lower chloride levels. All of the specimens were fabricated with the same chloride contaminated concrete and the same non-chloride concrete grout, so the chloride levels were expected to be the same. The half-cell potential values for the specimens that were not treated with the corrosion inhibitors were generally less negative than the specimens that were treated.

The new specimens, along with the remaining specimens from the initial study, were placed in a new exposure tank. The exposure tank that had been used for the study described in Chapters 5 and 6 had started experiencing problems with leaking. The new exposure tank was built out of concrete and lined with epoxy to prevent leaking and corrosion of the reinforcing in the tank. Figure 8.8 is a photograph of the exposure environment.

Figure 8.8 Specimens in the exposure tank.

The specimens will continue to be exposed to wet/dry cycles consisting of the one week wet followed by two weeks air drying. Half-cell potential readings are planned after every cycle for the embedded probes and after every four cycles for the surface half-cell potential readings.

Chapter 9

Summary and Conclusions

9.1 SUMMARY

Corrosion of steel reinforcing in concrete is one of the greatest threats to the durability of reinforced concrete. It is the single most expensive corrosion related problem, and affects the integrity of thousands of reinforced concrete structures. Bridges located in aggressive environments, such as exposure to seawater or deicing salts are highly susceptible to corrosion activity.

Fiber reinforced plastic (FRP) composite wraps have recently been suggested to be used in repair of damage to concrete that resulted from corrosion activity. FRP composite wraps have been proven to strengthen concrete members and improve ductility. Over the last decade, they have performed well in seismic retrofit applications.

Little is known about the long-term effectiveness of FRP composite wrap in prevention of corrosion in reinforced concrete. The FRP may act as a barrier to protect the concrete from moisture and chlorides, which can lead to corrosion, or it may trap already existing moisture and chlorides in the concrete, allowing for the corrosion process to continue undetected.

In this study, laboratory specimens that represent conditions present in chloride contaminated concrete were exposed to an accelerated aggressive environment. The specimens were monitored and evaluated for corrosion activity.

In addition, bridge overpasses that have been wrapped with FRP after experiencing corrosion related damage were monitored for corrosion activity.

9.2 REVIEW OF FINDINGS

The following observations were noted in the laboratory and the field.

9.2.1 CORROSION ACTIVITY

The monitoring methods used in this study: half-cell potential, linear polarization, and embedded probes indicated that corrosion activity was likely in all of the specimens in the study. Corrosion activity generally corresponded with areas that had the most severe exposure to wetting and drying; typically in the damaged portions of the concrete, especially at crack locations.

9.2.2 ROLE OF FRP AS A BARRIER

The FRP composite wrap did provide a barrier for chlorides and moisture for the downstream ends of the rectangular block specimens and the upper halves of the cylinder specimens. Very little corrosion activity was found in those areas for the concrete specimens without the cast-in-chlorides. Corrosion activity was found in those locations for the chloride contaminated specimens. In the case of the cylinder specimens, increased chlorides were found in the splash zone. This included a cylinder specimen that was fully wrapped and did not contain cast-in-chlorides. In addition, trapped moisture was found underneath the wrap in four out of five of the fully wrapped specimens when the wrap was removed. The

moisture was found near the edge of the wrap, since the specimens were not fully encapsulated Accelerated corrosion was also found near the locations of the trapped moisture. There was some section loss of a steel stirrup in one of the specimens.

9.2.3 EFFECT OF REPAIR MATERIALS

Corrosion activity was further accelerated at locations of patches of repair material in the chloride contaminated concrete. Corrosion was also found near the patch location in the downstream end of a fully wrapped rectangular block that did not contain cast-in-chlorides. The activity was minor compared to corrosion activity taking place near the patch locations of the chloride contaminated concrete.

9.2.4 FIELD OBSERVATIONS

In the field study, high chloride levels were found in portions of concrete that were not showing signs of damage due to corrosion at the time repairs were made. The linear polarization testing indicates that low to moderate corrosion activity is most likely taking place in the structures after the members were wrapped. It was observed that some surface areas on the tops of the bridge bents were left exposed near the edge of the wrap around the bearing pads. Corrosion rates were higher in such locations compared with areas where the surface was completely sealed. Also, one bridge bent had visible signs of corrosion activity

taking place. Rust stains were found on the underside of the bent at the seams in the FRP wrap.

9.3 PRELIMINARY CONCLUSIONS AND RECOMMENDATIONS

The following conclusions and recommendations were drawn from this study.

9.3.1 EFFECTIVENESS OF FRP IN CORROSION PREVENTION

Wrapping of chloride contaminated concrete does not appear to prevent corrosion. There is a serious risk that corrosion may continue in areas where moisture may infiltrate, and also in areas with dissimilar repair materials. Macrocells may develop between existing chloride contaminated concrete and the repair material even in areas where moisture infiltration is unlikely. However, very little corrosion activity was found in the wrapped portions of chloride free, undamaged concrete. This is most likely due to the ability of the FRP composite wrap to act as a barrier to chlorides and moisture.

9.3.2 FRP AS A BARRIER

In the laboratory study, the FRP composite wrap appeared to provide a barrier to chlorides and moisture. However, moisture was able to enter the wrapped portions of concrete through adjacent exposed concrete surface. Increased chlorides and trapped moisture was found in the concrete near the edge

of the wrap. It does not appear to be feasible to totally wrap bridge members in the field.

9.3.3 CORROSION MONITORING

The half-cell potential, linear polarization, and embedded probes all proved to be viable options for evaluating corrosion activity. Linear polarization is the only method that establishes the degree of corrosion activity taking place. The half-cell potential is limited to determining whether corrosion activity is taking place. In a laboratory environment where corrosion activity is expected, half-cell potential readings provide little information after the onset of corrosion.

Because FRP composite wraps obscure the concrete surface, all corrosion monitoring is limited to predetermined locations where access to the concrete is provided. As a result, corrosion activity may appear to be more severe than it actually is, or corrosion activity may take place undetected. The corrosion activity at the location being monitored may not necessary reflect conditions a short distance away.

9.3.4 RECOMMENDATIONS FOR FIELD APPLICATIONS

It is recommended that all chloride contaminated concrete should be removed before FRP composite wrap is applied when repairing concrete damage due to corrosion activity. It is also recommended that care should be taken to seal exposed concrete near the edge of the wrap on structures that are exposed to deicing salts. The less exposed concrete, the lower the amount of moisture and

chlorides that are likely to enter bridge members. In marine environments, preventing moisture and chlorides from entering bridge columns is an area of concern. It may be difficult to prevent capillary action from taking place. In addition, it is recommended that embedded probes be installed in areas that may be susceptible to corrosion activity in order to monitor the structure.

9.4 RECOMMENDATIONS FOR CONTINUING RESEARCH

Further research is needed into the long-term effects of corrosion activity of reinforcing steel in FRP composite wrapped concrete. While corrosion activity has been found in the specimens examined, the extent of corrosion activity over a longer period of time is unknown.

In addition to long-term studies, more research is needed to assess the effectiveness of FRP composite wrap in preventing or reducing corrosion activity in concrete that has been repaired properly. Adequate preparation includes the removal of all chloride contaminated concrete and sealing of cracks. The use of surface applied corrosion inhibitors needs further exploration, especially where chloride contaminated concrete is involved.

Appendix A

Table A1 Parameters for Chloride Contaminated Cylinders

Specimen*	FRP Wrap		Resin system	Initial concrete condition	Concrete repair material[+]	Corrosion Inhibitor
	Fabric type	Length, in				
CC1	Fibrwrap	24	TYFO S	Cracked		Ferrogard
CC2	Generic	30	TYFO S	Wet	LMC	
CC3	Fibrwrap	24	TYFO S		EG	
CC4	Fibrwrap	24	TYFO S		LMC	
CC5	Generic	36	Epoxy	Cracked	EG	
CC6	Generic	36	Vinyl Ester	Cracked	EG	Ferrogard
CC7	Fibrwrap	24	TYFO S	Cracked		
CC8	Fibrwrap	36	TYFO S	Cracked	LMC	
CC9	Fibrwrap	24	TYFO S			
CC10	None					Ferrogard
CC11	None					
CC12	Generic	30	Epoxy	Wet		
CC13	Generic	24	Epoxy	Cracked		
CC14	Generic	24	Epoxy		LMC	Ferrogard
CC15	Generic	24	Epoxy	Cracked		Ferrogard
CC16	None				EG	
CC17	None				LMC	
CC18	None			Cracked		
CC19	Generic	24	Vinyl Ester		LMC	
CC20	Generic	24	Vinyl Ester			Ferrogard
CC21	None			Cracked		Ferrogard

Table A2 Parameters for Non-Chloride Cylinders

Specimen*	FRP Wrap		Resin system	Initial concrete condition	Concrete repair material+	Corrosion Inhibitor
	Fabric type	Length, in				
CNC1	Generic	27	Epoxy	Cracked, Wet	EG	
CNC2	Generic	36	Epoxy	Cracked		
CNC3	Generic	24	Epoxy			Ferrogard
CNC4	Fibrwrap	24	TYFO S			
CNC5	Fibrwrap	36	TYFO S	Cracked		
CNC6	Generic	24	Vinyl Ester	Cracked, Wet	EG	
CNC7	None					Ferrogard
CNC8	None			Cracked		Ferrogard
CNC9	Generic	24	Vinyl Ester		LMC	
CNC10	Fibrwrap	24	TYFO S	Cracked		
CNC11	None				LMC	
CNC12	None				EG	
CNC13	Generic	24	Epoxy	Cracked		Ferrogard
CNC14	Generic	36	Epoxy	Cracked		Ferrogard
CNC15	None			Cracked		
CNC16	Fibrwrap	24	TYFO S		LMC	
CNC17	Fibrwrap	24	TYFO S		EG	
CNC18	Generic	24	Epoxy		LMC	Ferrogard
CNC19	Generic	24	Epoxy			
CNC20	None					

Table A3 Parameters for Chloride Contaminated Rectangular Blocks

Specimen*	FRP Wrap		Resin system	Initial concrete condition	Concrete repair material[+]	Corrosion Inhibitor
	Fabric type	Length, in				
RC1	Generic	27	Epoxy		LMC	Ferrogard
RC2	Generic	31	Vinyl Ester	Cracked		
RC3	Fibrwrap	24	TYFO S	Cracked		
RC4	None			Cracked		
RC5	Fibrwrap	27	TYFO S		LMC	
RC6	Fibrwrap	33	Epoxy		LMC	
RC7	Generic	30	Epoxy	Cracked		
RC8	None				LMC	
RC9	Fibrwrap	24	Epoxy	Cracked		Ferrogard

Table A4 Parameters for Non-Chloride Rectangular Blocks

Specimen*	FRP Wrap		Resin system	Initial concrete condition	Concrete repair material[+]	Corrosion Inhibitor
	Fabric type	Length, in				
RNC1	Fibrwrap	24	TYFO S			
RNC2	None					
RNC3	Generic	27	Epoxy			Ferrogard
RNC4	Generic	36	Vinyl Ester	Cracked	LMC	
RNC5	Fibrwrap	30	TYFO S	Cracked		
RNC6	Fibrwrap	3030	Epoxy	Cracked	LMC	
RNC7	None			Cracked		
RNC8	Generic	24	Epoxy	Cracked		

* The first letter represents the specimen geometry (C for cylinder, R for rectangular block). The following letters denote which concrete mix was used (C for cast-in-chlorides, NC for no chlorides).

[+] The notation EG is for the epoxy grout, and the notation LMC is for the latex-modified concrete.

Appendix B

Table B1 Half-cell Potential Readings for Group A

(mV vs. $Cu/CuSO_4$)

Date	CC7	CC18	CNC8	CNC13	CNC14	CNC19	RC4	RC7
02/26/99		-18	-66				-24	
05/13/99		-221	-326				-377	
06/11/99		-310	-333				-307	
07/02/99		-340	-361				-380	
07/28/99		-251	-347				-387	
08/25/99		-411	-417				-447	
09/15/99		-443	-437				-423	
10/06/99	-547	-501	-513	-574	-425	-471		
11/03/99		-544	-565				-572	-386
11/26/99		-546	-584				-574	
12/15/99		-579	-586				-574	
01/06/00		-683	-521				-606	
01/28/00	-588	-528	-584	-597	-507	-507	-566	-397
02/29/00		-610	-659				-607	
03/25/00		-616	-674				-615	
04/18/00	-608	-590	-667	-611	-535	-556	-609	-411

Table B2 Half-cell Potential Readings for Group B

(mV vs. $Cu/CuSO_4$)

Date	CC3	CC5	CC6	CNC10	RNC6	RNC7
02/26/99						-32
05/13/99						-392
06/11/99						-398
07/02/99						-487
07/28/99						-486
08/25/99						-476
09/15/99						-499
10/06/99	-288	-589	-583	-449		
11/03/99					-276	-589
11/26/99						-589
12/15/99						-585
01/06/00						-606
01/28/00	-355	-606	-580	-524	-375	-555
02/29/00						-620
03/25/00						-414
04/14/00						-670
05/08/00						-640
06/07/00	-409	-638	-658	-560	-488	-645
07/03/00						-588
07/26/00						-621
08/17/00						-640
10/15/00	-255	-513	-510	-394	-316	-547
02/05/01	-212	-460	-459	-356	-228	-462

Appendix C

CORROSION RATE DATA SHEETS FOR GROUP B

Corrosion Rate Measurement Data Sheet Project 1774 Sheet __1___	
Date	5/22/01
Sample ID #	CC5
Sample Location: 4" above waterline	**Comments:** Bar with clamp
Polarization Data: **PRMonitor:** Ecorr = -411.0 mV Icorr = 4.269 $\mu A/cm^2$ Rate = 1.95 mpy	
Concrete Surface Description: Was previously covered with wrap. Some cracking noted.	
Half-Cell Potential (mV vs. $Cu/CuSO_4$)	-411 mV
PR Monitor Filename	cc5mid

Corrosion Rate Measurement Data Sheet Project 1774 Sheet __2___	
Date	5/22/01
Sample ID #	CC5
Sample Location: 6” from bottom	**Comments:** One bar to the right of the bar with clamp
Polarization Data: **PRMonitor:** Ecorr = -474.7 mV Icorr = 4.882 μA/cm^2 Rate = 2.23 mpy	
Concrete Surface Description: Was previously covered with wrap, uneven surface remains. Large crack with rust stain. Honeycombed area at bottom of specimen.	
Half-Cell Potential (mV vs. Cu/CuSO$_4$)	-475 mV
PR Monitor Filename	cc5bot

Corrosion Rate Measurement Data Sheet Project 1774 Sheet __3___	
Date	5/22/01
Sample ID #	CNC10
Sample Location: 4” above waterline	**Comments:** Bar with clamp
Polarization Data: **PRMonitor:** Ecorr = -275.1 mV Icorr = 1.270 μA/cm^2 Rate = 0.58 mpy	
Concrete Surface Description: Was previously covered with wrap, uneven surface remains. Some cracking noted. Minor honeycombing.	
Half-Cell Potential (mV vs. Cu/CuSO$_4$)	-275 mV
PR Monitor Filename	cnc10mid

Corrosion Rate Measurement Data Sheet Project 1774 Sheet __4___	
Date	5/22/01
Sample ID #	CNC10
Sample Location: 6” from bottom	**Comments:** One bar to the left of the bar with clamp
Polarization Data: **PRMonitor:** Ecorr = -549.4 mV Icorr = 8.45 μA/cm^2 Rate = 3.86 mpy	
Concrete Surface Description: Was previously exposed. Some epoxy above the sample remains. Large crack with rust stain.	
Half-Cell Potential (mV vs. Cu/CuSO$_4$)	-549 mV
PR Monitor Filename	cnc10bot

Corrosion Rate Measurement Data Sheet Project 1774 Sheet __5___	
Date	5/22/01
Sample ID #	CC3
Sample Location: 4" above waterline	**Comments:** Bar with clamp
Polarization Data: **PRMonitor:** Ecorr = -247.9 mV Icorr = 0.744 $\mu A/cm^2$ Rate = 0.34 mpy	
Concrete Surface Description: Was previously covered with wrap, uneven surface remains. Extensive microcracking noted. Epoxy grout patch below sample.	
Half-Cell Potential (mV vs. Cu/$CuSO_4$)	-248 mV
PR Monitor Filename	cc3mid

Corrosion Rate Measurement Data Sheet Project 1774 Sheet __6___	
Date	5/22/01
Sample ID #	CC3
Sample Location: 6” from bottom	**Comments:** One bar to the right of bar with clamp
Polarization Data: **PRMonitor:** Ecorr = N/A Icorr = N/A Rate = N/A	Inconsistent drift
Concrete Surface Description: Was previously exposed. Epoxy resin covers the concrete surface. Epoxy grout patch at sample location. No cracks noted. Cannot wet the concrete surface.	
Half-Cell Potential (mV vs. Cu/$CuSO_4$)	N/A
PR Monitor Filename	cc3bot

Corrosion Rate Measurement Data Sheet Project 1774 Sheet __7___	
Date	5/22/01
Sample ID #	CC6
Sample Location: 4” above waterline	**Comments:** Bar with clamp
Polarization Data: **PRMonitor:** Ecorr = -458.3 mV Icorr = 5.232 μA/cm^2 Rate = 2.39 mpy	
Concrete Surface Description: Was previously covered with wrap, smooth surface. Large cracks noted. Rust stains noted. Epoxy grout patch above sample.	
Half-Cell Potential (mV vs. Cu-CuSO$_4$)	-458 mV
PR Monitor Filename	cc6mid

Corrosion Rate Measurement Data Sheet Project 1774 Sheet __8___	
Date	5/22/01
Sample ID #	CC6
Sample Location: 6” from bottom	**Comments:** One bar to the left of the bar with clamp
Polarization Data: **PRMonitor:** Ecorr = -504.3 mV Icorr = 3.087 μA/cm^2 Rate = 1.41 mpy	
Concrete Surface Description: Was previously covered with wrap, smooth surface. Extensive cracking noted. Rust stains.	
Half-Cell Potential (mV vs. Cu/CuSO$_4$)	-504 mV
PR Monitor Filename	cc6bot

Appendix D

PHOTOGRAPHS OF STEEL REINFORCING FOR GROUP A

Figure D1 Specimen CC7

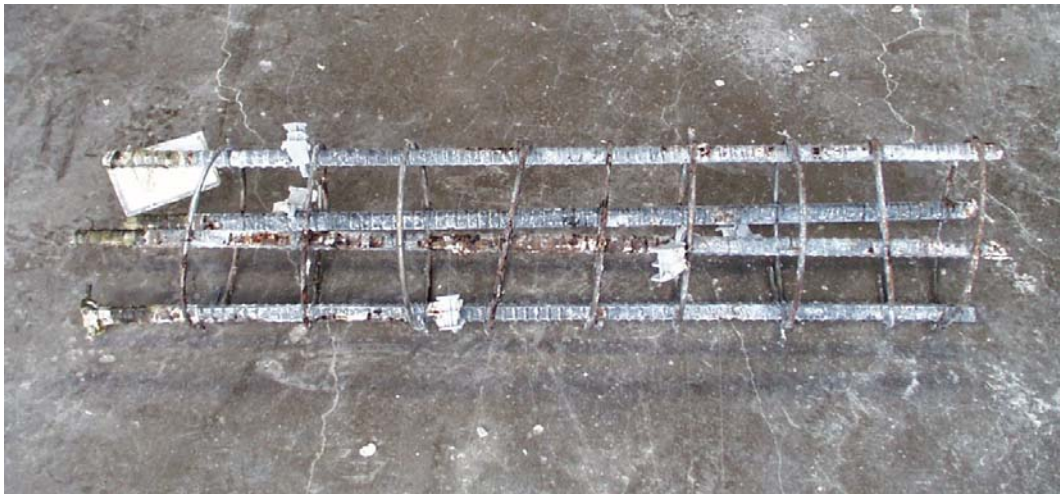

Figure D2 Specimen CC18

Figure D3 Specimen CNC8

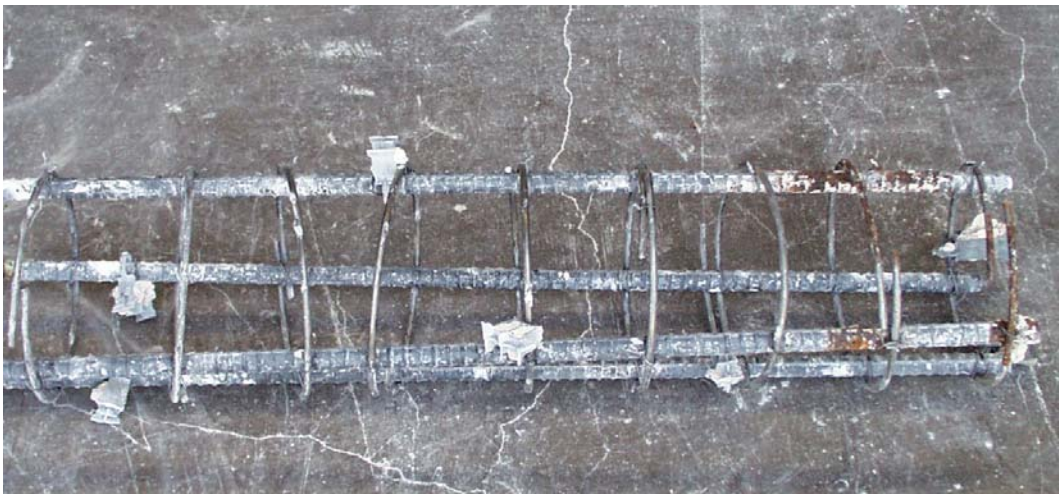

Figure D4 Specimen CNC13

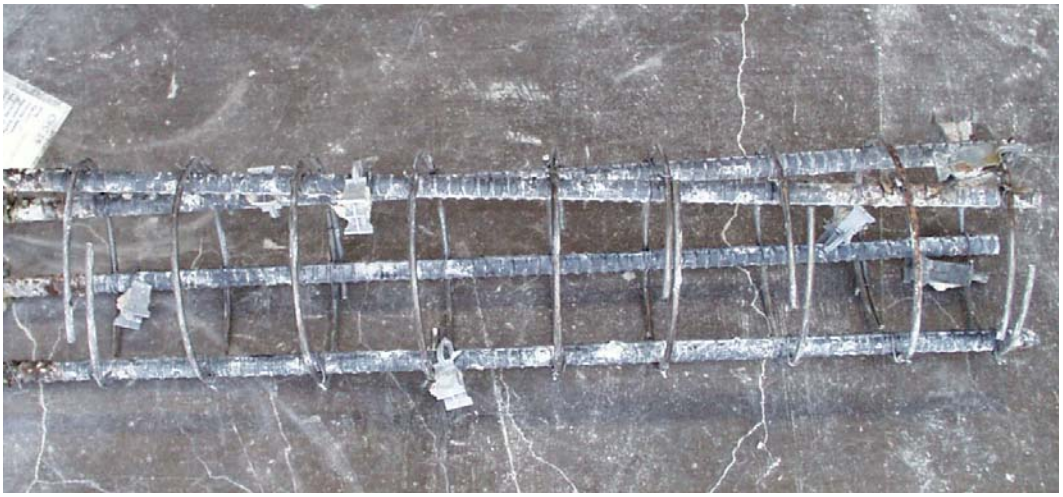

Figure D5 Specimen CNC14

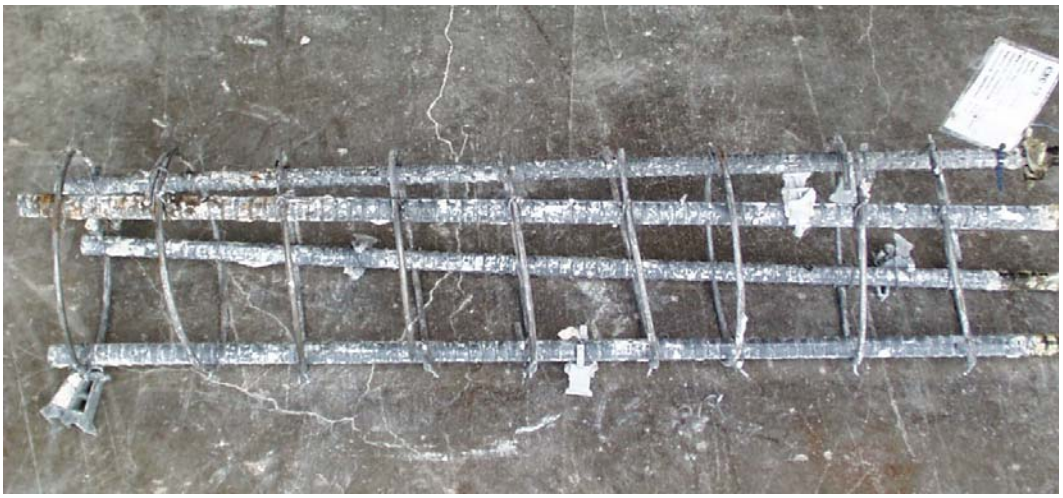

Figure D6 Specimen CNC19

Figure D7 Specimen RC4

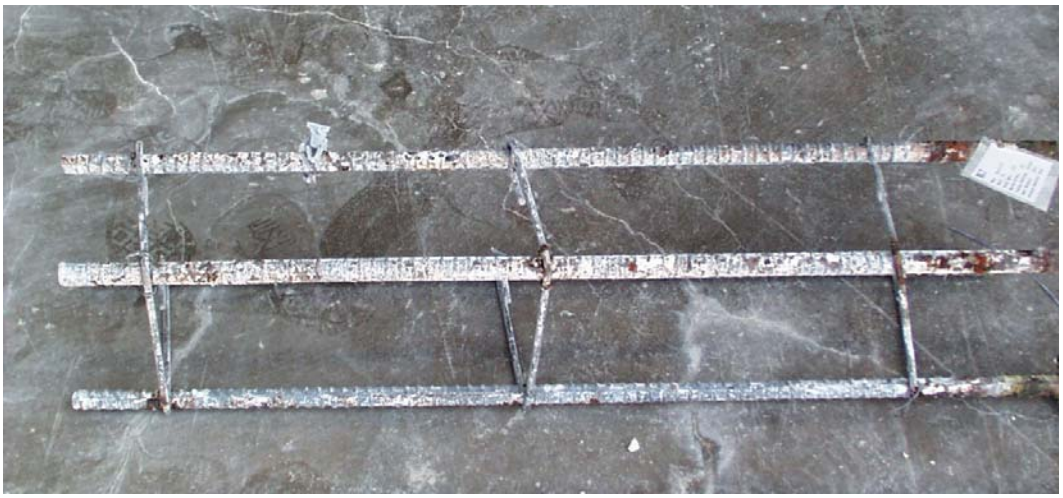

Figure D8 Specimen RC7

PHOTOGRAPHS OF STEEL REINFORCING FOR GROUP B

Figure D9 Specimen CC3

Figure D10 Specimen CC5

Figure D11 Specimen CC6

Figure D12 Specimen CNC10

Figure D13 Specimen RNC6

Figure D14 Specimen RNC7

Appendix E

CORROSION RATE DATA SHEETS FOR EMBEDDED PROBES

Corrosion Rate Measurement Data Sheet Project 1774 Sheet __1___	
Date	5/17/00
Bridge Location	WB 62/82 over Loop 289
Bridge ID #	Structure #7
Sample ID #	7.1
Sample Location: 1st bent from east end.	**Comments:** Located 7.5' from end.
Polarization Data: **PRMonitor:** Ecorr = -243.8 mV Icorr = 0.569 $\mu A/cm^2$ Rate = 0.26 mpy	
Concrete Surface Description: Covered with wrap.	
Half-Cell Potential (mV vs. $Cu/CuSO_4$)	-244 mV
PR Monitor Filename	sam9

Corrosion Rate Measurement Data Sheet Project 1774 Sheet __2___	
Date	5/17/00
Bridge Location	WB 62/82 over Loop 289
Bridge ID #	Structure #7
Sample ID #	7.2
Sample Location: 1st bent from east end.	**Comments:** Located 4' from end. Cord #9.
Polarization Data: **PRMonitor:** Ecorr = -476.6 mV Icorr = 1.598 $\mu A/cm^2$ Rate = 0.73 mpy	
Concrete Surface Description: Covered with wrap.	
Half-Cell Potential (mV vs. $Cu/CuSO_4$)	-477 mV
PR Monitor Filename	sam8

Corrosion Rate Measurement Data Sheet Project 1774 Sheet __3___	
Date	5/17/00
Bridge Location	EB 62/82 over Loop 289
Bridge ID #	Structure #8
Sample ID #	8.1
Sample Location: 4rd bent from east end.	**Comments:** Located 5' from end. Cord #12.
Polarization Data: **PRMonitor:** Ecorr = -328.8 mV Icorr = 0.438 μA/cm^2 Rate = 0.20 mpy	
Concrete Surface Description: Covered with wrap.	
Half-Cell Potential (mV vs. Cu/CuSO$_4$)	-329 mV
PR Monitor Filename	sam6

Corrosion Rate Measurement Data Sheet Project 1774 Sheet __4___	
Date	5/17/00
Bridge Location	EB 62/82 over Loop 289
Bridge ID #	Structure #8
Sample ID #	8.2
Sample Location: 4rd bent from east end.	**Comments:** Located 4' from end. Cord #3.
Polarization Data: **PRMonitor:** Ecorr = -361.9 mV Icorr = 1.357 μA/cm^2 Rate = 0.62 mpy	
Concrete Surface Description: Covered with wrap.	
Half-Cell Potential (mV vs. Cu/CuSO$_4$)	-362 mV
PR Monitor Filename	sam4

Corrosion Rate Measurement Data Sheet Project 1774 Sheet __5___	
Date	5/17/00
Bridge Location	EB 62/82 over Loop 289
Bridge ID #	Structure #8
Sample ID #	8.3
Sample Location: 3rd bent from east end.	**Comments:** Located 5' from end. Cord #3.
Polarization Data: **PRMonitor:** Ecorr = -376.7 mV Icorr = 0.569 μA/cm^2 Rate = 0.26 mpy	
Concrete Surface Description: Covered with wrap.	
Half-Cell Potential (mV vs. Cu/CuSO$_4$)	-377 mV
PR Monitor Filename	sam3

Corrosion Rate Measurement Data Sheet Project 1774 Sheet __6___	
Date	5/17/00
Bridge Location	EB 62/82 over Loop 289
Bridge ID #	Structure #8
Sample ID #	8.4
Sample Location: 3rd bent from east end.	**Comments:** Located 4' from end. Cord #5.
Polarization Data: **PRMonitor:** Ecorr = -351.0 mV Icorr = 0.985 μA/cm^2 Rate = 0.45 mpy	
Concrete Surface Description: Covered with wrap.	
Half-Cell Potential (mV vs. Cu/CuSO$_4$)	-351 mV
PR Monitor Filename	sam2

Corrosion Rate Measurement Data Sheet Project 1774 Sheet __7___	
Date	5/17/00
Bridge Location	EB 84 over FM 400
Bridge ID #	Structure #12
Sample ID #	12.1
Sample Location: 1st bent from west end.	**Comments:** Located 4' from end.
Polarization Data: **PRMonitor:** Ecorr = -304.9 mV Icorr = 3.371 $\mu A/cm^2$ Rate = 1.54 mpy	
Concrete Surface Description: Large area under girders is exposed.	
Half-Cell Potential (mV vs. $Cu/CuSO_4$)	-305 mV
PR Monitor Filename	sam11

Corrosion Rate Measurement Data Sheet Project 1774 Sheet __8___	
Date	5/17/00
Bridge Location	EB 84 over FM 400
Bridge ID #	Structure #12
Sample ID #	12.2
Sample Location: 1st bent from west end.	**Comments:** Located 4' from end.
Polarization Data: **PRMonitor:** Ecorr = -384.2 mV Icorr = 2.693 $\mu A/cm^2$ Rate = 1.23 mpy	
Concrete Surface Description: Large area under girders is exposed.	
Half-Cell Potential (mV vs. $Cu/CuSO_4$)	-384 mV
PR Monitor Filename	sam10

Corrosion Rate Measurement Data Sheet Project 1774 Sheet __9___	
Date	5/17/00
Bridge Location	EB 84 over FM 400
Bridge ID #	Structure #12
Sample ID #	12.3
Sample Location: 3rd bent from west end.	**Comments:** Located 4' from end.
Polarization Data: **PRMonitor:** Ecorr = N/A Icorr = N/A Invalid results Rate = N/A	
Concrete Surface Description: Covered with wrap.	
Half-Cell Potential (mV vs. $Cu/CuSO_4$)	N/A
PR Monitor Filename	sam12

Corrosion Rate Measurement Data Sheet Project 1774 Sheet __10__	
Date	10/19/00
Bridge Location	WB 62/82 over Loop 289
Bridge ID #	Structure #7
Sample ID #	7.1
Sample Location: 1st bent from east end.	**Comments:** Located 7.5' from end.
Polarization Data: **PRMonitor:** Ecorr = -250.6 mV Icorr = 0.372 $\mu A/cm^2$ Rate = 0.17 mpy	
Concrete Surface Description: Covered with wrap. Some debris.	
Half-Cell Potential (mV vs. $Cu/CuSO_4$)	-251 mV
PR Monitor Filename	oct006

Corrosion Rate Measurement Data Sheet Project 1774 Sheet __11__	
Date	10/19/00
Bridge Location	WB 62/82 over Loop 289
Bridge ID #	Structure #7
Sample ID #	7.2
Sample Location: 1st bent from east end.	**Comments:** Located 4' from end. Cord #9.
Polarization Data: **PRMonitor:** Ecorr = -425.7 mV Icorr = 1.094 $\mu A/cm^2$ Rate = 0.50 mpy	
Concrete Surface Description: Covered with wrap. FRP frayed under girder.	
Half-Cell Potential (mV vs. $Cu/CuSO_4$)	-426 mV
PR Monitor Filename	oct005

Corrosion Rate Measurement Data Sheet Project 1774 Sheet __12__	
Date	10/19/00
Bridge Location	EB 62/82 over Loop 289
Bridge ID #	Structure #8
Sample ID #	8.1
Sample Location: 4rd bent from east end.	**Comments:** Located 5' from end. Cord #12.
Polarization Data: **PRMonitor:** Ecorr = -306.3 mV Icorr = 0.241 μA/cm^2 Rate = 0.11 mpy	
Concrete Surface Description: Covered with wrap. Some debris.	
Half-Cell Potential (mV vs. Cu/CuSO$_4$)	-306 mV
PR Monitor Filename	oct004

Corrosion Rate Measurement Data Sheet Project 1774 Sheet __13__	
Date	10/19/00
Bridge Location	EB 62/82 over Loop 289
Bridge ID #	Structure #8
Sample ID #	8.2
Sample Location: 4rd bent from east end.	**Comments:** Located 4' from end. Cord #3.
Polarization Data: **PRMonitor:** Ecorr = -352.3 mV Icorr = 0.941 μA/cm^2 Rate = 0.43 mpy	
Concrete Surface Description: Covered with wrap. Some debris. Wrap pulled away from under girder.	
Half-Cell Potential (mV vs. Cu/CuSO$_4$)	-352 mV
PR Monitor Filename	oct003

Corrosion Rate Measurement Data Sheet Project 1774 Sheet __14__	
Date	10/19/00
Bridge Location	EB 62/82 over Loop 289
Bridge ID #	Structure #8
Sample ID #	8.3
Sample Location: 3rd bent from east end.	**Comments:** Located 5' from end. Cord #3.
Polarization Data: **PRMonitor:** Ecorr = -392.4 mV Icorr = 0.328 μA/cm^2 Rate = 0.15 mpy	
Concrete Surface Description: Covered with wrap. Some debris. Wrap coming up under girders.	
Half-Cell Potential (mV vs. Cu/CuSO$_4$)	-392 mV
PR Monitor Filename	oct20002

Corrosion Rate Measurement Data Sheet Project 1774 Sheet __15__	
Date	10/19/00
Bridge Location	EB 62/82 over Loop 289
Bridge ID #	Structure #8
Sample ID #	8.4
Sample Location: 3rd bent from east end.	**Comments:** Located 4' from end. Cord #5.
Polarization Data: **PRMonitor:** Ecorr = -460.6 mV Icorr = 0.788 μA/cm^2 Rate = 0.36 mpy	
Concrete Surface Description: Covered with wrap. Some debris.	
Half-Cell Potential (mV vs. Cu/$CuSO_4$)	-461 mV
PR Monitor Filename	oct001

Corrosion Rate Measurement Data Sheet Project 1774 Sheet __16__	
Date	10/19/00
Bridge Location	EB 84 over FM 400
Bridge ID #	Structure #12
Sample ID #	12.1
Sample Location: 1st bent from west end.	**Comments:** Located 4' from end.
Polarization Data: **PRMonitor:** Ecorr = -315.8 mV Icorr = 0.591 $\mu A/cm^2$ Rate = 0.27 mpy	
Concrete Surface Description: Wrap is not well grouted around bearing pad.	
Half-Cell Potential (mV vs. $Cu/CuSO_4$)	-316 mV
PR Monitor Filename	oct008

Corrosion Rate Measurement Data Sheet Project 1774 Sheet __17__	
Date	10/19/00
Bridge Location	EB 84 over FM 400
Bridge ID #	Structure #12
Sample ID #	12.2
Sample Location: 1st bent from west end.	**Comments:** Located 4' from end.
Polarization Data: **PRMonitor:** Ecorr = -303.0 mV Icorr = 2.080 $\mu A/cm^2$ Rate = 0.95 mpy	
Concrete Surface Description: Wrap is not well grouted around bearing pad.	
Half-Cell Potential (mV vs. $Cu/CuSO_4$)	-303 mV
PR Monitor Filename	oct007

Corrosion Rate Measurement Data Sheet Project 1774 Sheet __18__	
Date	10/19/00
Bridge Location	EB 84 over FM 400
Bridge ID #	Structure #12
Sample ID #	12.3
Sample Location: 3rd bent from west end.	**Comments:** Located 4' from end.
Polarization Data: **PRMonitor:** Ecorr = N/A Icorr = N/A Invalid results Rate = N/A	
Concrete Surface Description: Covered with wrap.	
Half-Cell Potential (mV vs. $Cu/CuSO_4$)	N/A
PR Monitor Filename	oct009

Corrosion Rate Measurement Data Sheet Project 1774 Sheet __19__	
Date	5/30/01
Bridge Location	WB 62/82 over Loop 289
Bridge ID #	Structure #7
Sample ID #	7.1
Sample Location: 1st bent from east end.	**Comments:** Located 7.5' from end.
Polarization Data: **PRMonitor:** Ecorr = -252.5 mV Icorr = 0.372 $\mu A/cm^2$ Rate = 0.17 mpy	
Concrete Surface Description: Covered with wrap. Dirt and debris. Wrap around bearing pad is not painted. Smoother finish around bearing pad than ID #7.1.	
Half-Cell Potential (mV vs. $Cu/CuSO_4$)	-253 mV
PR Monitor Filename	may006

Corrosion Rate Measurement Data Sheet Project 1774 Sheet __20__	
Date	5/30/01
Bridge Location	WB 62/82 over Loop 289
Bridge ID #	Structure #7
Sample ID #	7.2
Sample Location: 1st bent from east end.	**Comments:** Located 4' from end. Cord #9.
Polarization Data: **PRMonitor:** Ecorr = -527.6 mV Icorr = 1.817 $\mu A/cm^2$ Rate = 0.83 mpy	
Concrete Surface Description: Covered with wrap. Dirt and debris. Wrap is very frayed and not painted along bearing pad.	
Half-Cell Potential (mV vs. $Cu/CuSO_4$)	-528 mV
PR Monitor Filename	may005

Corrosion Rate Measurement Data Sheet Project 1774 Sheet __21__	
Date	5/30/01
Bridge Location	EB 62/82 over Loop 289
Bridge ID #	Structure #8
Sample ID #	8.1
Sample Location: 4rd bent from east end.	**Comments:** Located 5' from end. Cord #12.
Polarization Data: **PRMonitor:** Ecorr = -344.0 mV Icorr = 0.438 μA/cm^2 Rate = 0.20 mpy	
Concrete Surface Description: Covered with wrap. Dirt and debris. Paint is starting to wear away. Wrap is frayed along bearing pad.	
Half-Cell Potential (mV vs. Cu/CuSO$_4$)	-344 mV
PR Monitor Filename	may004

Corrosion Rate Measurement Data Sheet Project 1774 Sheet __22__	
Date	5/30/01
Bridge Location	EB 62/82 over Loop 289
Bridge ID #	Structure #8
Sample ID #	8.2
Sample Location: 4rd bent from east end.	**Comments:** Located 4' from end. Cord #3.
Polarization Data: **PRMonitor:** Ecorr = -384.3 mV Icorr = 1.423 μA/cm^2 Rate = 0.65 mpy	
Concrete Surface Description: Covered with wrap. Dirt and debris. Paint is starting to wear away. Wrap is frayed along bearing pad.	
Half-Cell Potential (mV vs. Cu/CuSO$_4$)	-384 mV
PR Monitor Filename	may003

Corrosion Rate Measurement Data Sheet Project 1774 Sheet __23__	
Date	5/30/01
Bridge Location	EB 62/82 over Loop 289
Bridge ID #	Structure #8
Sample ID #	8.3
Sample Location: 3rd bent from east end.	**Comments:** Located 5' from end. Cord #3.
Polarization Data: **PRMonitor:** Ecorr = -395.4 mV Icorr = 1.226 μA/cm^2 Rate = 0.56 mpy	
Concrete Surface Description: Covered with wrap. Dirt and debris.	
Half-Cell Potential (mV vs. Cu/CuSO$_4$)	-395 mV
PR Monitor Filename	may002

Corrosion Rate Measurement Data Sheet Project 1774 Sheet __24__	
Date	5/30/01
Bridge Location	EB 62/82 over Loop 289
Bridge ID #	Structure #8
Sample ID #	8.4
Sample Location: 3rd bent from east end.	**Comments:** Located 4' from end. Cord #5.
Polarization Data: **PRMonitor:** Ecorr = -358.9 mV Icorr = 1.313 μA/cm^2 Rate = 0.60 mpy	
Concrete Surface Description: Covered with wrap. Dirt and debris.	
Half-Cell Potential (mV vs. Cu/$CuSO_4$)	-359 mV
PR Monitor Filename	may001

Corrosion Rate Measurement Data Sheet Project 1774 Sheet __25__	
Date	5/30/01
Bridge Location	EB 84 over FM 400
Bridge ID #	Structure #12
Sample ID #	12.1
Sample Location: 1st bent from west end.	**Comments:** Located 4' from end.
Polarization Data: **PRMonitor:** Ecorr = -392.2 mV Icorr = 2.189 $\mu A/cm^2$ Rate = 1.00 mpy	
Concrete Surface Description: Large area under girders is exposed. Wrap is starting to fray. Dirt and debris.	
Half-Cell Potential (mV vs. $Cu/CuSO_4$)	-392 mV
PR Monitor Filename	may008

Corrosion Rate Measurement Data Sheet Project 1774 Sheet __26__	
Date	5/30/01
Bridge Location	EB 84 over FM 400
Bridge ID #	Structure #12
Sample ID #	12.2
Sample Location: 1st bent from west end.	**Comments:** Located 4' from end.
Polarization Data: **PRMonitor:** Ecorr = -435.7 mV Icorr = 2.452 $\mu A/cm^2$ Rate = 1.12 mpy	
Concrete Surface Description: Large area under girders is exposed. Wrap is starting to fray. Dirt and debris.	
Half-Cell Potential (mV vs. $Cu/CuSO_4$)	-436 mV
PR Monitor Filename	may007

Appendix F

CORRESPONDENCE INHIBITORS SHEETS*

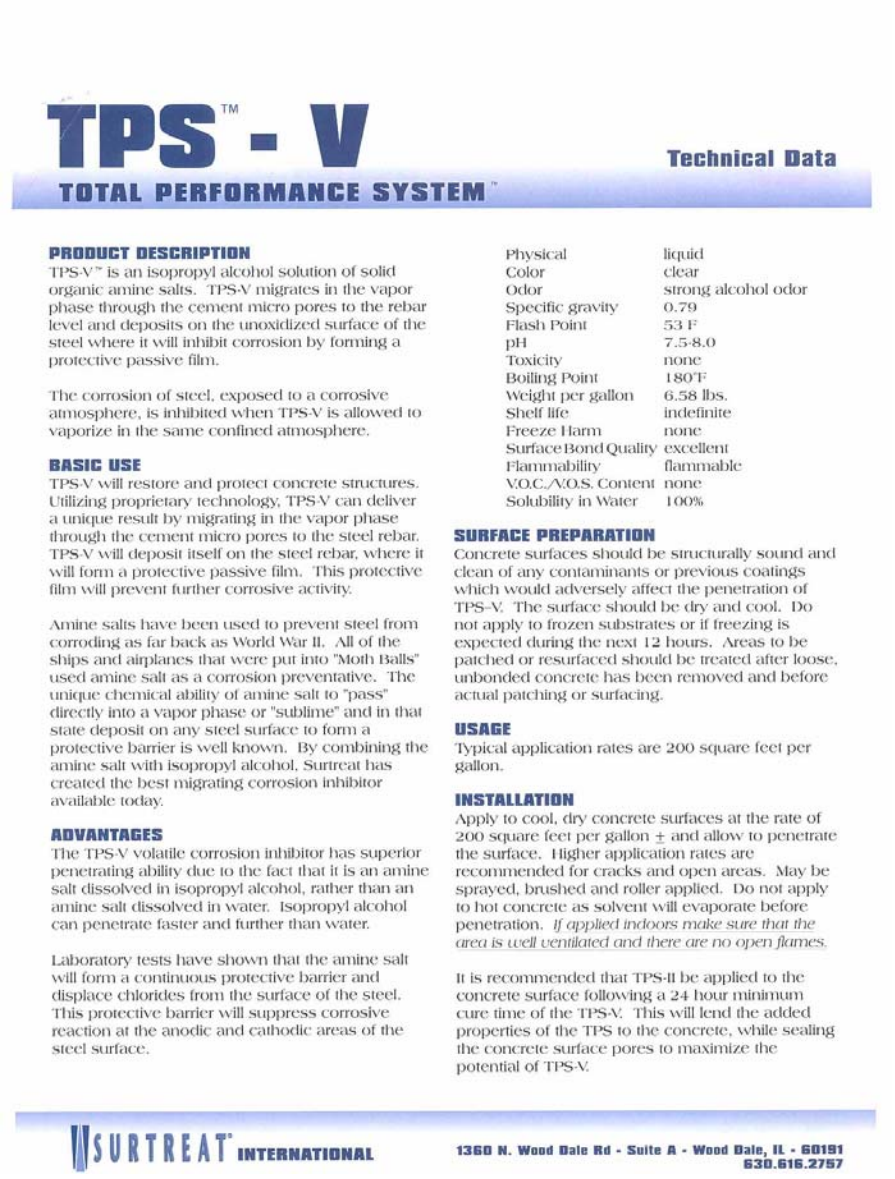

TPS™ - V

TOTAL PERFORMANCE SYSTEM™

Technical Data

PRODUCT DESCRIPTION

TPS-V™ is an isopropyl alcohol solution of solid organic amine salts. TPS-V migrates in the vapor phase through the cement micro pores to the rebar level and deposits on the unoxidized surface of the steel where it will inhibit corrosion by forming a protective passive film.

The corrosion of steel, exposed to a corrosive atmosphere, is inhibited when TPS-V is allowed to vaporize in the same confined atmosphere.

BASIC USE

TPS-V will restore and protect concrete structures. Utilizing proprietary technology, TPS-V can deliver a unique result by migrating in the vapor phase through the cement micro pores to the steel rebar. TPS-V will deposit itself on the steel rebar, where it will form a protective passive film. This protective film will prevent further corrosive activity.

Amine salts have been used to prevent steel from corroding as far back as World War II. All of the ships and airplanes that were put into "Moth Balls" used amine salt as a corrosion preventative. The unique chemical ability of amine salt to "pass" directly into a vapor phase or "sublime" and in that state deposit on any steel surface to form a protective barrier is well known. By combining the amine salt with isopropyl alcohol, Surtreat has created the best migrating corrosion inhibitor available today.

ADVANTAGES

The TPS-V volatile corrosion inhibitor has superior penetrating ability due to the fact that it is an amine salt dissolved in isopropyl alcohol, rather than an amine salt dissolved in water. Isopropyl alcohol can penetrate faster and further than water.

Laboratory tests have shown that the amine salt will form a continuous protective barrier and displace chlorides from the surface of the steel. This protective barrier will suppress corrosive reaction at the anodic and cathodic areas of the steel surface.

Physical	liquid
Color	clear
Odor	strong alcohol odor
Specific gravity	0.79
Flash Point	53 F
pH	7.5-8.0
Toxicity	none
Boiling Point	180F
Weight per gallon	6.58 lbs.
Shelf life	indefinite
Freeze Harm	none
Surface Bond Quality	excellent
Flammability	flammable
V.O.C./V.O.S. Content	none
Solubility in Water	100%

SURFACE PREPARATION

Concrete surfaces should be structurally sound and clean of any contaminants or previous coatings which would adversely affect the penetration of TPS–V. The surface should be dry and cool. Do not apply to frozen substrates or if freezing is expected during the next 12 hours. Areas to be patched or resurfaced should be treated after loose, unbonded concrete has been removed and before actual patching or surfacing.

USAGE

Typical application rates are 200 square feet per gallon.

INSTALLATION

Apply to cool, dry concrete surfaces at the rate of 200 square feet per gallon ± and allow to penetrate the surface. Higher application rates are recommended for cracks and open areas. May be sprayed, brushed and roller applied. Do not apply to hot concrete as solvent will evaporate before penetration. *If applied indoors make sure that the area is well ventilated and there are no open flames.*

It is recommended that TPS-II be applied to the concrete surface following a 24 hour minimum cure time of the TPS-V. This will lend the added properties of the TPS to the concrete, while sealing the concrete surface pores to maximize the potential of TPS-V.

SURTREAT® INTERNATIONAL

1360 N. Wood Dale Rd - Suite A - Wood Dale, IL - 60191
630.616.2757

* Reproduced from Manufacturers' Product Data Sheets

PRECAUTIONS
Flammable formulation containing isopropyl alcohol. Use in a well ventilated area and avoid exposure to ignition sources.

WALLS AND STEEP SLOPES
Apply TPS-V, as described above, from the bottom up with a fan spray pattern overlapping 20 to 30%.

CLEAN UP
Clean equipment using water and mild soap. Never store spray equipment without cleaning and following manufacturer's recommendations for storage between usage.

SHELF LIFE
Shelf life is indefinite provided containers are kept tightly sealed when not in use.

PACKAGING
TPS-V is packaged in 5 gallon containers. 55 gallon drums are available upon request.

MAINTENANCE
Special maintenance of treated area is not required.

TECHNICAL SERVICES
Technical information and assistance in addition to this data can be obtained from the TPS Technical Services Department at 412-281-1202.

TEST RESULTS
Laboratory test reports from Pittsburgh testing laboratories are available. Contact your local agent or call 412-281-1202.

WARNING
Avoid contact with skin or eyes. May cause irritation. If on skin: wash promptly with soap and water. Get medical attention if irritation occurs. if in eyes: rinse with plenty of water for at least 15 minutes. If swallowed: Do not induce vomiting. Drink plenty of water, call physician. Misuse of empty containers can be hazardous. Do not reuse containers. Cutting, welding or exposure to open flame, heat or pressure may cause fire or explosion of toxic fumes and residues. Drain container completely, seal bung hole, and dispose of container in a proper manner.

HAZARD INDEX
4 - Severe hazard
3 - Serious hazard
2 - Moderate hazard
1 - Slight hazard
0 - Minimal hazard

HEALTH	**1**
FLAMMABILITY	**3**
REACTIVITY	**1**

PERSONAL PROTECTION
SAFETY GLASSES & GLOVES

SURTREAT® INTERNATIONAL
1360 N. Wood Dale Rd - Suite A - Wood Dale, IL - 60191
630.616.2757

Sika FerroGard® 903

3/00

Penetrating, corrosion inhibiting, impregnation coating for hardened concrete

DESCRIPTION

Sika FerroGard 903 is a corrosion inhibiting impregnation coating for hardened concrete surfaces. It is designed to penetrate the surface and then to diffuse in vapor or liquid form to the steel reinforcing bars embedded in the concrete. Sika FerroGard 903 forms a protective layer on the steel surface which inhibits corrosion caused by the presence of chlorides as well as by carbonation of concrete.

HOW IT WORKS

Sika FerroGard 903 is a combination of aminoalcohols, and organic and inorganic inhibitors that protects both the anodic and cathodic parts of the corrosion cell. This dual action effect dramatically delays the initiation of corrosion and greatly reduces the overall corrosion activity.

Sika FerroGard 903 protects the embedded steel by depositing a physical barrier in the form of a protective layer on the surface of the steel reinforcement. This barrier inhibits corrosion of the steel.

WHERE TO USE

Sika FerroGard 903 is recommended for all steel-reinforced, prestressed, precast, post tensioned or marine concrete. Use of Sika FerroGard 903:

- ▲ Steel-reinforced concrete, bridges and highways exposed to corrosive environments (deicing salts, weathering)
- ▲ Building facades and balconies
- ▲ Steel-reinforced concrete in or near a marine environment
- ▲ Parking garages
- ▲ Piers, piles, and concrete dock structures
- ▲ As part of Sika's system approach for buildings and civil engineering structures

ADVANTAGES

Sika FerroGard 903 offers owners, specifiers, port authorities, DOTs, and engineers, a new technology in corrosion inhibition that can easily be applied to the surface of existing concrete to extend the service life of any reinforced concrete structure.

- ▲ Protects against the harmful effects of corrosion by penetrating the surface of even the most dense concrete and diffusing to the steel to inhibit corrosion.
- ▲ Enhances the durability of reinforced concrete.
- ▲ Does not require concrete removal.
- ▲ Environmentally sound.
- ▲ Does not contain calcium nitrite.
- ▲ Easily applied by either spray or roller to all existing reinforced concrete.

TYPICAL DATA FOR SIKA FERROGARD 903 (at 73F / 23C)	
SHELF LIFE	18 month minimum in original, unopened container
STORAGE CONDITIONS	Store at 40-95F (4-35C). Protect from freezing. If frozen, discard.
COLOR	Pale Yellow
VISCOSITY	15 cps
FLASH POINT	None (water based)
DENSITY	1.13 (9.4 lbs./gal.)
pH	11 (±1)
APPLICATION RATE	100-150 ft²/gal. total application rate

SIGNIFICANT PROOF OF PERFORMANCE

Key Criteria	Performance Level	Test Method/ Institute
Corrosion inhibition	FerroGard corrosion inhibitors delay the onset of corrosion and reduce the rate of corrosion by 65% versus control specimen after 1 year.	1
Penetration Rate in hardened concrete	FerroGard 903 penetrates independently of orientation (horizontal, vertical, overhead) at a rate of 1/10 to 4/5 inches (2.5 to 20 mm)per day, depending on the density of the concrete.	2
Depth of Penetration	FerroGard 903 penetrates at least 3 inches (76 mm) in 28 days.	2
Protective layer on steel	FerroGard 903 forms a protective layer on the reinforcing steel of high integrity measured at 100 Å thickness.	3
Displacement of chlorides from steel surface	FerroGard 903 forms a continuous film on the reinforcing steel and displaces chloride ions from the steel surface.	3

Test Method/Institute:

1. Cracked Concrete Beam Test (adapted from ASTM G109).
2. Secondary Neutron Mass Spectroscopy (SNMS) / Institute for Radiochemistry, Karlsruhe (Germany), Prof. Dr. J. Goschnick.
3. X-ray Photon Spectroscopy (XPS) and Secondary Ion Mass Spectroscopy (SIMS) / Brundle and Associates, San Jose, CA and University Heidelberg (Germany), Prof. M. Grunze.

- ▲ Can be applied to reinforced concrete that already exhibits corrosion.
- ▲ Adds additional benefits when used prior to protective coatings in concrete restoration systems.
- ▲ Water based for easy handling and application.
- ▲ Not a vapor barrier; allows vapor diffusion.
- ▲ FerroGard has been proven effective in both laboratory (ASTM G109/Cracked Beams) and field analysis.

COVERAGE

For normal concrete, application is 200-300 ft²/gal. each coat. A minimum of two coats is always required.

For dense concrete, application may exceed 300 ft²/gal. Therefore, more than two coats may be required to achieve the **total application rate: 100-150 ft²/gal.**

PACKAGING

5 gallon pails with spout, 55 gallon drums.

HOW TO USE

SURFACE PREPARATION

Before applying Sika FerroGard 903 be sure the surface is clean and sound. Remove all dirt, dust, oil, grease, efflorescence or existing coatings from concrete surface by steam cleaning, waterblasting or slightly sandblasting. Allow concrete surface to dry prior to application of Sika FerroGard 903. The dryer the surface the better the penetration and effectiveness.

APPLICATION

Sika FerroGard 903 is applied by roller, brush or spray on concrete surfaces. When spraying, use a conventional airless spray system or hand-pressure equipment. **A minimum of two coats is always required.** Dense substrates may require more coats. Waiting time between coats of Sika FerroGard 903 is at least 1 hour.

When Sika FerroGard 903 is used prior to the application of a repair mortar or a concrete overlay, care must be taken to remove any residue from the treatment before the mortar or concrete is applied. This can be achieved by carefully rinsing with water, pressure washing or grit blasting. Allow a minimum of 1 day to allow Sika FerroGard 903 to dry and penetrate. The use of Sika Armatec 110 EpoCem as a bonding agent prior to the application of repair mortars or concrete overlays is suggested.

If substrates treated with Sika FerroGard 903 are to be overcoated (protective coatings, Sikafloor Systems, etc.), any residue from the treatment must be removed by carefully rinsing with water, pressure washing or grit blasting. After that, allow the substrate to dry before applying coatings. Drying time depends on environmental conditions, absorbency of the substrate and maximum recommended moisture content for the subsequently applied system.

LIMITATIONS

- ▲ Minimum ambient and substrate temperatures 35F.
- ▲ Do not apply when temperature is expected to fall below 35F within 12 hours.
- ▲ Substrate should be as dry as possible prior to the application.
- ▲ Protect glass, wood, brick, galvanized steel, copper and exposed aluminum during the application.
- ▲ Maximum chloride content of concrete structures intended to be treated with Sika FerroGard 903 is 6 lbs./y³ (measured at the level of the reinforcing steel). For levels up to 10 lbs./y³, consult technical service.

CAUTION

Irritant - Skin and eye irritant. Vapors may cause respiratory tract irritation. Use only with adequate ventilation. Use of safety goggles and chemical resistant gloves is recommended. Remove contaminated clothing.

FIRST AID

In case of skin contact, wash thoroughly with soap and water. For eye contact, flush immediately with plenty of water for at least 15 minutes; contact physician immediately. For respiratory problems, remove person to fresh air. Wash clothing before re-use.

CLEAN UP:

In case of spills or leaks, wear suitable protective equipment, contain spill, collect with absorbent material, and transfer to a suitable container. Ventilate area. Avoid contact. Dispose of in accordance with current, applicable local, state, and federal regulations.

Product Code 197-643. Sika and FerroGard are registered trademarks. Made in USA. Printed in USA. March, 2000.

KEEP CONTAINER TIGHTLY CLOSED **KEEP OUT OF REACH OF CHILDREN**

NOT FOR INTERNAL CONSUMPTION **FOR INDUSTRIAL USE ONLY**

CONSULT MATERIAL SAFETY DATA SHEET FOR MORE INFORMATION

Sika warrants its products to be free from manufacturing defects and to meet Sika's current published properties when applied in accordance with Sika directions and tested in accordance with ASTM and Sika Standards. User determines suitability of product for use and assumes all risks. Buyer's sole remedy shall be limited to the purchase price or replacement of product and excludes labor or the cost of labor. Any claim for breach of this warranty must be brought within one year of the date of purchase.

NO OTHER WARRANTIES EXPRESSED OR IMPLIED INCLUDING ANY WARRANTY OF MERCHANTIBILITY OR FITNESS FOR A PARTICULAR PURPOSE SHALL APPLY. SIKA SHALL NOT BE LIABLE FOR ANY CONSEQUENTIAL OR SPECIAL DAMAGES OF ANY KIND, RESULTING FROM ANY CLAIM OF BREACH OF WARRANTY, BREACH OF CONTRACT, NEGLIGENCE OR ANY LEGAL THEORY. SIKA ASSUMES NO LIABILITY FOR USE OF THIS PRODUCT IN A MANNER TO INFRINGE ON ANOTHER'S PATENT.

Visit our website at www.sikausa.com
1-800-933-SIKA NATIONWIDE
Regional Information and Sales Centers
For the location of your nearest Sika sales office, contact your regional center.

Sika Corporation
201 Polito Avenue
Lyndhurst, NJ 07071
Phone: 800-933-7452
Fax: 201-933-6225

Sika Canada Inc.
601 Delmar Avenue
Pointe Claire
Quebec H9R 4A9
Phone: 514-697-2610
Fax: 514-694-2792

Sika Mexicana S.A. de C.V.
Carretera Libre Celaya Km. 8.5
Corregidora, Queretaro
C.P. 76920 A.P. 136
Phone: 52 42 25 0122
Fax: 52 42 25 0537

Quality Certification Numbers: Lyndhurst: 93-062B, Marion: 93-086B, Kansas City: 94-258B, Santa Fe Springs: 94-195C

MIGRATORY CORROSION INHIBITOR™ (MCI®) PRODUCTS FOR CONCRETE

MCI-2020

PRODUCT DESCRIPTION

MCI-2020 is a surface applied corrosion inhibitor designed to migrate through even the densest concrete structures and seek out the steel reinforcement bars in concrete. MCI-2020 also protects a multitude of metals including carbon steel, galvanized steel and aluminum. The unique feature of Migrating Corrosion Inhibitors™ (MCI®) is that if not in direct contact with metals, the inhibitor will migrate a considerable distance through concrete to provide protection. MCI-2020 will stop further corrosion of reinforcing metals and extend the service life of the structure. A high viscosity version of MCI-2020 is available-MCI-2020 HV, specifically designed for vertical and overhead applications.

WHERE TO USE

MCI-2020 is recommended for:

- All reinforced, precast, prestressed, post-tensioned or marine concrete structures
- Steel-reinforced concrete bridges, highways and streets exposed to corrosive environments (carbonation, deicing salts and atmospheric attack)
- Parking decks, ramps and garages
- Preventive maintenance of all reinforced concrete commercial and civil engineered structures
- Concrete piers, dams, offshore platforms, piles, pillars, pipes and utility poles
- Restoration and repair of all reinforced concrete commercial and civil engineered structures
- Plant floors subject to chemical and/or acid attack
- Buildings and foundations of all types
- Cooling towers and portable water tanks

ADVANTAGES

- MCI-2020 offers engineers, owners, contractors, DOTs and government agencies a time proven corrosion inhibiting technology that will extend the life of all reinforced concrete structures.
- Protects against the harmful effects of corrosion by migrating into even in the densest concrete
- Migrating corrosion inhibitor reduces further corrosion of the most rusted metals
- Easily applied by spray, roller, squeegee or paint brush to any concrete surface, reducing the high cost of labor and equipment
- Does not contain any calcium nitrite
- Water-based and non-flammable for easy handling
- Does not require the removal of sound concrete
- Organic, safe and environmentally friendly
- Enhances the durability of reinforced concrete
- Lab and field tested worldwide
- Allows concrete to breathe and vapor to diffuse, is not a vapor barrier
- Protects both anodic and cathodic areas
- Proven effective in the Strategic Highway Research Program (SHRP) funded by the federal government and state DOTs
- NSF approved for potable water applications (certified by Underwriters Laboratories)
- Confirmed effective in international documented field evaluation (ASTM G-109, JIS, Korean, etc.)
- Proven to migrate to adjacent areas to protect surrounding metals
- No cure time is required. Traffic may resume minutes after application, if necessary
- Available in high viscostiy form for hard-to-reach or vertical surfaces

CORTEC CORPORATION
Environmentally Safe VCI/MCI® Technologies

COVERAGE
150 ft²/1.7 lb. Dense substrates may require two coats at the rate of 2.4 lb (5.52 m²/1 kg).

PACKAGING
MCI-2020 and MCI-2020 HV is available in 5 gallon (19 liter) pails and 55 gallon (208 liter) drums.

SURFACE PREPARATION
Surface should be dry, sound, clean and free of all dirt, oil, grease efflorescence, sealers, coatings, membranes and asphalt. Cleaning may be done by steam cleaning, water-blasting or sandblasting.

APPLICATION
Apply the solution by spray (conventional airless or hand pressure spray equipment), roller, squeegee or paint brush to any concrete surface. Dense substrates may require two coats with a minimum of 7.5 hours between coats. When applying a sealer, coating, repair mortar or concrete overlay, the surface should be rinsed with water, pressure washed or blastcleaned to remove any residue.

LIMITATIONS
The substrate and ambient temperature should be above freezing and below 125°F (50°C). Do not apply if the temperature is expected to fall below freezing within 12 hours. MCI® will not penetrate film-forming sealers, coatings, paints, membranes or asphalt.

PHYSICAL PROPERTIES

MCI-2020	
Specific gravity	1.03 - 1.05
Appearance	Clear amber
pH	9.0 - 9.5
Flash point	N/A (Water-based)
Storage/Shelf Life	24 months in sealed drums
Storage	Minimum 32°F(0°C) Maximum 212°F(100°F) *Do not freeze*

MCI-2020 HV	
Specific gravity	1.03 - 1.06
Appearance	Clear, yellow, viscous
pH	9.0 - 9.7
Non volatile content	20 - 27%
Viscosity	2600 cps at room temperature
Flash point	N/A (Water-based)
Storage/Shelf Life	24 months in sealed drums
Storage	Minimum 32°F(0°C) Maximum 212°F(100°F) *Do not freeze*

MCI® Migrating Corrosion Inhibitor™ is a registered trademark of Cortec Corporation.

FOR INDUSTRIAL USE ONLY
KEEP OUT OF REACH OF CHILDREN
KEEP CONTAINER TIGHTLY CLOSED
NOT FOR INTERNAL CONSUMPTION
CONSULT MATERIAL SAFETY DATA SHEET FOR MORE INFORMATION

LIMITED WARRANTY

All statements, technical information and recommendations contained herein are based on tests Cortec Corporation believes to be reliable but the accuracy or completeness thereof is not guaranteed.

Cortec Corporation warrants Cortec® products will be free from defects when shipped to customer. Cortec Corporation's obligation under this warranty shall be limited to replacement of product that proves to be defective. No ribbon replacement product under this warranty the customer must notify Cortec Corporation of the claimed defect within six months after shipment of product to customer. All freight charges for replacement products shall be paid by customer.

Cortec Corporation shall have no liability for any injury, loss or damage arising out of the use of or the inability to use the products.

BEFORE USING, USER SHALL DETERMINE THE SUITABILITY OF THE PRODUCT FOR ITS INTENDED USE, AND USER ASSUMES ALL RISK AND LIABILITY WHATSOEVER IN CONNECTION THEREWITH. No representation or recommendation not contained herein shall have any force or effect unless in a written document signed by an officer of Cortec Corporation.

THE FOREGOING WARRANTY IS EXCLUSIVE AND IN LIEU OF ALL OTHER WARRANTIES, EXPRESS, IMPLIED OR STATUTORY, INCLUDING WITHOUT LIMITATION ANY IMPLIED WARRANTY OF MERCHANTABILITY OR OF FITNESS FOR A PARTICULAR PURPOSE. IN NO CASE SHALL CORTEC CORPORATION BE LIABLE FOR INCIDENTAL OR CONSEQUENTIAL DAMAGES.

CORTEC CORPORATION
4119 White Bear Parkway, St. Paul, MN 55110 USA
Phone (651) 429-1100, Fax (651) 429-1122
Toll Free (800) 4-CORTEC, E-mail info@cortecvci.com
Internet http://www.cortecvci.com

Distributed by:

Bibliography

Abu-Tair, A.L., E. Burley, and S.R. Rigden. (1995). "Evaluating the Pull-Off Bond Strength of Three Repair Materials Subjected to Different Loading and Exposure Conditions," *Proceedings of the Fifth International Conference, Structural Faults and Repairs*, Volume 2, Engineering Technics Press, Edinburgh, UK, pp. 355-364.

Allen, R.T.L., S.C. Edwards, and J.D.N. Shaw, ed. (1993). The Repair of Concrete Structures, Second Edition, Blackie Academic & Professional, Glasgow, UK.

American Concrete Institute. (1995). Building Code Requirements for Structural Concrete (ACI 318-95) and Commentary (ACI 318R-95), American Concrete Institute, Farmington Hills, MI.

American Concrete Institute. (1992). "Control of Cracking in Concrete Structures," 224R-92, American Concrete Institute, Detroit, MI.

American Society of Civil Engineers. (2001). "Report Card for America's Infrastructure: Bridges," American Society of Civil Engineers.

ASTM. (1989). "Standard Test Method for Half-Cell Potential of Uncoated Reinforcing Steel in Concrete," Annual Book of ASTM Standards, Designation: C876-87, ASTM, West Conshohocken, PA, pp. 428-432.

Babaei, Khossrow and Neil M. Hawkins. (1991). "Evaluation of Bridge Deck Protective Strategies," Concrete Durability: Corrosion Protection, ACI Compilation 25, American Concrete Institute, Detroit, MI, pp. 18-28.

Ballinger, Craig A. (1991). "Development of Composites for Civil Engineering," Advanced Composites Materials in Civil Engineering Structures, American Society of Civil Engineers, NY.

Bassett, Susan. (1998). Composites for Infrastructure: A guide for Civil Engineers, Ray Publishing, Wheat Ridge, CO.

Berke, Neal S. (1991). "Corrosion Inhibitors in Concrete," Concrete Durability: Corrosion Protection, ACI Compilation 25, American Concrete Institute, Detroit, MI, pp. 14-17

.

Broomfield, John P. (1997). Corrosion of Steel in Concrete, E.& F.N. Spon, London, UK.

Concorr. (1998). "Corrosion Rate Probe and Connection Detail," Concorr, Inc., Ashburn, VA.

Corrosion Monitoring Systems. (2000). VETEK Product Information.

Cortec Corporation. (2000). MCI-2020 Product Data Sheet.

CRC Handbook on Nondestructive Testing of Concrete. (1991). CRC Press, Boca Raton, FL.

Delta Structural Technology, Inc. (2000). Composite Fiberwrap, Delta Structural Technology, Inc., Humble, TX.

Emmons, Peter H., Alexander M. Vaysburd, and Jay Thomas. (1998). "Strengthening Concrete Structures, Part II," *Concrete International*, April, pp. 56-60.

Erki, M.A. and S.H. Rizkalla. (1993). "FRP Reinforcement for Concrete Structures," *Concrete International*, June, pp. 48-53.

Feld, Jacob and Kenneth L. Carper. (1997). Construction Failure, Second Edition, John Wiley & Sons, Inc., NY.

Ferguson Structural Engineering Laboratory. (1999). "Effect of Wrapping Chloride Contaminated Structural Concrete With Layers of Glass Fiber/Composites and Resin," Center for Transportation Research, Austin, TX.

Fuentes, Laura Alexandra. (1999). "Implementation of Composite Wrapping Systems on Reinforced Concrete Structures Exposed to a Corrosive Laboratory Environment," Thesis, Civil Engineering Department, University of Texas at Austin.

Fyfe, Edward R., (1995). "Testing and Field Performance of High Strength Fiber Wrapping System," Restructuring: America and Beyond, *Proceedings of Structures Congress XIII*, Volume 1, pp. 603-606.

Gaynor, R. (1987). "Understanding Chloride Percentages," Corrosion, Concrete, and Chlorides. Steel Corrosion in Concrete: Causes and Restraints, (SP102-11), American Concrete Institute, Detroit, MI, pp. 161-165.

Gu, Ping, et al. (1997). "Electrochemical Incompatibility of Patches in Reinforced Concrete," *Concrete International*, August, pp. 68-72.

Hansson, Carolyn M. and Birgit Sorensen. (1990). "The Threshold Concentration of Chloride in Concrete for the Initiation of Reinforcement Corrosion," Corrosion Rates of Steel in Concrete, ASTM STP 1065, Philadelphia, PA, pp. 3-16.

James Instruments, Inc. Test CL-500 To Determine the Total Content of Chlorides in Concrete, James Instruments, Inc., Chicago, IL.

John, D.G., et al. (1995). "Corrosion Management of Reinforced & Pre-stressed Concrete Bridges Using Permanently Embedded Sensors," *Proceedings of the Fifth International Conference, Structural Faults and Repairs*, Volume 1, Engineering Technics Press, Edinburgh, UK, pp. 123-128.

Jones, Denny A. (1996). Principles and Prevention of Corrosion, Second Edition, Prentice Hall, Upper Saddle River, NJ.

Karbhari, Vistasp M., Frieder Seible, and Gilbert A. Hegemier. (1996). "On the Use of Fiber Reinforced Composites for Infrastructure Renewal- A Systems Approach," Materials for the New Millennium, American Society of Civil Engineers, NY, pp. 1091-1100.

Kay, Ted. (1992). Assessment and Renovation of Concrete Structures, Longman Scientific & Technical, NY.

Krauss, Paul, Gu, Gordon Ping, and Alexander Vaysburd. (1999). "Perspectives on Corrosion Inhibitors," Repair Perspectives, Publication #R970154, The Aberdeen Group.

Labossiere, P., Neale, K.W., and Martel, S. (1997). "Strengthening Existing Structures With Composite Materials: Practical Applications in Quebec," *Recent Advances in Bridge Engineering*, July, pp. 89-97.

Leeming, M.B. and V. Peshkam. (1995). "Robust Solution to Strengthening Bridges," *Proceedings of the Fifth International Conference, Structural Faults and Repairs*, Volume 1, Engineering Technics Press, Edinburgh, UK, pp. 161-164.

Long, A.E. and A. McC. Murray. (1984). "The "Pull-Off" Partially Destructive Test for Concrete," In Situ/Nondestructive Testing of Concrete, (SP 82-17), Amercian Concrete Institute, Detroit, MI, pp. 327-350.

Mailvaganam, Noel P., ed. (1992). Repair and Protection of Concrete Structures, Institute for Research in Construction, National Research Council of Canada, CRC Press, Inc., Ottawa, Ontario.

Mallick, P. K. ed. (1997). Composites Engineering Handbook, University of Michigan-Dearborn, Dearborn, MI.

Mirmiran, Amir and Mohsen Shahawy. (1997). Behavior of Concrete Columns Confined by Fiber Composites," *Journal of Structural Engineering*, May, pp. 583-590.

Nanni, Antonio. (1995). "Concrete Repair With Externally Bonded FRP Reinforcement," *Concrete International*, June, pp. 22-26.

Neale, Kenneth W. and Pierre Labossiere. (1998). "Fiber Composite Sheets in Cold Climate Rehab," *Concrete International*, June, pp. 22-24.

Ohta, Toshitaka, et al. (1992). "Deterioration in a Rehabilitated Prestressed Concrete Bridge," *ACI Materials Journal*, July-August, pp. 328-336.

Ohtsu, Masayasa, Toshifumi Yamamoto, and Kimitoshi Matsuyama. (1997). "Quantitative NDE Estimation for Rebar Corrosion in Concrete," *Proceedings of the Seventh International Conference, Structural Faults and Repairs*, Volume 2, Engineering Technics Press, Edinburgh, UK, pp. 265-273.

Perkins, P.H. (1997). Repair, Protection and Waterproofing of Concrete Structures, E.& F.N. Spon, London, UK.

Saadatmanesh, H., M.R. Ehsani, and M.W. Li. (1994). "Strength and Ductility of Concrete Columns Externally Reinforced with Fiber Composite Straps," *ACI Structural Journal*, July-August, pp. 434-447.

Scannell, William T., Ali A. Sohanghpurwala, and Moavin Islam. (1996). "Assessment of Physical Condition of Concrete Bridge Components," *FHWA-SHRP Showcase Participant's Workbook*, Concorr, Inc., Ashburn, VA .

Shahawy, Mohsen and Thomas E. Beitelman. (1995). “Structural Applications of Advanced Composite Materials in Bridge Construction and Repair,” Restructuring: America and Beyond, *Proceedings of Structures Congress XIII*, Volume 1, pp. 607-621.

Shaw, Mark. (1997). “Migrating Corrosion Inhibitors fro Reinforced Concrete Protection,” *Proceedings of the Seventh International Conference, Structural Faults and Repairs*, Volume 2, Engineering Technics Press, Edinburgh, UK, pp. 317-324.

Sherwin Williams (2001). Macropoxy 920 Pre-Prime Data Sheet.

Sheikh, S. et al. (1999) “Repair of Delaminated Circular Pier Columns by ACM., Ontario Joint Transportation Research Report, MTO Reference Number 31902.

Sika Corporation. (2000). Sika FerroGard 903 Product Data Sheet.

Sika Corporation. (1996). Construction Products Catalog.

Sohanghpurwala, Ali and William T. Scannell. (1994). “Repair and Protection of Concrete Exposed to Seawater,” *Concrete Repair Bulletin*, July-August, pp. 8-11.

Soudki, Khaled A. and Mark F. Green. (1997). “Freeze-Thaw Response of CFRP Wrapped Concrete,” Concrete Interational, August, pp. 64-67.

Surtreat International. (2000). Total Performance System Technical Data.

Tang, Benjamin. (1997). "Fiber Reinforced Polymer Composites Applications in USA," *First Korea/U.S.A. Road Workshop Proceedings*.

Teng, Ming-Hung, Elisa D. Sotelino, and Wang Chen. (2000). "Monitoring of Long-Term Performance of Highway Bridge Columns Retrofitted by Advanced Composite Jackets in Indiana," Joint Transportation Research Program, West Lafayette, Indiana.

Thomas, Jay, et al. (1996). "Externally Bonded Carbon Fiber For Strengthening Concrete," Materials for the New Millennium, American Society of Civil Engineers, NY, pp. 924-931.

Toutanji, H. and P. Balaguru. (1998). "Durability Characteristics of Concrete Columns Wrapped with FRP Tow Sheets," *Journal of Materials in Civil Engineering*, February, pp. 52-57.

Verhulst, Stewart Mason. (1999). "Evaluation and Performance Monitoring of Corrosion Protection Provided by Fiber-Reinforcing Wrapping," Thesis, Civil Engineering Department, University of Texas at Austin.

Watson, Ronald J. (2000). "Wrapping it Up," *ASTM Standardization News*, February, pp. 22-25.

Whitmore, David, Sean Abbott, and Emmanuel Velivasakis. (1999). "Battling Concrete Corrosion," *Civil Engineering*, January, pp. 46-48.

Yeomans, S. R. (1991). “Comparative Studies of Galvanized and Epoxy Coated Steel Reinforcement in Concrete,” Durability of Concrete, Second International Conference, Volume I, (SP 126-19), American Concrete Institute, Detroit, MI, pp. 355-370.